Aus der Poliklinik für Kieferorthopädie
der Heinrich-Heine-Universität Düsseldorf
Direktor: Univ.-Prof. Dr. med. dent. Dieter Drescher

Analysis of osteocytic gene and associated protein expression in cells surrounding orthodontic mini-implants migrating in bone – an LCM/ Immunofluorescence/ micro-CT study in the rodent model

Dissertation

zur Erlangung des Grades eines Doktors der Zahnmedizin
der Medizinischen Fakultät der Heinrich-Heine-Universität Düsseldorf

vorgelegt von
Nicole Jasmin Rauch

2022

Als Inauguraldissertation gedruckt mit der Genehmigung der

Medizinischen Fakultät der Heinrich-Heine-Universität Düsseldorf

gez.:

Dekan/ in: Prof. Dr. med. Nikolaj Klöcker

Erstgutachter/in: Prof. Dr. med. dent. Dieter Drescher

Zweitgutachter/in: Prof. Dr. med. dent. Jürgen Becker

“So come with me, where dreams are born, and time is never planned.

Just think of happy things, and your heart will fly on wings”

— J.M. Barrie

Teile dieser Arbeit wurden veröffentlicht:

Becker, K., Rauch, N., Brunello, G., Azimi, S., Beller, M., Hüfner, M., Nienkemper, M., Schwarz-Herzke, B., Drescher, D., (2021), Bone remodelling patterns around orthodontic mini-implants migrating in bone: an experimental study in rat vertebrae. European Journal of Orthodontics, (Volume 43, Issue 6) Pages 708 - 717

Zusammenfassung

Die vorliegende Arbeit möchte das bislang nur klinisch zu beobachtende Phänomen der Implantatmigration durch Analyse der lokalen Gen- und Proteinexpression im umgebenen Knochen hinterleuchten - histologisch und mittels Real-Time-PCR. Implantatmigration beschreibt den Prozess, bei dem enossale Implantate – entgegen ihrer bislang vermuteten Ortsstabilität – unter dem Einwirken einer entsprechenden Kraft eine Positionsänderung im Knochen erfahren. Teile dieser Dissertation wurden 2021 bereits unter dem Titel „Bone remodelling patterns around orthodontic mini-implants migrating in bone: an experimental study in rat vertebrae“ im Journal of European Orthodontics veröffentlicht (Becker et al. 2021).

In unserer Pilotstudie (Becker et al. 2019) wurden hierfür in die Schwanzwirbel von n = 61 weiblichen Ratten jeweils zwei spezielle Mini-Implantate inseriert und mit einer NiTi-Feder verbunden, die eine jeweils konstante Kraft ausübte (0 N, 0,5 N, 1,0 N, 1,5 N). Dadurch konnten periimplantäre Knochenareale je nach Richtung in Druck- und Zugzonen unterteilt werden. Für die vorliegende Arbeit standen n = 26 Tiere zur Verfügung, von denen jeweils 13 nach zwei bzw. acht Wochen getötet wurden. n = 15 Proben wurden bei -80 °C konserviert und deren Osteozyten durch *Lasermikrodissektion* (LCM) extrahiert. Die aus ihnen isolierte mRNA wurde mittels reverser Transkription in DNA umgeschrieben, um die lokale Genaktivität von Runx2, SP7, SOST und CTSK zu analysieren. Weitere n = 11 Proben wurden entkalkt, um die Expression von Osteocalcin und Cathepsin K durch Immunfluoreszenz zu untersuchen.

Die Ergebnisse zeigten, dass Druck- und Zugkräfte keinen statistisch signifikanten Einfluss auf die Gen- und Proteinexpression hatten. Lokale Tendenzen konnten dennoch festgestellt werden: Einige anabolische Marker (Runx2 und Osteocalcin) und alle katabolischen Marker (SOST, CTSK und Cathepsin K) waren nach zwei Wochen besonders in den Druckzonen erhöht, während der Appositionsmarker SP7 verstärkt in den Zugzonen exprimiert wurde. Dies lässt nach zwei Wochen auf ein erhöhtes Knochenremodelling in Bewegungsrichtung der Implantate schließen, mit tendenziell dominierender Knochenresorption in den Druckzonen und einer relativ dazu erhöhten Knochenapposition in den Zugzonen. Nach acht Wochen zeigten die Gene und Proteine einen Expressionsabfall und das Erreichen eines Gleichgewichtszustandes. Beides lässt auf eine mit der Zeit stagnierende Implantatmigration schließen.

Trotz ein paar weniger Einschränkungen konnte diese Studie aufzeigen, dass die Migration kieferorthopädischer Mini-Implantate durch belastungsinduziertes Knochenremodelling im periimplantären Gewebe ausgelöst zu werden scheint.

Abstract

The aim of the present study is to enlighten the phenomenon of implant migration, which has so far only been observed clinically, by analyzing the local gene and protein expression in the implants' surrounding bone tissue - histologically and by real-time PCR. Implant migration describes the process by which endosseous implants - contrary to their previously assumed local stability - undergo a change in position in the surrounding bone under the influence of a corresponding force. Parts of this dissertation have already been published under the title 'Bone remodeling patterns around orthodontic mini-implants migrating in bone: an experimental study in rat vertebrae' in the Journal of European Orthodontics 2021 (Becker et al. 2021).

For this purpose, in a prior pilot study (Becker et al. 2019), two customized mini-implants were inserted into the caudal vertebrae of n = 61 female Wistar rats and connected to each other with a NiTi spring, each exerting a constant force (0 N, 0.5 N, 1.0 N, 1.5 N). This allowed the peri-implant bone areas to be subdivided into compression and tension zones depending on the direction. For the present work, n = 26 animals were available, 13 of which were killed either after two or eight weeks, respectively. Samples from n = 15 animals were preserved at -80 °C and the osteocytes they contained were subsequently extracted by *laser-capture-microdissection* (LCM). The mRNA isolated from the osteocytes was transcribed into DNA by reverse transcription to analyze the local activity of genes such as Runx2, SP7, SOST and CTSK. Another n = 11 samples were decalcified to analyze the expression of osteocalcin and cathepsin K using immunofluorescence.

The analyses showed that compressive and tensile forces did not have statistically significant effects on gene and protein expression. Local trends regarding an increased expression of bone anabolic and resorptive markers could be detected, though: some anabolic markers (Runx2 and osteocalcin) and all catabolic markers (SOST, CTSK and cathepsin K) were increased after two weeks, mainly in the compression zones, whereas the apposition marker SP7 was strongly expressed in the traction zones. These observations indicate a general increased bone remodeling in the direction of implant movement after two weeks, with a tendency of a more dominant bone resorption in the pressure zones and relatively increased bone apposition in the traction zones. After eight weeks, genes and proteins showed a decrease in their expression and the achievement of an equilibrium. Both suggest that implant migration stagnates over time.

Despite some limitations, this study demonstrated that migration of orthodontic mini-implants appears to be triggered by load-induced bone remodeling in the peri-implant tissue.

Table of Abbreviations

μCT ..... Microcomputed tomography
BAp ..... Bone alkaline phosphatase
BIC ..... Bone-to-implant-contact
BMU ..... Basic multicellular unit
BV/ TV ..... Bone volume fraction
Cbfa1 ..... Core-binding factor alpha 1
cDNA ..... complementary Deoxyribonucleic acid
Ct ..... Cycle threshold
CTSK ..... Gene coding Cathepsin K
Cx43 ..... Connexin-43
DAPI ..... 4′,6-Diamidin-2-phenylindol
DNA ..... Deoxyribonucleic acid
ECM ..... Extracellular matrix
fcc ..... face centered cubic
FELASA ..... Federation of European Laboratory Animal Science Associations
FEM ..... Finite element method
FOV ..... Field of view
H1.0 ..... Histone H1.0
hcp ..... hexagonal close-packed
IgG ..... Immunoglobuline G
LANUV ..... Landesamt für Natur, Umwelt und Verbraucherschutz Nordrhein-Westfalen
LCM ..... Laser-capture-microdissection
LPC ..... Laser-pressure-catapulting
mRNA ..... messenger Ribonucleic acid
N ..... Newton
nanoCT ..... Nanocomputed tomography
NF-κB ..... Nuclear factor 'kappa-light-chain-enhancer' of activated B-cells
NiTi ..... Nickel-titanium
O.C.T. ..... Optimal cutting temperature
OA/TA ..... Occupied area per tissue area
Pa ..... Pascal
PBS ..... Phosphate-buffered saline
PMMA ..... Polymethylmethacrylate e
qPCR ..... quantitative Polymerase chain reaction
Ra ..... Arithmetic average of the roughness profile

RANKL ..... Receptor Activator of NF-κB Ligand
RNA ..... Ribonucleic acid
RNAses..... Ribonucleases
Runx2 ..... Runt-related transcription factor 2
SAS..... Skeletal anchorage systems
SLA ..... sandblasted, large-grit, acid-etched
SOST ..... Gene coding Sclerostin
SP7 ..... Specifity Protein 7
VEGF ..... Vascular Endothelial Growth Factor
Wnt ..... Wingless Int-1

Table of Contents

1. Introduction

1.1. Background

For the orthodontic movement of teeth within their surrounding bone, anchorage is of crucial importance (Angle 1900) as it compensates the reactive forces occuring according to Newton‘s 3rd law (actio = reactio) (Angle 1900, Upendran et al. 2021, Nienkemper et al. 2013, Nienkemper et al 2014). In the last two decades, skeletal anchorage using orthodontic mini-implants gained popularity (Pauls et al. 2013, Nienkemper et al. 2014).

1.2. Anchorage in Orthodontics

The origin of correcting malpositioned teeth with the help of orthodontic appliances is not clear. However, the first person to be mention is Fauchard (1726), who invented an expansion arch for the correction of transversal discrepancy (Angle 1900). Multiple other devices have followed thereafter, all of them in need for sufficient anchorage to avoid undesired site effects.

Angle determined two requirements for the orthodontic movement of teeth as 1) the applied force has to be appropriate and 2) the anchorage has to be ‘sufficient to resist this force’ and therefore arise from ‘a fixed base’, if the anchorage unit itself is not supposed to be displaced during the movement (Angle 1900). Burstone subdivided different kinds of anchorage according to the anchorage quality determined by the movement of both the active unit (teeth intended to be moved) and the anchorage device itself (Smith/ Burstone 1984): he considered a 1) critical anchorage, when the active unit is moved up to 25 % and whenever the anchorage unit undergoes a simultaneous movement of 75 %; 2) minimal anchorage is defined by a movement of 50 % of both the active unit and the anchorage device at the same time. 3) Moderate anchorage is defined by a movement of 75 % of the active unit and 25 % of the anchorage unit in return.

The term ‘skeletal anchorage’ found its way into literature at the second half of the 20th century with the invention of endosseus devices, that are ‘osseointegrated’ in the bone (Melsen 2005). In this context, when the active unit is about to move 100 % and the anchorage unit remains stationary stable (movement of 0 %) we achieve 4) maximum anchorage [Fig. 1].

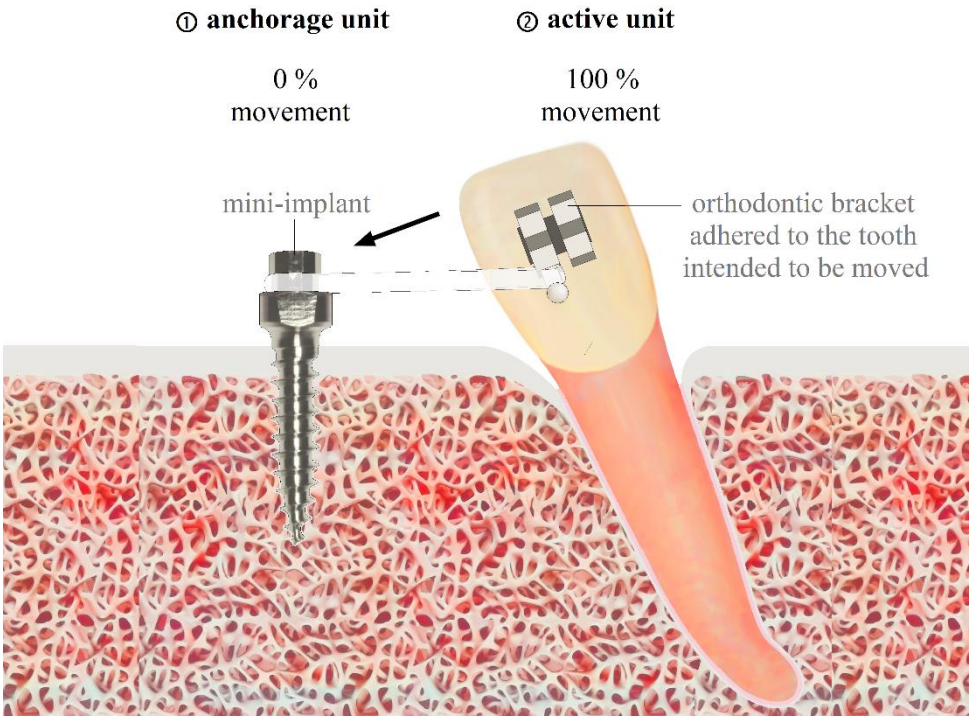

Fig. 1: **Movement ratio of active and anchorage unit in case of maximal anchorage. The anchorage unit is considered to be stationary stable (0 % movement), whereas the active unit is moving in the bone (100 % of the movement).**

As early as 1945, first experiments were carried out on dogs' jaws to test skeletal anchorage using vitallium screws that were inserted into the anterior part of the mandibular ramus. The screws were connected with an elastic band to an appliance in the dogs' maxilla and then subjected to a tensile force. However, these initial approximations of skeletal anchorage failed, as implant loss of all implants occurred within the first sixteen to thirty days. Microscopic destruction of the peri-implant bone tissue was subsequently observed (Gainsforth/ Higley 1945).

Further efforts in developing *skeletal anchorage systems* (SAS) were made to generate sufficient skeletal anchorage, which – according to their structure - can be subdivided into different modalities. 38 years after the attempts of Gainsforth and Higley, Creekmore endeavored to place screw implants in the area of the anterior nasal spine in order to achieve skeletal anchorage for the intrusion of maxillary anterior teeth (Creekmore/ Eklund 1983). In 1990, Roberts developed another system for orthodontic 'rigid' anchorage with the placement of endosseous implants in the retromolar region for the mesialization of lower molars, which have shown to get osseointegrated (Roberts et al. 1990).

In order to generate a supposedly less invasive skeletal anchorage element, Triaca later invented a flat screw implant in 1992, which was the first skeletal anchorage element to find application in the anterior palate (Triaca et al. 1992). Three years later, Block and Hoffmann were also investigating solutions for the insertion of anchorage elements within the palate and therefore developed a so-called 'onplant', which was supposed to guarantee greater anchorage due to a larger diameter of 10 mm and a hydroxyl apatite coated surface for purely subperiosteal insertion (Block/ Hoffman 1995). Because of their large diameter, these implants have not found application in clinical practice.

In 1988, Shapiro was the first to introduce dental implants as anchorage elements for the use in orthodontics (Shapiro/ Kokich 1988).

A further development with regard to a reduced width of the endosseous screws was the invention of the 'orthosystem' by H. Wehrbein, in which screws made of pure titanium with a smaller diameter were inserted in the palatal region (Wehrbein et al. 1996).

The 'mini-implants' developed later were the very first to be described by R. Kanomi in 1997 (Kanomi 1997). They have been used in regular practice since then because they offer the possibility of being placed almost anywhere (Costa et al. 1998).

In addition to mini-implants, miniplates have also found application in clinical practice, first described by Umemori in 1999 and intended for insertion in the zygomaticoalveolar crest (Umemori et al. 1999), and still used in the present (Hourfar et al. 2014, Nagasaka et al. 2009).

A rather newer design belonging to the class of miniplates is the Mentoplate, which is inserted into the chin region and is used for early therapy of class III patients with the help of elastics fixation (Wilmes et al. 2011).

1.2.1. Orthodontic Mini-implants

With the invention of mini-implants, provision of additional anchorage became possible (Nienkemper et al 2014, Becker et al. 2018). Even though the mini-implants remain in bone only temporary, they belong to the group of endosseous implants (Liou et al. 2004). Mini-implants are placed transmucosally, with the implant head being exposed to the oral cavity [Fig. 2] (Upendran et al. 2021). In contrast to dental implants used for prosthetic purposes, mini-implants exhibit a 'reduced diameter' (Becker et al. 2019) (Upendran et al. 2021) and are mostly made out of 'titanium alloys' (Becker et al. 2019) (Kuphasuk et al. 2001, Deguchi et al. 2003, Cotrim-Ferreira et al. 2010, de Morais et al. 2009, Upendran et al. 2021), or

stainless steel (Brown et al. 2014, Bollero et al. 2018, Chang et al. 2019, Mecenas et al. 2020). In addition, to ease explantation upon their temporary usage, a machined surface is commonly used. Advantages compared to other devices providing skeletal anchorage are the ease of use and the possibility to be inserted even in narrow anatomical locations (Liou et al. 2004, Papageorgiou et al. 2012, Upendran et al. 2021). Furthermore, the insertion and removal process are hardly invasive (Nienkemper et al. 2013), and the post-insertional time until mini-implants can be orthodontically loaded is short as they can be loaded 'immediately' (Becker et al. 2019) after placement (Liou et al. 2004). Also, their clinical failure rate is rather small (Papageorgiou et al. 2012), reflecting in an overall 'high success rate[s]' (Becker et al. 2019) of 87.7 % (Papadopoulos et al. 2011).

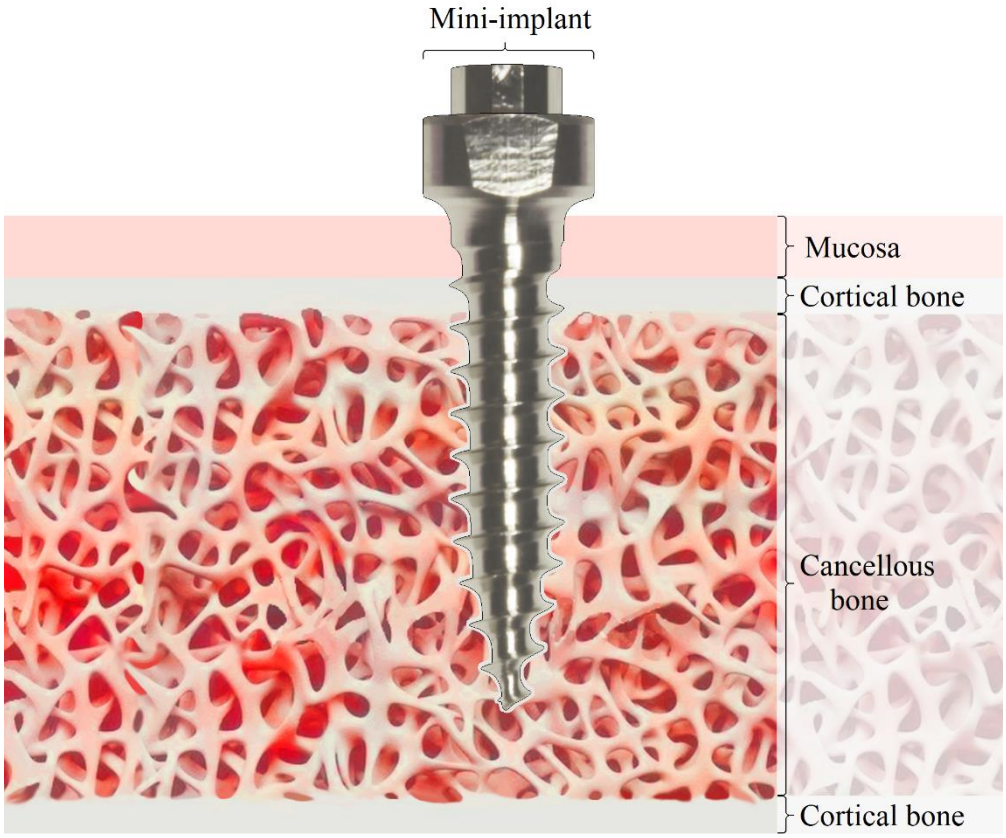

Fig. 2: **Mechanism of a mini-implant inserted into the bone matrix**

1.2.2. Examples for the Usage of Mini-implants in Orthodontics

There are different indications for which mini-implants were shown to be effective during orthodontic therapy:

1) Tooth intrusion: for tooth intrusion, mini-implants were reported to be highly suitable compared to other orthodontic devices (Jain et al. 2014, Wilmes et al. 2014, Nosouhian et al. 2015, Asok et al 2019), and they were described to be efficacious for closing an open bite (intrusion of upper molars) (Hart et al. 2015, Pinzan-Vercelino et al. 2017).
2) Tooth extrusion: extrusion of impacted or retained teeth can be achieved using mini-implants (Nienkemper et al. 2012, Nosouhian et al. 2015). Additionally, deep bite can be successfully corrected through molar extrusion (Sosly et al. 2020). When the clinical crown of a tooth needs to be prolonged for prosthetic purposes, an extrusion can be successfully achieved with the help of orthodontic mini-implants (Greco/ Derton 2012).
3) Front retraction: units consisting of all anterior teeth can be retracted with significant lower anchorage loss compared to other devices (Nosouhian et al. 2015, Becker et al. 2018).
4) Mesialization/ distalization: Mini-implants can be used for the closure of spaces (Becker et al. 2018) or to distalize teeth (Wilmes et al. 2014). The latter is used for the correction of mesially migrated lateral teeth (Upadhyay et al. 2008, Nosouhian et al. 2015) or the preoperative orthodontic correction prior to orthognathic surgery for class II or class III treatment (Upadhyay et al. 2009, Upadhyay et al. 2012, Tozlu et al. 2013, Gurgel et al. 2013, Nosouhian et al. 2015, Rodríguez de Guzmán-Barrera et al. 2017, Meyns et al. 2018).
5) Transversal expansion: in case of a transversal discrepancy between upper and lower jaw, mini-implants can be used as an alternative to a palatal expansion for a transversal tipping of the upper molars in a relation to the lower molars (Carlson et al. 2016, Nojima et al. 2018, Lyu et al. 2019).
6) Orthopedic purposes (early treatment of class III patients) (Wilmes et al. 2014, Lombardo et al. 2020): if the upper jaw is retrognathic to the lower jaw and therefore affects the skeletal development in the early growth, mini-implants are used as anchorage devices for an anterior displacement of the upper jaw in a sagittal direction.

1.2.3. Different Anchorage Concepts

Depending on the anchorage mechanism used for tooth movement, we can further distinguish between direct and indirect anchorage (Wilmes et al. 2009, Wilmes et al. 2014, Wilmes et al. 2019).
1) Direct anchorage: in the concept of direct anchorage, the tooth to be moved is directly connected to the anchorage element, and the force required for tooth movement is applied directly to the implants.

2) Indirect anchorage: in contrast, in indirect anchorage, the anchorage element serves as an intermediate component for transmitting force to the tooth to be moved. This intermediate element is intended, for example, to stabilize a row of teeth serving as an anchorage unit against retraction forces.
In both concepts, mini-implants can be used as such anchorage elements.

1.2.4. Implant Migration

While the periodontal ligament is considered to play an important role for the movement of teeth within bone under the application of orthodontic force systems (Angle 1900, Dyment/ Synge 1935, Yoshikawa 1981), an endosseous implant is considered to be stationary stable (Becker et al. 2019) as it is directly connected to the peri-implant bone. Herein, stationary implant stability is an important criterion for treatment success, especially when indirect anchorage is utilized.
Implant stability can be subdivided into primary (directly after insertion) and secondary stability (after healing). Secondary stability depends on bone formation at the bone-to-implant surface (Nahm et al. 2015): like dental implants, mini-implants are assumed to integrate with their surrounding bone through a process called osseointegration, even though the fraction of bone in contact with the implants' surface is usually lower compared to dental implants (Liou et al. 2004, Vande Vannet et al. 2007, Dhaliwal et al. 2017, Alves et al. 2019).
The term osseointegration was introduced by Brånemark in 1983 and refers to a direct contact between the implant surface and its surrounding bone without the interposition of soft tissue (Brånemark et al. 1983, Mavrogenis et al. 2009, Wróbel et al. 2010).
Although the effectiveness of mini-implants in orthodontics is reflected by numerous publications, 'recent clinical studies' (Becker et al. 2019) (Liou et al. 2004, El-Beialy et al. 2009, Pittman et al. 2014, Nienkemper et al. 2014, Becker et al. 2021) revealed that mini-implants seem to 'migrate within bone when subjected to orthodontic loading' (Becker et al. 2021) [Fig. 3]. However, the underlying biological and 'molecular patterns' are poorly understood (Becker et al. 2019, Becker et al. 2021).

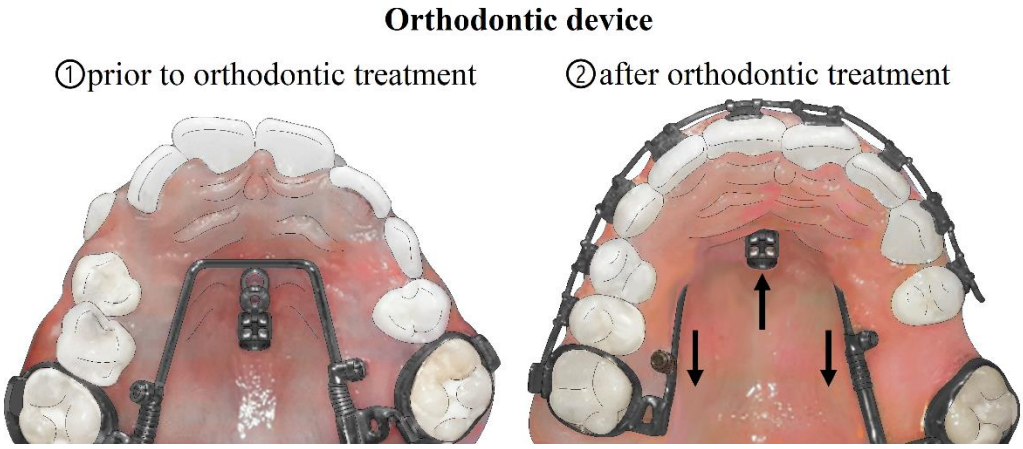

Fig. 3: **Clinical observation of an implant migration (modified after a clinical picture)**

1.2.5. Site-specific Gene and Protein Distribution in the peri-implant Areas

Orthodontic tooth movement has long been assumed to involve site-specific stress distribution in the bone tissue surrounding the root surface (Davidovitch 1991). As early as 1888, the bending of the peri-radicular bone was suspected to be a requirement for tooth movement within the bone tissue (Farrar 1888). This conjecture was to be reconciled with Wolff's law, according to which bone architecture can change by the application of mechanical forces (Wolff 1892). Based on this, Sandstedt et al. were able to show that changes in the peri-radicular bone tissue appear to be controlled by processes in the periodontal ligament, and that newly formed bone was found in areas where the periodontal ligament was subjected to tensile stress, while bone resorption was found in areas of compression (Sandstedt 1904). More recent techniques such as the *finite element method* (FEM) – which is able to contribute to 'a more accurate assessment of the local stresses and strains' (Becker et al. 2021) - have further confirmed the suspected inhomogeneous stress distribution within the periodontal ligament during tooth movement, showing that the peri-radicular bone surface can be divided into compression zones (in the direction of tooth movement) and tension zones (contrary to the direction of tooth movement) depending on the center of rotation of the tooth (Tanne et al. 1987).

'Therefore, the traditional terminology from orthodontic tooth movements was adopted' (Becker et al. 2021) within this study, so that results from areas subjected to mechanical pressure within this study are marked in red, while the regions that were subjected to tension are colored in green [Fig. 4].

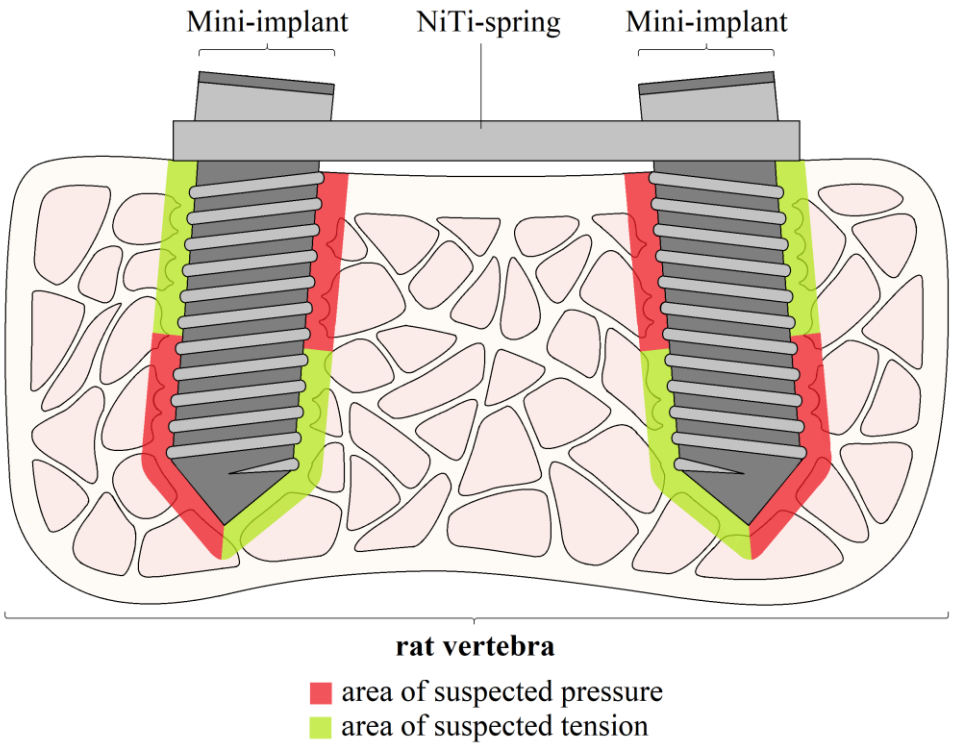

Fig. 4: **Suspected distribution of peri-implant areas of pressure (red) and tension (green) (modified after Becker et al. 2021)**

1.3. The Peri-implant Area

Bone is described as a dynamic organ in which cells are communicating with each other to maintain its structural and physiological integrity. This communication is assumed to be crucial in order to respond to mechanical loading (Novack 2011).

Bone consists of water (10 %), organic or non-mineralized matrix (25 %) (Sheldon/ Robinson 1957, Shoulders/ Raines 2009) and inorganic or mineralized components (65 %) (Scheele 1931, Rey et al. 1995, Rey et al. 2009, Mahamid et al. 2008).

According to the organic parts, 90 % are made of collagen fibers; the other 10 % are made of so called non-collagenous proteins (NCPs). Collagen fibrils are connected with each other by so called ‘cross-links’ (Shoulders/ Raines 2009, McNerny et al. 2015) and are arranged along to force trajectories to resist mechanical forces: longitudinal fibers can be found where bone is under tension, whereas transversal arranged fibers are primarily in regions of mechanical pressure (Peterlik et al. 2006, Granke et al. 2013, Schrof et al. 2016).

The inorganic parts are made of hydroxyl apatite deposited next to or in between the collagen fibrils (Sheldon/ Robinson 1957, Tertuliano/ Greer 2016, Reznikov et al. 2015). The bone

surface is covered by soluble carbonates, phosphates or hydroxyl ions, which can be easily resorbed under acidification (Bushinsky/ Frick 2000).

Upon this, water plays an important role within bone tissue: on the one hand, it is firmly bound to collagen fibers, and on the other hand it is distributed soluble within empty bone cavities (Robinson 1979, Granke et al. 2015). In the latter case, water can be redistributed under mechanical loading within the bone matrix, which then leads to a detection by the osteocytes, 'the principal sensory cells responding to mechanical stimuli' (Becker et al. 2021). This is important for the orchestration of osteocyte mediated bone remodeling (Dallas et al. 2013, Qin et al. 2020).

1.3.1. Bone Remodeling

Bone remodeling is defined as a result of bone formation (apposition of new bone) and bone resorption (removal of existing bone) (Costa et al. 2011) and is directly influenced by mechanical loading (Nomura/ Takano-Yamamoto 2000). Bone resorption and bone apposition occur side by side within the bone tissue, with a shift of the balance in favor of either apposition or resorption (Enlow et al. 1969)

Frost first termed the collection of osteoblasts, osteoclasts and supplying blood vessels as the so called *basic multicellular unit* (BMU), where bone remodeling takes place as a balance of bone formation and bone resorption on the bone surface in response to mechanical loading (Frost 1990, Kenkre/ Bassett 2018).

1.3.2. Osteoclasts and Bone Resorption

Bone resorption frequently starts with the 'osteocyte apoptosis' (Becker et al. 2021), i.e. in locations where damage has happened (Kennedy et al. 2012, Kennedy et al. 2014, Jilka et al. 2013, Goldring 2015). Osteocytes in closest proximity to those dying osteocytes release cytokines (i.e. *Receptor Activator of NF-κB Ligand* (RANKL), *Vascular Endothelial Growth Factor* (VEGF)), that recruit osteoblastic and osteoclastic precursor cells to the bone surface (Goldring 2015). There, osteoclastic precursor cells differentiate and fuse to mature multinucleated osteoclasts (Miyamoto et al. 2011, Xing/ Boyce 2012). Like osteoblasts, osteoclasts attach to the bone surface via integrins that form a so called 'sealing zone' on a local region on the top of the bone surface. Within this zone, ions (hydrogen and chloride ions) are released, which acidify the bone matrix for the subsequent resorption of the exposed organic bone matrix by enzymes in charge of bone resorption, such as proteases (Novack

2011). Those ions contribute to an increase in the pH value within the sealing zone, and result in dissolving of bone minerals (Schlesinger et al. 1994, Schlesinger et al. 1997, Schaller et al. 2005, Supanchart/ Kornak 2008). This demineralization leads to an envelope of collagen fibers, which get resorbed in a second step (Everts et al. 2002). When bone resorption is finished, osteoclasts either detach from the bone surface and remain inactivated until further needed (Chambers 1982, Martin/ Ng 1994, Miller/ Bowman 2007), or undergo apoptosis (Xing/ Boyce 2005, Wang et al. 2015, Soysa/ Alles 2019).

1.3.3. Osteoblasts and Bone Formation

Osteoblasts are responsible for the formation of new bone by depositing the bone matrix called osteoid made out of collagen type I onto the bone surface. The osteoid later gets mineralized by the deposition of calcium and phosphate ions; the anorganic part of mineralized bone is called hydroxyapatite (Bonucci et al 1970, Pugliarello et al. 1970, Iwayama et al. 2019). Once bone formation is completed, osteoblasts get enclosed by their surrounding bone matrix. Later, they may become either osteocytes or undergo apoptosis (Nefussi et al. 1991, Franz-Odendaal et al. 2006). The *Wnt*-signaling (Wingless Int-1) pathway plays an important role in the osteoblastic differentiation (Novack 2011) and therefore 'favours bone formation' (Becker et al. 2021); upon others, *Runt-related transcription factor 2* (Runx2) is a transcription factor within the Wnt-signaling pathway that is crucial for the forming of the typical osteoblastic phenotype (Komori et al. 2010).

1.3.4. Osteocytes and Mechanical Stimuli

Osteocytes are former osteoblasts that got buried within bone lacunas (Wassermann/ Yaeger 1965, Nefussi et al. 1991, McNamara et al. 2009). Through small channels, so called canaliculi, osteocytes send about 50 dendritic processes into the *extracellular matrix* (ECM). Two dendritic processes are connected with each other via gap junctions, among them *Connexin-43* (Cx43) (Goldring 2015, Riquelme et al. 2020).

Trigger for the process of bone remodeling are mechanical stimuli. In recent years it turned out that – beside other cells in charge of bone homeostasis, such as macrophages (Cho et al, 2014, Kaur et al. 2016, Chen et al. 2020), fibroblasts (Chiquet et al. 2003, Chiquet et al. 2009) and immune cells (Yang/ Liu 2021) - osteocytes also seem to be one of the target cells in sensing mechanical stimuli and in return activating osteoblastic and osteoclastic bone remodeling (Novack 2011): a change in the fluid direction within the canalicular space leads

to a deflection of integrins, which in return activates signal transductions within the osteocytes' stroma. This induces G-protein-coupled signaling pathways (Wang et al. 2007, Geoghegan et al. 2019). In response, osteocytes produce cytokines, such as sclerostin, which inhibts the Wnt-pathway and is also considered to be a bone resorption marker (it inhibits bone formation). Signals that also derive from a movement in the integrins lead to the expression of Runx2, which is a prominent transcription factor for the maturation of osteoblasts (Franceschi et al. 2003). On the other hand, osteocytes activate osteoclastic mediated bone resorption through their own apoptosis (Bellido 2014), 'which has been shown to trigger osteoclast formation' (Becker et al. 2021).

1.3.5. Cytokines in Bone

Among multiple signaling pathways, the Wnt- and the *Nuclear factor 'kappa-light-chain-enhancer' of activated B-cells* (NF-κB)-signaling pathway play an important role in the control of bone remodeling [Fig. 5]. Via the Wnt-signaling pathway, osteocytes mediate the maturation of osteoblasts (Takada et al. 1994, Greco et al. 1996, Glass et al. 2005, Moorer/ Riddle 2018). Through its activation, the expression of target genes in charge of bone formation, such as Runx2, increase, which in return leads to the expression of further genes in favor of both bone formation and resorption (Sevetson et al. 2004, Ma/ Hottiger 2016). The Wnt-signaling pathway has shown to be activated under mechanical loading of bone tissue (Bullock et al. 2019). As mentioned above, osteocytic apoptosis induces the recruitment of osteoclasts. In contrast to this, mechanical loading and the activation of the Wnt-signaling pathway can prevent osteocytes' apoptosis (Bellido 2014). Cytokines such as sclerostin are capable of inhibiting the Wnt-signaling pathway due to a downregulation of bone formation (Cao/ Chen 2005, Goldring 2015). In opposite to the Wnt-signaling pathway, NF-κB has shown to inhibit and 'downregulate' the osteoblastogenesis instead, i.e. via cathepsin K (Novack 2011, Dai et al. 2020).

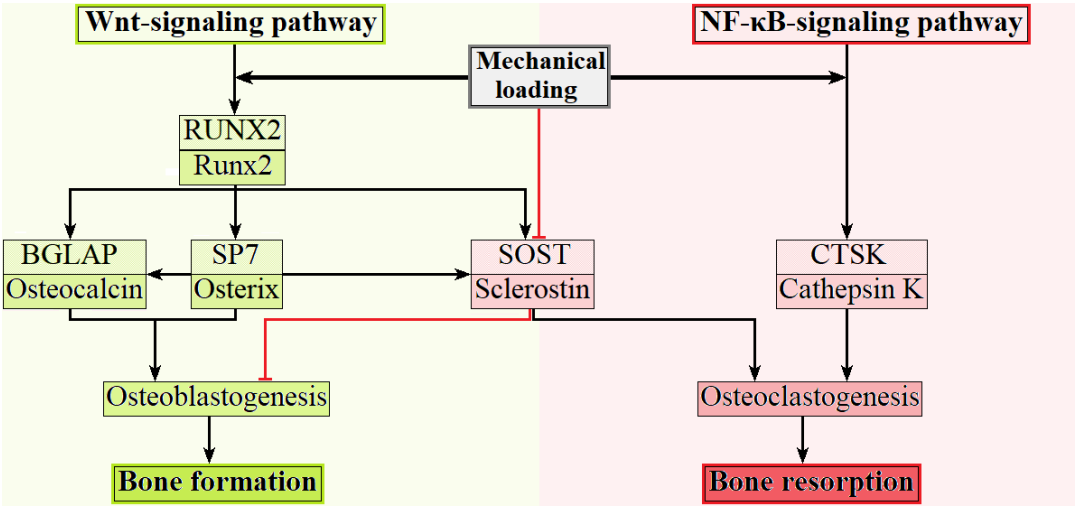

Fig. 5: **Interaction between genes and proteins involved in bone formation and resorption (in capital letters: genes in charge of bone remodeling, in small letters: associated proteins: RUNX2 encoding for Runx2, BGLAP encoding for osteocalcin, SP7 encoding for osterix, SOST encoding for sclerostin, CTSK encoding for cathepsin K)**

1.3.5.1. Runx2

Runx2, also referred to as *Core-binding factor alpha 1* (Cbfa1), is located on chromosome 6p2. Alterations in the gene locus lead to the clinical appearance of the cleidocranial dysplasia (Mundlos 1999). In its physiological function, Runx2 is supposed to manage processes in bone formation, as it is expressed within cells of the osteoblastic lineage: while it reaches its highest expression in 'immature osteoblasts', its activity decreases when osteoblasts get mature (Komori 2019). Besides this, 'there is [only] scarce information on their role in osteocytes' (Becker et al. 2021) As a major key player in the Wnt-signaling pathway, it is responsible for the induction of the expression of *Specifity Protein 7* (SP7) (Komori 2019, Komori 2020), but also SOST (Sevetson et al. 2004) as it is, below others, their transcriptional factor (Komori 2018). Via Runx2, the Wnt-signaling pathway inhibits the differentiation of osteoclasts (Kovács et al. 2019). This also plays an important role in bone apposition at the bone-to-implant interface (Nahm et al. 2015).

1.3.5.2. SP7/ Osterix

As a downstream product of Runx2 (Komori 2006), osterix also functions as 'an essential transcription factor for bone formation' (Becker et al. 2021) by contributing to the differentiation of osteoblasts (Chen et al. 2019). Its gene locus is on chromosome 12q13.13

(Gao et al. 2004). Upon others, it regulates the expression of osteocalcin. In its absence, the amount of mineralized bone mass decreases (Chen et al. 2019).

Additionally, SP7 can inhibit the Wnt signaling pathway and therefore negatively influence the proliferation of osteoblasts (Zhang et al. 2008), as it contributes to the expression of SOST (Yang et al. 2010).

1.3.5.3. Osteocalcin

Osteocalcin is one of the NCPs within the ECM and only secreted by osteoblasts (Wei/ Karsenty 2015, Moriishi et al. 2020). This secretion is mediated by both Runx2 and SP7 (Chen et al. 2019, Komori 2020). NCPs play a key role in the formation of the ECM (Bailey et al. 2017, Komori 2020). In its function as an NCP, osteocalcin has an impact on bone's mechanical properties (Moriishi et al. 2020). Together with osteopontin, osteocalcin is built 'during bone formation and late in the mineralization process'. They both play 'important roles in determining bone size, shape, and strength' (Bailey et al. 2017). Recent studies have revealed a different understanding of the physiological function of osteocalcin in bone tissue: Osteocalcin consists of three glutamic acids that are initially decarboxylated (Wei/ Karsenty 2015). Whilst the decarboxylated state of osteocalcin was assumed to work as a hormone, the carboxylated form has a high attraction to calcium ions: this fact found to be a major reason for its ability to inhibit growth in hydroxyl apatite crystals (Moriishi et al. 2020, Komori 2020). In addition, carboxylated osteocalcin was reported to attract precursors of osteoclastic cells and subsequently lead to the differentiation of these precursor cells into osteoclasts (Lambert et al. 2016, Moriishi et al. 2020, Komori 2020), therefore being responsible for bone resorption and the inhibition of bone formation (Moriishi et al. 2020).
The studies that showed an inhibition of bone resorption in the absence of osteocalcin were not reproducible in subsequent studies performed afterwards though (Komori et al. 2020). Usually, *bone alkaline phosphatase* (BAp) is arranged along the c-axis of hydroxyl apatite crystals and hence also parallel to the orientation of collagen fibrils (Moriishi et al. 2020). In recent studies with osteocalcin knockout rats instead of mice, Komori was able to show that only the orientation of BAp along the c-axis is 'disrupted' in comparison to the usual arrangement in wild type animals; the alignment of the collagen fibrils along the longitudinal axis still remained the same in between both groups (Moriishi et al. 2020). Consequently, they concluded that osteocalcin is not responsible of bone formation itself, but affects the correct arrangement of BAp along the same axis as the collagen fibrils. A disruption of this

usual arrangement of BAp to the collagen fibrils led to a reduction in the bone's Young's module (Moriishi et al. 2020, Komori 2020). With these results, Komori et al. claimed that osteocalcin would not be responsible for the process of bone resorption, but for aspects in bone quality, such as bone strength (Moriishi et al. 2020, Komori 2020).

1.3.5.4. SOST/ Sclerostin

As identified by van Buchem in 1976, sclerostin is a product of the SOST gene located on chromosome 17q12-q21 (Van Hul et al. 1998, Goldring 2015) and in charge of the van Buchem disease. It is expressed by osteocytes, osteoblasts and osteoclasts and controls osteoblastic bone formation (Cao/ Chen 2005, Li et al. 2005, Lin et al. 2009). Sclerostin is an inhibitor of the Wnt signaling pathway (Cao/ Chen 2005, Semënov et al. 2005, Li et al. 2005, Bellido 2014, Goldring 2015): the result of this inhibition is a decrease of osteoblastic differentiation (Cao/ Chen 2005), as well as an increase of the amount of RANKL, which has shown to promote osteoclastogenesis (Wijenayaka et al. 2011). By doing so, it acts as an antagonist to bone formation (Bellido 2014). Runx2 and SP7 do both have an impact on the expression of SOST as they bind to its promotor (Sevetson et al. 2004, Pérez-Campo et al. 2016, Becker et al. 2021). Pérez-Campo et al. showed that a higher expression in Runx2 and SP7 both contributed to a higher expression in SOST in human bone (Pérez-Campo et al. 2016).

Mechanical loading influences the expression of osteocytic SOST, as mechanical pressure leads to an activation of the Wnt signaling pathway with a concomitant decrease of SOST expression (Robling et al. 2008, Lin et al. 2009, Tu et al. 2012, Spatz et al. 2015). A decreased expression of osteocytic SOST can therefore be found in regions where mechanical strain and subsequent bone formation is high (Goldring 2015). In contrast, Spatz et al. found that osteocytes also sense mechanical unloading and then contribute to an increase in the expression of SOST (Spatz et al. 2015).

1.3.5.5. CTSK/ Cathepsin K

Cathepsin K (and its associated gene CTSK) belongs to a family of proteins called papain-like cysteine proteases located within the lysosomes (Costa et al. 2011, Novinec/ Lenarčič 2013, Dai et al. 2020). Found on chromosome 1q21 (Haagerup et al. 2000), it is expressed within osteoclasts, but can also be secreted in osteoblasts and osteocytes under mechanical loading (Costa et al. 2011, Novinec/ Lenarčič 2013, Dai et al. 2020, Bonnet at al. 2017). As

mentioned above, its expression is mediated by NF-κB, an important ligand in the process of osteoclastogenesis. When preosteoclasts mature into osteoclasts and bone resorption is intended, osteoclasts release cathepsin K into the sealing zone (Dai et al. 2020), where cathepsin K then hydrolases type I collagen (Costa et al. 2011, Borel et al. 2012, Novinec/ Lenarčič 2013, Dai et al. 2020). Physiologically, cathepsin K gets released from osteocytes in the case of mechanical compression (Bonnet at al. 2017).

1.3.5.6. RANK/ RANKL/ OPG

Within bone metabolism, the interplay between three other mediators takes on a very important role: Receptor Activator of NF-κB (RANK), RANKL and osteoprotegerin (OPG). The decoding of their interaction due to the activity of osteoblasts and osteoclasts took place in the second half of the 20th century. Without understanding the exact context, it was already shown in the 1980s that the activity and maturation of osteoclasts is regulated through the contact of osteoblasts with hematopoietic osteoclastic precursor cells (Chambers 1982). Initially only found on the surface of dendritic cells and later also on osteoclasts, RANK was then identified as a membrane-bound receptor belonging to the Tumor necrosis factor (TNF) receptor family (Anderson et al 1997). Its activation depends on binding to a ligand that has been named RANKL (Anderson et al 1997). RANKL is a soluble ligand expressed by osteoblasts and belongs to the family of TNF. When RANKL binds to RANK, osteoclastogenesis is activated (Anderson et al. 1997, Wong et al. 1997): the binding of RANKL to RANK induces an intracellular signaling cascade occurring in osteoclastic progenitor cells by activating NF-κB, which subsequently enters the nucleus and affects the transcription of various genes responsible for osteoclastogenesis (Siebenlist et al. 1994). As a result, osteoclastic progenitor cells become mature multinuclear osteoclasts (Jansen et al. 2012). In the course of bone resorption, this also leads to osteoclasts settling on the bone surface, forming a so-called rufled border, and starting bone resorption (Schlesinger et al. 1997).

To control the interplay between RANKL and RANK, another protein is expressed in bone tissue, which can inhibit osteoclastogenesis in return (Simonet et al. 1997, Tsuda et al. 1997): OPG. OPG is also expressed by osteoblasts, and, since it has a similar N-terminal protein sequence as RANK (Nelson et al 2012), is able to act as a decoy receptor by binding to RANKL (Lacey et al. 1998, Yasuda et al. 1998).

1.4. Methods for the Analysis of the Bone Remodeling Processes

For the analysis of bone remodeling, multiple approaches are listed in literature, reaching from invasive to non-invasive, *in* and *ex vivo* methods. Among them, the reconstruction of X-ray based images as well as the preparation of histological specimens were utilized in the present study, like also in prior investigations already (Becker et al. 2019).

1.4.1. Micro-computed tomography analyses

Microcomputed tomography (µCT) is an X-ray based imaging method suitable for non-invasive *in* and *ex vivo* analyses (Boerckel et al. 2014). Invented by Hounsfield (Hounsfield 1973), Feldkamp later developed an algorithm for a micro-computed tomography that was able to produce images with an even higher resolution (Feldkamp et al. 1984). Nowadays, even *nanocomputed tomographies* (nanoCTs) are available, that provide images with a voxel size from 60 nm (Bruker Co.) up to 400 nm (Kampschulte et al. 2016).

µCT is a widely used analysis method in the research of the bone tissue (Müller 2009, Boerckel et al. 2014, Becker et al. 2017, Trelenberg-Stoll et al. 2021). Besides its application in *ex vivo* analyses, µCT has become an ideal tool for *in vivo* analyses of 'living animals' (Becker et al. 2019), i.e. in combination with intravenous X-ray contrast agents for the analysis of vascular and cardial phenomena (Badea et al. 2008). In addition to one-point analyses it has also facilitated vast advantages in multi-step analyses of the same object of interest within a certain time interval (Yang et al. 2003, Wehrle et al. 2019, Ning et al. 2019, Scheuren et al. 2020), as images from 'different time points' (Becker et al. 2019) can be registered and changes over time can be detected, 'as multiple high-resolution scans can be obtained from the same animal' (Becker et al. 2021). In a previous study (Becker et al. 2019), we were already able to investigate changes in the peri-implant bone microstructure over time with the help of µCT. We were able to show that 'bone resorption took place mainly in areas at which pressure was suspected to occur, whereas newly formed bone was observed at the initial implant positions' (Becker et al. 2021). However, these findings 'are limited to end-point analyses' (Becker et at. 2021) and 3D reconstructed images, which only suggest to be bone tissue on the basis of their gray scale. Little to not yet mineralized bone matrix cannot be depicted by radiological imaging techniques, which is why they are not included in quantitative analyses of radiological images. A prove of this finding can only be confirmed by performing histological and histomorphometric *ex vivo* analyses, which are considered to

be complementary and ‘can overcome [the] limitations’ mentioned above (Becker et al. 2021).

1.4.2. Analyses using Immunofluorescence

Multiple efforts in the labelling of antigens with specialized enzymes were achieved in the past. In addition to immunofluorescence, immunohistochemical labeling of enzymes with horseradish peroxidase made a vast approach onto a more precise labelling of antigens of interest - both for *in vivo* and and *ex vivo* purposes. The subsequent invention of avidin-biotin staining proved to be equally evident down the road (Graham et al. 1966, Nakane/ Pierce 1966, Hsu et al. 1981). Although there have been approaches to uniform definitions for evaluating immunohistochemical stainings (e.g., ‘microanatomical distribution of staining, proportion of positively stained cells [and the] staining intensity’ (Seidal et al. 2001), these results appeared to be rather descriptive, as quantification of purely immunohistochemically stained preparations was hardly possible (Matos et al. 2010). This makes immunofluorescence an even more favorable method for the analysis of protein distribution, as each protein distribution appears as an immunofluorescence signal, which in return can be automatically detected and thus quantified using programs specifically designed for detecting immunofluoresence signals. Methods making use of fluorescence for immunolabelling were developed by Albert Coons in 1940 (Coons et al. 1941, Arthur 2016): after a fixation of the sample within formaldehyde (Donaldson 2015), the method is based on linking the epitope of an antigen of interest with a primary antibody, which, in a second step, gets linked to a fluorescence marked secondary antibody, also called ‘fluorophore’ (Donaldson 2015, Im et al. 2019). Immunofluorescence analyses are widely employed in clinical practice, especially in diagnostics of dermatological diseases such as autoimmune conditions (i.e. bullous autoimmune diseases, lichen planus or psoriasis) (Chhabra et al. 2012, Diercks et al. 2017, Jain/ Basavaraj 2019, Bresler et al. 2020), but also in malignant diseases associated with immune cells (Surace et al. 2019, Lee et al. 2020, Maliszewska-Olejniczak et al. 2020). A further advantage in the usage of immunofluorescence staining instead of immunochistochemical staining is the possibility to stain multiple antigens of interest within the same tissue section.

1.4.3. Cell capturing by Performing Laser-Capture-Microdissection (LCM)

The technique of LCM was developed by Emmert-Bruck et al. in 1996 (Emmert-Bruck et al. 1996). In contrast to other methods in analyzing gene expression within a whole sample, LCM provides the possibility of exclusively taking a look into a predefined enclosed area only within regions of interest. i.e. 'from areas subjected to different load qualities' (Becker et al. 2021). In contrast to earlier approaches in isolating single cells or a cell composite, either in a manual procedure (Zhuang et al. 1995, Going/ Lamb 1996) or with the help of ultraviolet radiation (Shibata et al. 1992), LCM provides the advantage of simultaneous observation of the tissue of interest under a microscope and the microdissection process itself. The initial technique made use of a carbon dioxide laser whose wavelength was appropriate for a precise cutting process without damaging the tissue itself. Nowadays also other types of lasers are in use (Curran et al. 2000). After the laser cutting process, the extracted material can be used for further analyses, such as *quantitative polymerase chain reaction* (qPCR), which has become a preferred procedure in current research (Lawrie/ Curran 2005, Silasi et al. 2008, Muruganandhan et al. 2018, Scheuren et al. 2020). In consideration of a further procedure with genetic material, an appropriate medium for tissue storage prior to LCM is needed. Like in most cases, fixation in formaldehyde was shown to make a subsequent qPCR analysis impossible (Goldsworthy et al. 1999, Curran et al. 2000). Although LCM has been used in the analysis of 'single cells from undecalcified cryosections' (Becker et al. 2021) of the bone tissue of mice in various studies (Xin et al. 2018, Wu et al. 2019, Marek et al. 2019, Scheuren et al. 2020), it has been utilized for the analyses of the bone tissue in rats in much smaller degree (Becker et al. 2019, Becker et al. 2021), probably due to the rat bone's thickness and hardness. Investigations on a sticky film for performing LCM within hard tissues are therefore a current research interest (Kawamoto 2003).

1.4.4. Analyses within Decalcified and Undecalcified Samples

Histomorphometric analyses or quantitative analyses such as qPCR were shown to be most suitable primarily for the examination of undecalcified bone tissue. In contrast, immunofluorescence staining of decalcified tissue still has to be demonstrated to be a suitable modality.

Keeping bone tissue undecalcified is crucial for the analysis of the microstructure of the hard components of bone or teeth. This also applies for the surface structure of implants that are in the region of interest (Donath/ Breuner 1982, Calvo-Guirado et al. 2015). The analysis of the *bone-to-implant-contact* (BIC) of the hard tissue to the surface of an endosseous implant is only possible when the bone's hard components are kept unchanged (Saulacic et al. 2012, Freitas et al. 2016). For the preparation of undecalcified bone samples the tissue is dehydrated by an ascending alcohol series and then processed by a special 'cutting-grinding-system' developed in 1982 by Donath and Breuner (Donath/ Breuner 1982, Gotfredsen et al. 1989) and further developed by the EXAKT Company in 1983 for commercial use (Cano-Sánchez et al. 2005). In case of subsequent genetic analyses, a decalcification would decrease the amount of *deoxyribonucleic acid* (DNA) and *ribonucleic acid* (RNA) available for qPCR (Singh et al. 2013). There are only few studies that have used the combination of the LCM-technique with subsequent qPCR in bone so far (Kawamoto/ Kawamoto 2014, Pacheco et al. 2018, Marek et al. 2019, Wu et al. 2019). An analysis of undecalcified bone makes it difficult to extract osteocytes though, as they are buried within lamellar bone. This might impair the overall yield of RNA deriving from osteocytes (Pérez-Campo et al. 2016). In contrast, immunofluorescence labelling is only possible when the tissue gets decalcified prior to the staining process, as antigens need to be uncovered from the overlaying hard tissue and exposed to the antibodies for immunolabelling (Idleburg et al. 2021, Felsenthal/ Zelzer 2021).

1.5. Aims

Null hypotheses:

- 1. Implant migration is independent of the force magnitude applied and not driven by the expression of genes and proteins involved in peri-implant bone remodeling.
- 2. This peri-implant gene and protein expression is
    - a) neither related to the location-specific occurrence of compressive or tensile forces
    - b) nor the observation period in terms of wound healing.

Therefore, the goals of the present study were

- 1. to assess the impact of the ‘magnitude of applied force’ (Becker et al. 2019) on the local ‘loaddependent’ (Becker et al. 2021) peri-implant osteocytic gene and associated protein expression.
- 2. and to find out whether
    - a) a difference among the differently stressed areas, i.e. ‘areas of compression and tension’ (Becker et al. 2021), exists
    - b) as well as to investigate if gene and protein expression is associated with the early or late period of wound healing.

2. Material and Methods

2.1. Surgical Procedure

Two ‘customized’ (Becker et al. 2019) titanium mini-implants (Titanium grade V, diameter = 0.8 mm, length = 3.0 mm, *arithmetic average of the roughness profile* (Ra) = 0.8 µm) (Becker et al. 2019) [Fig. 6], ‘connected with a *nickel-titanium* [NiTi] contraction spring’ (Becker et al. 2021) (RISystems, Landquart, Switzerland) [Fig. 7], were inserted into the ‘caudal […] vertebrae’ (Becker et al. 2019) of n = 61 female Wistar rats (Becker et al. 2019, Becker et al. 2021).

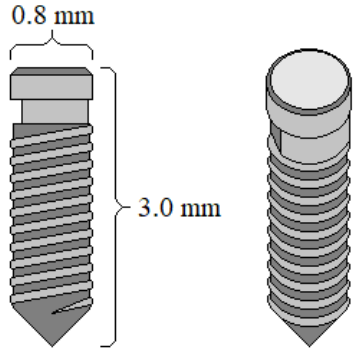

Fig. 6: **Mini-implant**
(modified after Becker et al. 2019)

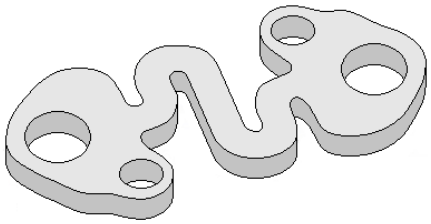

Fig. 7: **NiTi-spring**
(modified after Becker et al. 2019)

To elucidate the influence of mechanical forces on bone tissue, and to evaluate which inter- and intracellular factors ‘at a molecular and cellular level’ (Becker et al. 2021) constitute the basis of the process of implant migration, rat tail vertebrae were chosen for this study, as described earlier in literature (Wang et al. 2007, Webster et al. 2015, Renaud et al. 2016, Farkasdi et al. 2019).

Animal experiments can merely be considered as a model, which should approximate the issues in the target organism in as many criteria as possible, but will never achieve this completely: ‘The authors are aware that the animal model can affect the remodeling process and migrating level of implants’ (Becker et al 2021). Experiments on animals may therefore only be carried out under certain premises, that are historically anchored: in 1959, Russell and Burch established the concept of the 3Rs, which is based on 1) totally avoiding animal experiments if possible and replaceable by using alternative methods (Replace), 2) if nevertheless necessary, keeping the number of animals used for this purpose as low as possible (Reduce), as well as 3) limiting the suffering caused to the animals as low as

possible (Refine) (Russell/ Burch 1960). Today's Animal Protection Act also lists justifiable indications for the performance of animal experiments, such as the guarantee of detecting physiological states or function in humans or animals (Animal Protection Act 24.07.1972, Section 5, § 7a (1) b)), as well as testing for possible alternative methods to answer corresponding questions (Animal Protection Act 24.07.1972, Section 5, § 7a (2)). The present study has been 'approved by the appropriate local authority' *Landesamt für Natur, Umwelt und Verbraucherschutz Nordrhein-Westfalen* (LANUV) ('Ref. no. 84-02.04.2016.A380') (Becker et al. 2019, Becker et al. 2021), and all experimenters involved in the surgical implementation had the certificate of their expert knowledge in dealing with animal experiments according to the *Federation of European Laboratory Animal Science Associations* (FELASA).

An animal model was suitable for investigating the questions within this study, in particular because of the necessity of extracting (living) tissue for histological and molecular genetic examination. Extraction of human tissue would have been disproportionate, as it would not have been in conformity with the patients' further orthodontic therapy. Furthermore, the same samples used within this study were supposed to be used for longitudinal µCT examinations of the bone structure in our previous pilot study (Becker et al. 2019). Repeated sequential radiographic examinations in such a short time interval in humans would not have been justifiable. Furthermore, µCT investigations on living objects are reserved for small living beings due to space constraints, which is why only small animals such as mice, rats or rabbits would have been suitable for this experimental setup: the larger the experimental animals chosen for µCT research, the larger the *field of view* (FOV), which in return would have reduced the available magnification of the radiological images obtained. Because of their larger body size compared to rats or mice, rabbits were therefore not used for this experimental setup.

Due to anatomical features of these rodents, the use of rats has proven to be most beneficial – as previously performed by measurements on rat cadavers: this was due to the fact that rat vertebrae - in contrast to mice vertebrae - are longer. The larger extent between the proximal and distal end in rat vertebra was necessary for the present experimental setup, to achieve an appropriate distance of one mini-implant to the other in about 1 cm, in order to achieve a corresponding extension of the NiTi spring within its pseudoelastic interval (see below).

When selecting a suitable anatomical bone architecture to study peri-implant bone remodeling, several locations were taken into consideration:

1) Rat jaw: the selection of the rat jaw would have come closest to the anatomical localization used for mini-implants in humans. In contrast to human jaw bone, however, bone architecture of rat jaws 'contain[s] a huge amount of cortical bone tissue' (Becker et al. 2021), whereas cancellous bone is barely present (Fanghänel et al. 2006). This would have limited the comparability to peri-implant human bone remodeling.

2) Rat femur: rat femurs have been frequently used in the past for studies based on bone regeneration analysis (Harada et al. 2014). However, because bone architecture is always influenced by the action of mechanical forces (i.e. influence of inserting muscle fibers, which are particularly pronounced in the femur (Woittiez et al. 1985, Hamrick 2011)), rat femurs were not considered for the present questionings. Furthermore, rat femurs are strongly involved in hematopoiesis (Romaniuk et al. 2016), which could have additionally influenced the expression of genes meant to be analyzed within this study.

3. Rat tail vertebrae: 'The rat tail model has been sparsely mentioned in dental literature' (Becker et al. 2019). Tail vertebrae from rats have already found application in translational bone regeneration studies though – also with the aid of μCT studies (Renaud et al. 2016). With regard to the bone architecture of rat vertebrae, a homogeneous distribution of cancellous bone in the interior, a strong compacta at the surface, and a low level of hematopoiesis can be assumed (Blazsek et al. 1986, Becker et al. 2019). These anatomical conditions thus correspond most closely to those in the human jaw. In addition to their physiological properties, which are very close to human jawbone, their advantage also lies in the surgically easier access during the insertion of the mini-implants (Renaud et al. 2016).

2.1.1. Characteristics of NiTi-Alloys

NiTi alloys are frequently used in orthodontics because of their property of being 'superelastic'. Superelasticity is defined as specific materials' unique property (i.e. NiTi) to return to their initial shape after load relief. This mechanism is also termed pseudoelasticity or shape-memory (Auricchio/ Taylor 1996, Auricchio/ Lubliner 1997, Huang et al. 2003).

2.1.1.1. Austenite and Martensite

The reason for this pseudoelasticity is due to a so called thermoelastic martensitic phase change, firstly described by Adolf Martens: with a decrease in temperature, the *face centered cubic* (fcc) high temperature phase of a superelastic alloy, named austenite, converts into a *hexagonal close-packed* (hcp) crystal structure, named martensite [Fig. 8]. The transformation persists as long as the martensite is kept under a temperature below its transformation temperature. As soon as temperature passes a specific threshold, the martensite converts back to its former high temperature phase, austenite (Otsuka/ Wayman 1999, Yang et al. 2014).

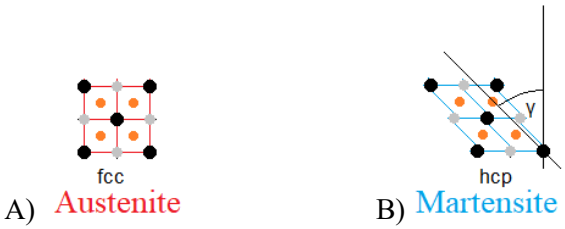

Fig. 8: **Changes in the crystal structure of a superelastic alloy.**
A) Austenite crystal structure. B) Martensite crystal structure (modified after Zhu et al. 2019).

2.1.1.2. Hysteresis and Pseudoelastical Interval

Phase transformations from austenite to martensite and back also take place within an interval of divergent extensions, as shown in Fig. 9: with an increasing extension, the austenite converts into a martensite; when extension decreases again, the martensite turns back into an austenite. These out- and backward transformations do not follow the same path though, but pass a hysteresis. Additionally, the strain-tension-curve is characterized by a plateau area between the martensitic and the austenitic state. Within this plateau, an immense extension can be performed without a notable change in strain. This strain plateau occurs in both directions, both during the straining process as well as the strain removal (Ortín/ Delaey 2002).

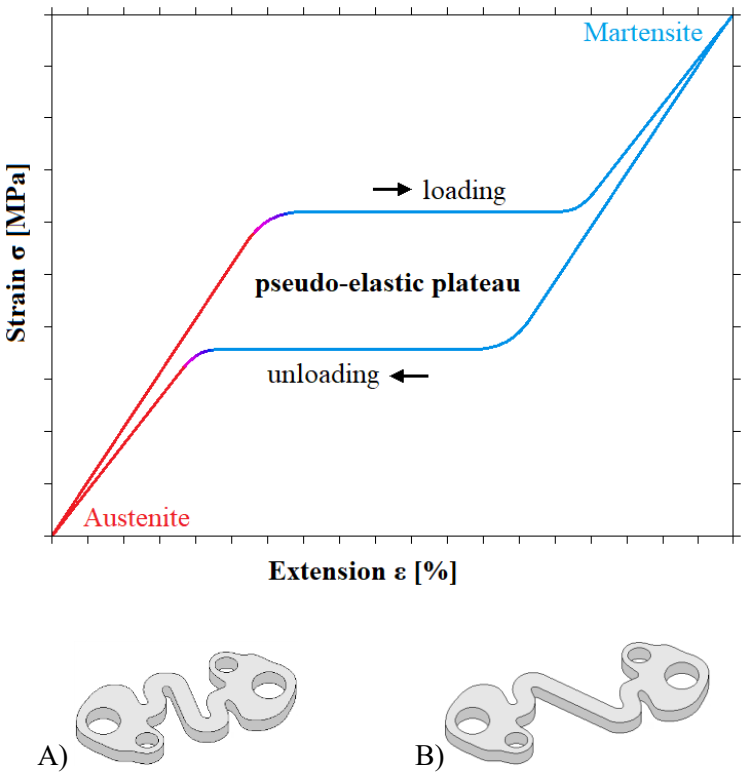

Fig 9: **Strain-tension-diagram of a NiTi-alloy (modified after Zhu et al. 2019). A) NiTi-spring without extension. B) NiTi-spring with extension.**

Since strain is expressed in the unit pressure p [Pascal = Pa], and is equivalent to the quotient of force F [Newton = N] per area A [mm^2], the acting strain is proportional to the acting force F [Formula (*1*].

$$(1) \qquad p = \frac{F}{A}, \qquad p \sim F$$

The 'optimal distance of [two] mini-implants' (Becker et al. 2019) within one vertebra therefore depended on the force that was intended to be applied for each group, which, because of their 'super-elastic range' (Becker et al. 2019), was dependent on the extension of the NiTi-springs in return [Fig. 10]: to determine the range in which the springs display superelastic behavior, i.e. nearly constant forces, each of them was subjected to a force/ tension analysis (Stäubli RX 60, Stäubli Tec-Systems, Kaiserslautern, Germany) (Becker et al. 2019). Since the tension of the spring was limited to the length of each vertebral body (1 cm in average), the force was adjusted by using springs of ascending thickness ('0.15 mm, 0.2 mm, and 0.25 mm' (Becker et al. 2019)) [Fig.11].

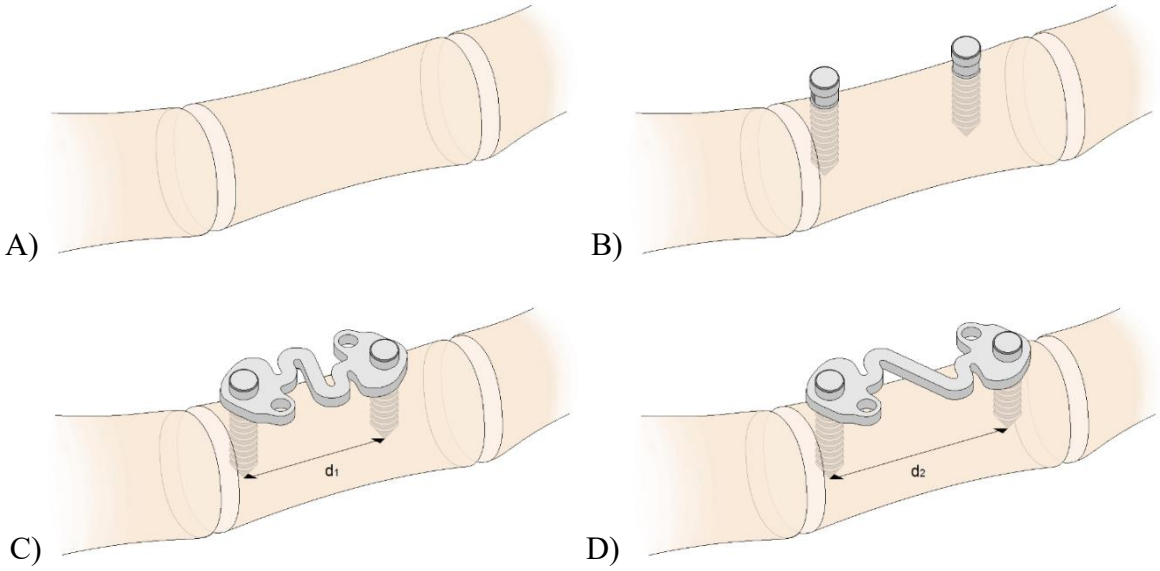

Fig. 10: **Two mini-implants inserted into a caudal proximal vertebra**
A) Exposed vertebrae. B) Insertion of two mini-implants in a definite distance to one another.
C) With force. D) Without force.

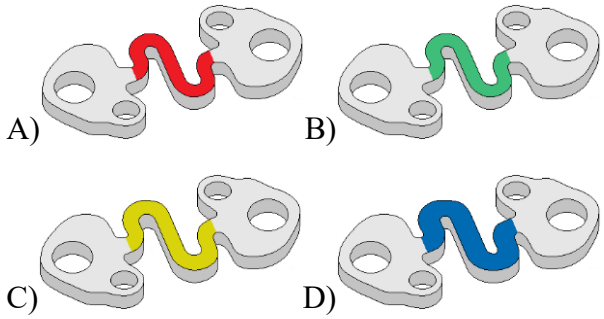

Fig.11: **NiTi-springs with different thicknesses.**
A) Width 200 µm, extension 0 mm, used in control group.
B) Width 200 µm, initial tension 1.5 mm, used in the 0.5 N group.
C) Width 250 µm, initial tension 1.5 mm, used in the 1.0 N group.
D) Width 300 µm, initial tension 1.5 mm, used in the 1.5 N group.

Animals were divided into three test groups - depending on the chosen spring and the concomitant force applied (0.5 N, 1.0 N, 1.5 N) – as well as one ‘control group’ (Becker et al. 2021) (with ‘no loading’ (Becker et al. 2019), 0 N). In the control group, the spring was only placed in a passive mode. Out of 26 animals available for this study, n = 13 animals were supposed to be sacrificed after ‘2 weeks’ (Becker et al. 2019, Becker et al. 2021), the other n = 13 animals after ‘8 weeks’ (Becker et al. 2019, Becker et al. 2021) with an overdose of intraperitoneal narcotic (300 mg/ kg pentobarbitale (Release®)). After scarification, samples were retrieved for further processing: half of the samples was analyzed using

immunofluorescence, the other samples were taken for gene expression analysis [Fig. 12] (Becker et al. 2021).

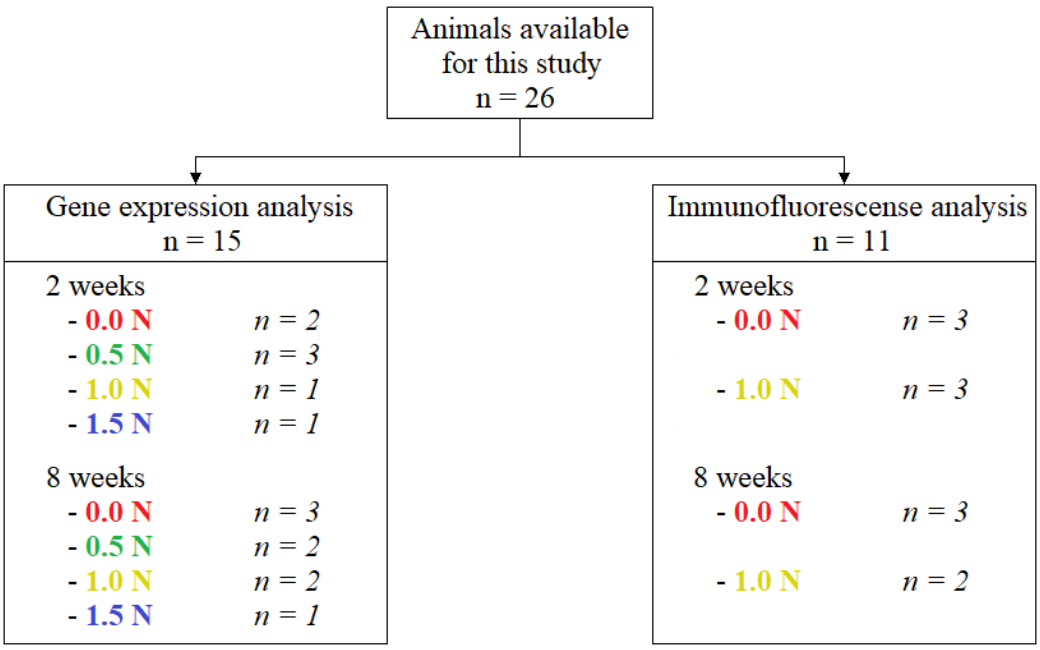

Fig. 12: **Overview of the different groups for the analysis in gene and protein expression (modified after Becker et al. 2021)**

2.2. Analysis of Gene Expression

For the samples chosen for gene expression analysis, the mini-implants and the spring were removed after biopsy harvesting [Fig. 13].

A) B)

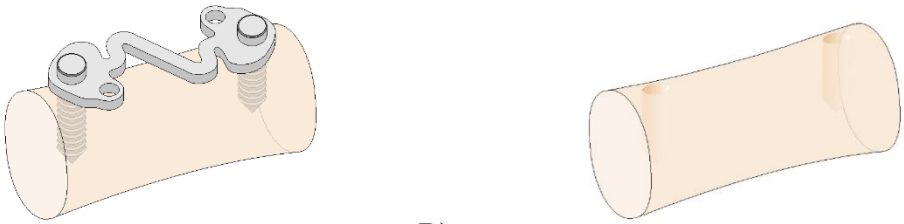

Fig. 13: **(A – B) Removal of mini screws and NiTi-spring**

After removal, the samples were frozen using dried ice and embedded in 'an *optimal cutting temperature*' (O.C.T.) medium (NEG-50™ Frozen Section Medium, Thermo Fisher Scientific, Waltham, Massachusetts, USA) (Becker et al. 2021). The fact these samples were not decalcified prior to embedding (in order to ease their subsequent sectioning) becomes

even more evident, as samples predicted to be analyzed by qPCR would lose their amount of DNA and RNA due to the decalcification process (Singh et al. 2013).

Until further procession, samples were stored in a freezer at '– 80 °C' (Becker et al. 2021). For the subsequent 'three-dimensional orientation' of the sample (anterior to posterior, left to right, bottom to top), a piece of absorbable suture (Vicryl®, Ethicon, Noderstedt, Germany) was additionally placed within the freezing container next to the right anterior top of the sample (Becker et al. 2021).

For µCT analyses of those samples, a special custom-made sample holder was constructed of polystyrene (and *polymethylmethacrylate* (PMMA)), that was able to store the samples under low temperatures during the scan process [Fig. 14].

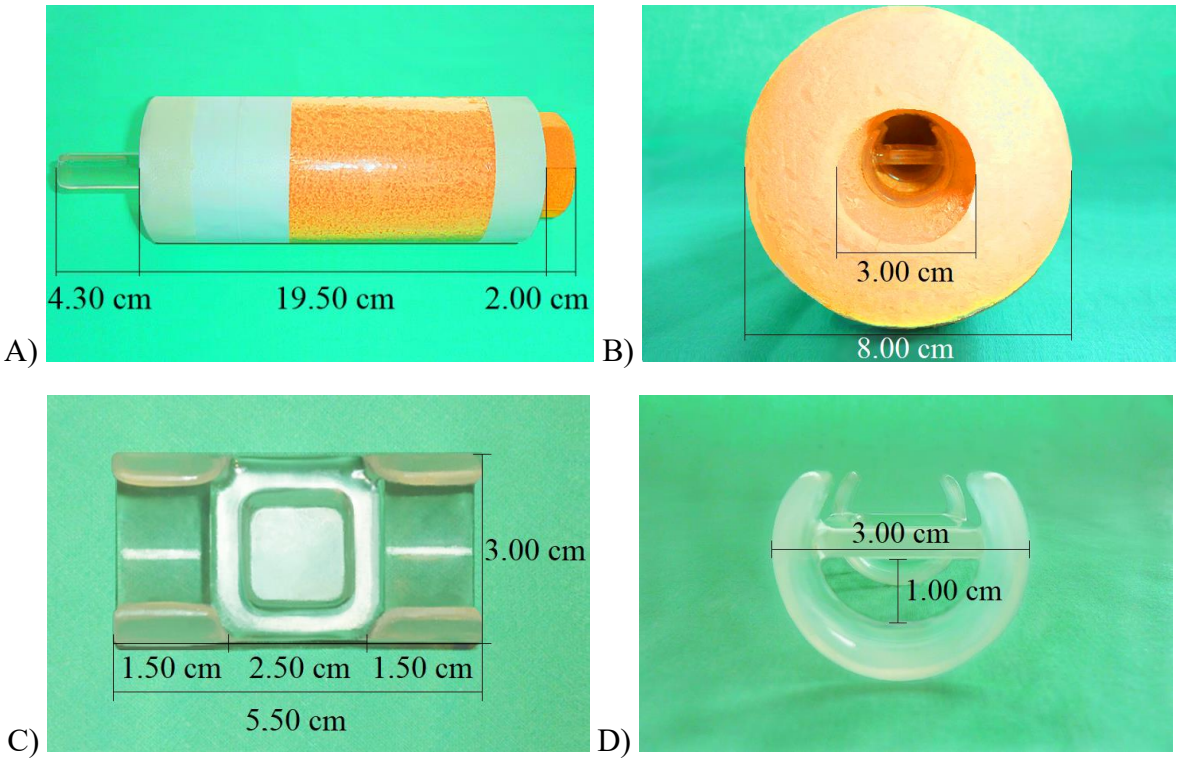

Fig. 14: **Sample holder for scanning under low temperature with dried ice.**
A) Outer insulation layer (polystyrene). B) Inner sample holder for specimen placement (PMMA).

2.2.1. Cryosectionings using a Cryofilm according to Kawamoto

The frozen samples were cryosectioned at a thickness of 3 µm 'orthogonally to the longitudinal axis of the implants' using a cryostat (Leica CM 3050 S, Leica AG, Wetzlar, Germany) and special 'blades for undecalcified tissues' (MX35 PREMMIER Microtome, Thermo Fisher Scientific, Waltham, Massachusetts, USA) (Becker et al. 2021). With a

chamber temperature of -25 °C and an object temperature of – 35 °C, the block was trimmed until the area of interest appeared on the cutting front.

In order to preserve the bone samples' shape, a cryofilm according to Kawamoto was placed 'onto the samples' longitudinal surface' (Becker et al. 2021) [Fig. 15, Fig. 16] (Kawamoto/ Kawamoto 2014). The film remained on top of the slide and both the film and the slide were then transferred to a sample slide. The sample slides themselves (Starfrost, Waldemar Knittel Glasbearbeitungs GmbH, Braunschweig, Germany) were previously self-prepared: a hole (1 x 0.5 cm) was cut into the center of each sample slide. At its sticky ends, the cryofilm was adhered onto the slide.

A) 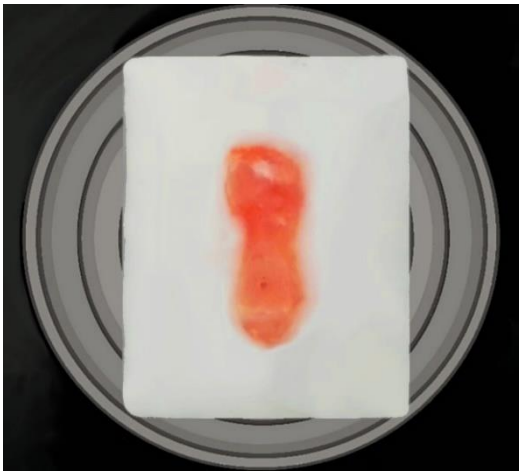 B) 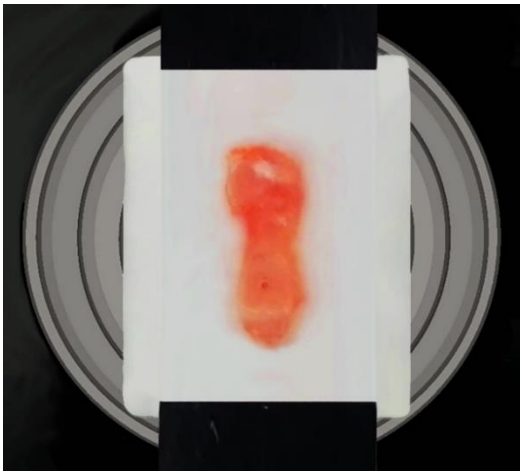

Fig. 15: **Fixation of the Kawamoto-film on top of the cryo samples within the cryostat. A) Sample without adhered cryofilm. B) Sample with adhered cryofilm)**

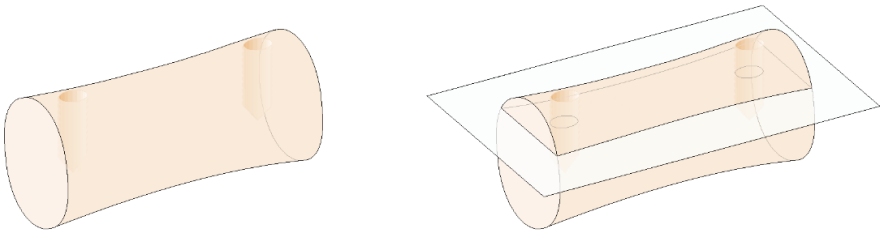

A) B)

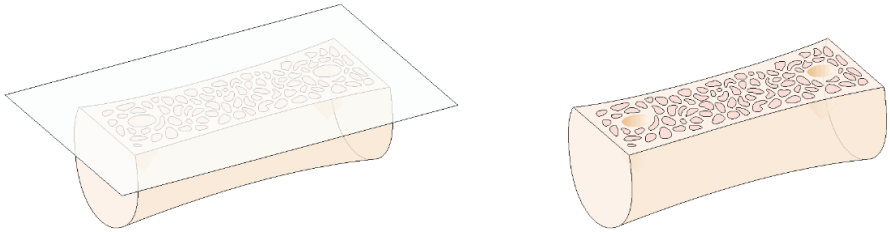

C) D)

Fig. 16: **(A – D) Orientation of the plain in samples for LCM-microscopy**

The cryosectioning method according to Kawamoto prevents the degradation of *messenger ribonucleic acid* (mRNA), as thawing processes are avoided through the usage of his adhesive film, which the author calls freeze-drying. This freeze-drying 'significantly inhibits the decomposition of mRNA' through endonucleases (Kawamoto/ Kawamoto 2014).

2.2.2. Cresyl Violet Stainings

For the staining procedure, the O.C.T. was removed by dipping each slide five to six minutes into ice-cold RNA-free water. After a fixation in 70 % ethanol for two minutes, slides were dipped into a custom made 1 % cresyl violet acetate solution for 30 sec. Excess stain was removed using absorbent surfaces. Subsequently, slides were dipped into an ascending alcohol series starting at 70 % and finally 100 %. In the end, the slides were air-dried on glass slides (Starfrost, Engelbrecht - Medizin und Labortechnik GmbH, Edermünde, Germany) for one to two minutes and stored at -80 °C for further processing [Fig. 17] (Becker et al. 2021).

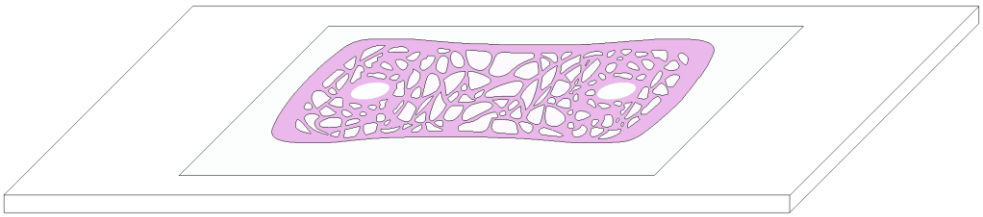

Fig. 17: **Undecalcified cresyl violet stained specimen (adhered to the cryofilm (light blue)) on glass slide for LCM-microscopy, scheme**

2.2.3. LCM Microscopy

Cryosectioned slices were examined using an LCM-microscope (PALM MicroBeam®, Zeiss, Oberkochen, Germany) [Fig. 18], where 'single osteocytes' within a mask of '100 µm from each implant site' (Becker et al. 2021) [Fig. 20] were laser cut using the following laser parameters: Cut energy 50 %, *laser pressure catapulting* (LPC) energy 10 %, Focus 64 %, Delta 0 % [Fig. 19] and the software's specific function 'Close & Cut + AutoLPC'. A free-hand drawn open figure was closed automatically and the tissue within this area cut and catapulted into 'adhesive caps' (AdhesiveCap Touch 500 opaque, Zeiss, Oberkochen, Germany) (Becker et al. 2021) [Fig. 21].

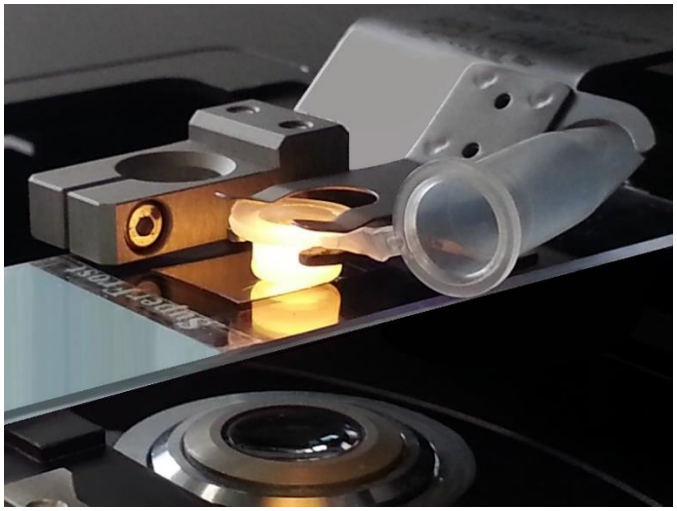

Fig. 18: **Adhesive cap mounted on top of the slide within the LCM-microscope**

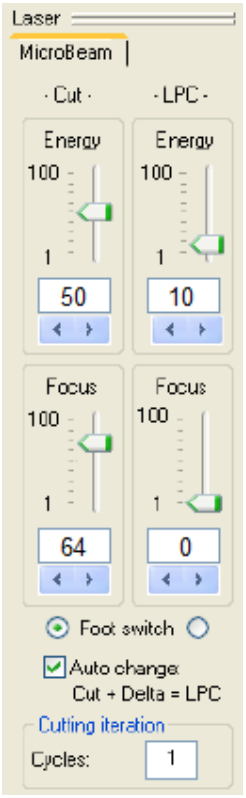

Fig. 19: **Specific laser parameters used in LCM microscopy**

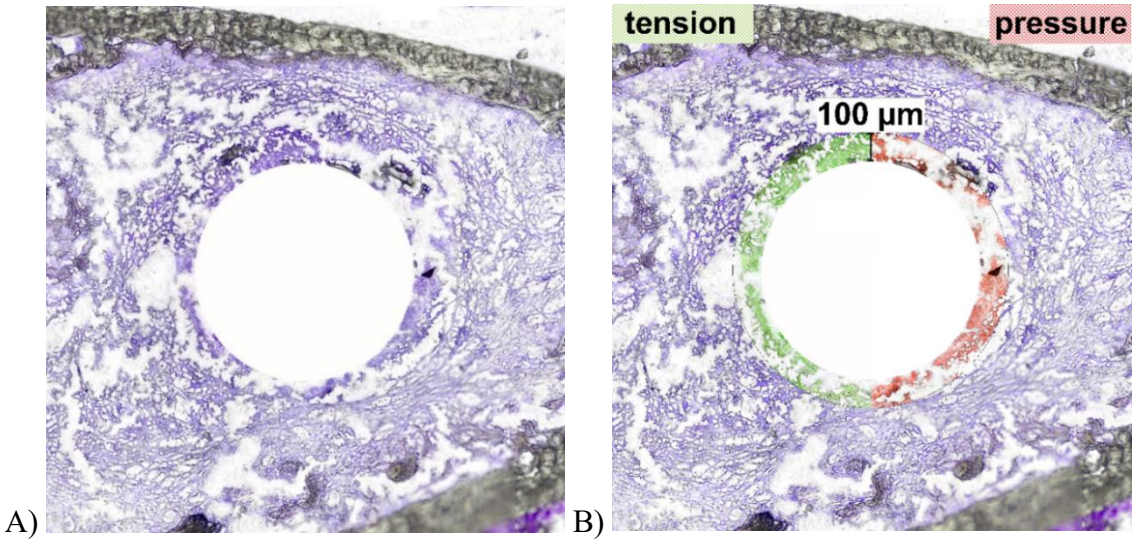

Fig. 20: **A) Cutout of peri-implant bone tissue B) divided into tension (green) and pressure (red) areas with a distance of 100 µm to the former implant localization (modified after Becker et al. 2021)**

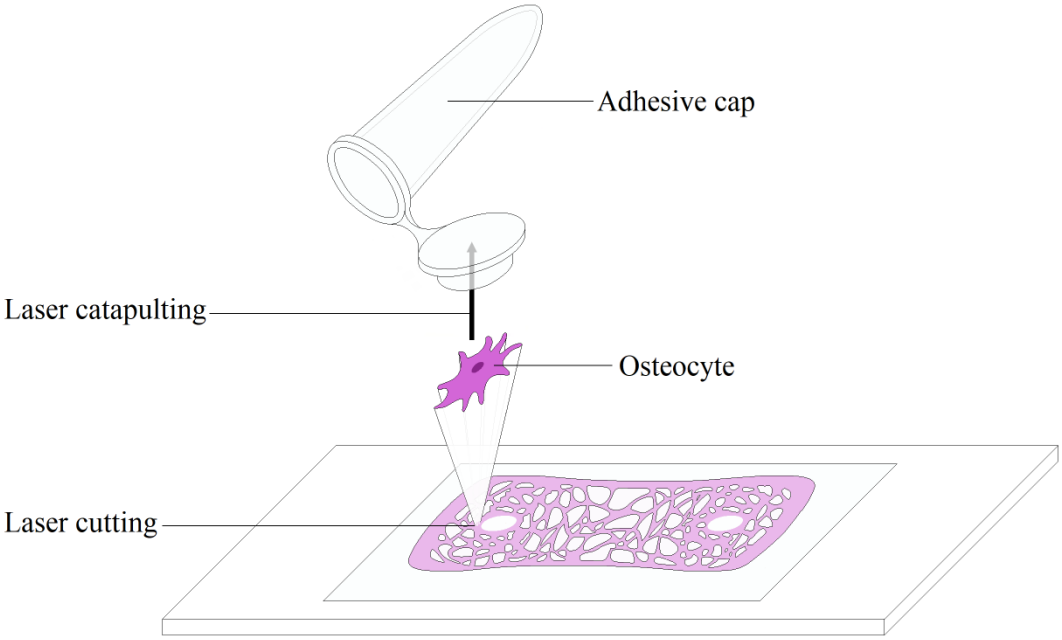

Fig. 21: **Principle of LCM-microscopy**

2.2.4. Real-Time-PCR

mRNA was extracted from the still living cells and then transformed into '*complementary DNA*' (cDNA) using a reverse DNA-transcriptase derived from the 'QuantiTect Reverse transcription kit' (Qiagen, Hilden, Germany) and a subsequent qPCR program (Applied Biosystems StepOneTM Real-Time PCR Systems). 'SYBR green reagents' (KAPA SYBR® FAST qPCR Kit master mix ABI Prism®, KAPA Biosystems, Cape Town, South Africa)

and the following primer sequences as well as *Histone H1.0* (H1.0) 'as a housekeeping gene' [Table 1] were used for the amplification (Becker et al. 2021):

Gene symbol	**Forward primer** (5' → 3')	**Reverse primer** (5' → 3')	**Product length** (bp)	**Encoding protein**
H1-0	CCAAGAGAAGGAAGAACCGCA	GTAGATGCGCGCCAGAGAC	113	Histone H1.0
RUNX2	ACAAATCCTCCCCAAGTGGC	GGATGAGGAATGCGCCCTAA	152	Runx2
SP7	TTTCTGCGGCAAGAGGTTCA	TTGCTCAAGTGGTCGCTTCT	126	Osterix
SOST	AGTCGAGTTCAAGTGGGCTG	TGTTCCATAGCCTCCTCCGA	156	Sclerostin
CTSK	TACCCATATGTGGGCCAGGA	TTCAGGGCTTTCTCGTTCCC	107	Cathepsin K

Table 1: **List of used primers (see also Becker et al. 2021)**

PCR cycles were performed using the following parameters: 15 min. at 42 °C, 1 min at 95 °C then at 4 °C. According to Vandesomple et al., the 'relative expression levels of Runx2, SP7, SOST and CTSK were calculated' (Becker et al. 2021) based on the *cycle threshold* (Ct) values of the housekeeping genes (Vandesompele et al. 2002).

2.3. Immunofluorescence Analysis

Another sixteen samples were meant to be further analyzed using immunofluorescence in order to explore the expression of certain proteins. After euthanasia, the mini-implants were removed and samples fixed in formalin 4 % (LaboChem, neoLab Migge GmbH, Heidelberg, Germany). For decalcification of the bone tissue, a 'custom-made solution of [34 g] Tris(hydroxymethyl)aminomethane' (Merck KGaA, Darmstadt, Germany) dissolved in 11 Aqua dest. and added by 100 g Ethylenenitrinoltetraacetic disodium-dihydrate (Tritriplex® III, Merck KGaA, Darmstadt, Germany) was prepared (Becker et al. 2021). The samples were stored within this solution for three weeks, and the solution was 'changed once a week' (Becker et al. 2021). Subsequently to the decalcification, each sample was cut 'along its longitudinal axis' with an exposure of one half of each former implant position [Fig. 22] and 'embedded in paraffin' (Becker et al. 2021). At a thickness of 3 µm, specimens were cut using a microtome (Leica CM3050 S, Leica Mikrosysteme Vertrieb GmbH, Wetzlar, Germany) and 'special blades' (MX35 Premier). Sections were placed onto glass slides (TOMO® Adhesion Microscope Slides, Matsunami Glass USA Inc., Bellingham, Washington, USA) [Fig. 23] (Becker et al. 2021).

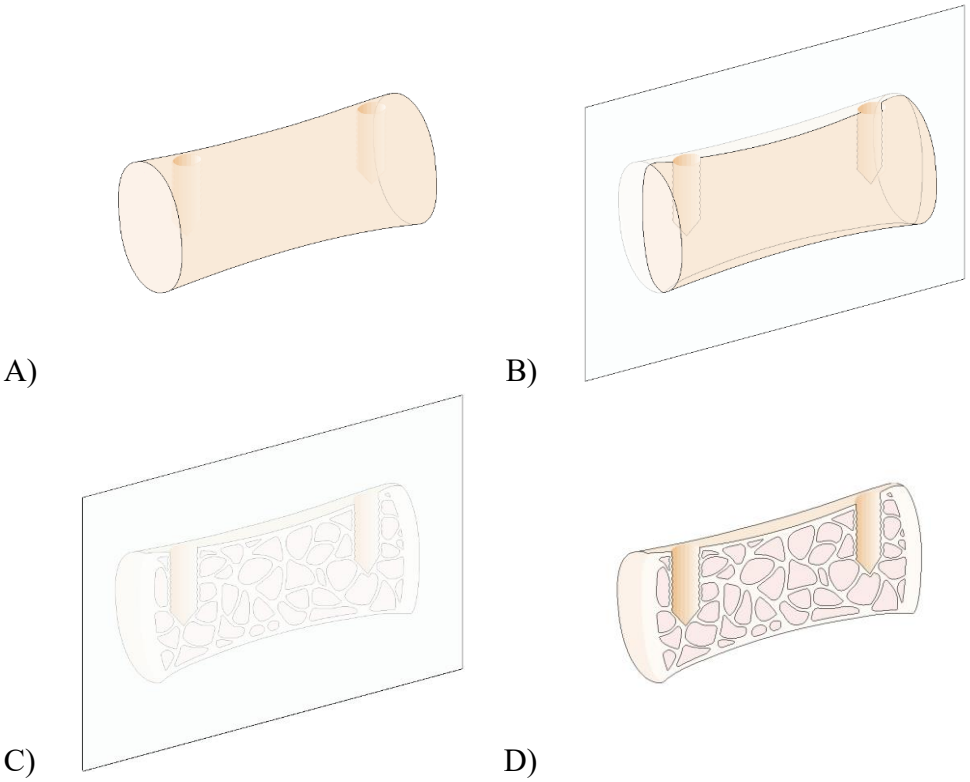

Fig. 22: **(A – D) Orientation of the plain in samples for immunofluorescence staining**

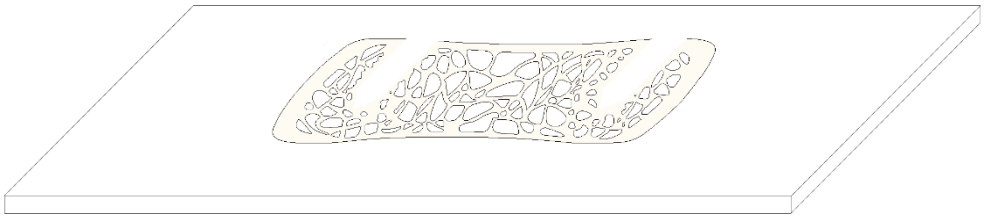

Fig. 23: **Paraffin specimen on glass slide for immunofluorescence staining, scheme**

2.3.1. Immunofluorescence Staining

For immunofluorescence staining, the manufacturer's protocol was slightly modified according to the preparation of the buffers used [Table 2].

Mixtures for immunofluorescence staining	
1.Alcohol mixture for dewaxing	
Ethanol	100 %
Methanol	100 %
Isopropanol	100 %
Liquids are mixed in a relation 18:1:1 and stirred well Two thirds of the solution are taken away to dilute each one third to a mixture of 95 % and 80 %	
2.Washing buffer (1 x PBS)	
NaCl	8 g

KCl	0,2 g	
Na_2HPO_4	1,44 g	
KH_2PO_4	0,24 g	
Destilled water	800 ml	
Adjustment of the pH-value of the compound to pH 7,2 with 1 N HCl		
Completion of the volume to 1 l using H_2O		
3.Blocking buffer (diluted 1:100 in PBS)		
Serum of the host species (in this case: goat) of the secondary antibody	5 %	70 µl
BSA (stabilizer)	1 %	14 µl (7 µl of a 2 % solution)
Triton X-100 (penetration enhancer)	0,1 %	14 µl
Tween 20 (detergent and surface tension reducer)	0,05 %	0.7 µl
Dilution in 1 x PBS		1242 µl

Table 2: **Mixtures for Immunofluorescence Staining**

0.5 µg of the primary *immunoglobuline G* (IgG) 'antibodies for osteocalcin' (Human/ Rat Osteocalcin Antibody, Monoclonal Mouse IgG, R&D Systems Inc., Minneapolis, Minnesota, USA) were diluted in 1 x *phosphate-buffered saline* (PBS) (Becker et al. 2021). This dilution was further diluted up to a concentration of 0.01 µg/ µl in the blocking buffer. The primary antibody for cathepsin K (Anti-Cathepsin K, Polyclonal Rabbit IgG, Abgent Inc., California, USA) was diluted 1:1000 in the blocking buffer according to the manufacturer's instructions [Fig. 24] (Becker et al. 2021).

The 'secondary antibodies' (Goat anti-Mouse for osteocalcin, Alexa Fluor® Plus 488, Thermo Fisher Scientific Inc., Waltham, Massachusetts, USA), (Goat anti-Rabbit for cathepsin K, Alexa Fluor® Plus 568, Thermo Fisher Scientific Inc., Waltham, Massachusetts, USA) were diluted 1:500 in the blocking buffer according to the manufacturer's instructions (Becker et al. 2021). Additionally, specimens were stained with *4′,6-Diamidin-2-phenylindol* (DAPI) 2 µl each to show nuclei (Becker et al. 2021).

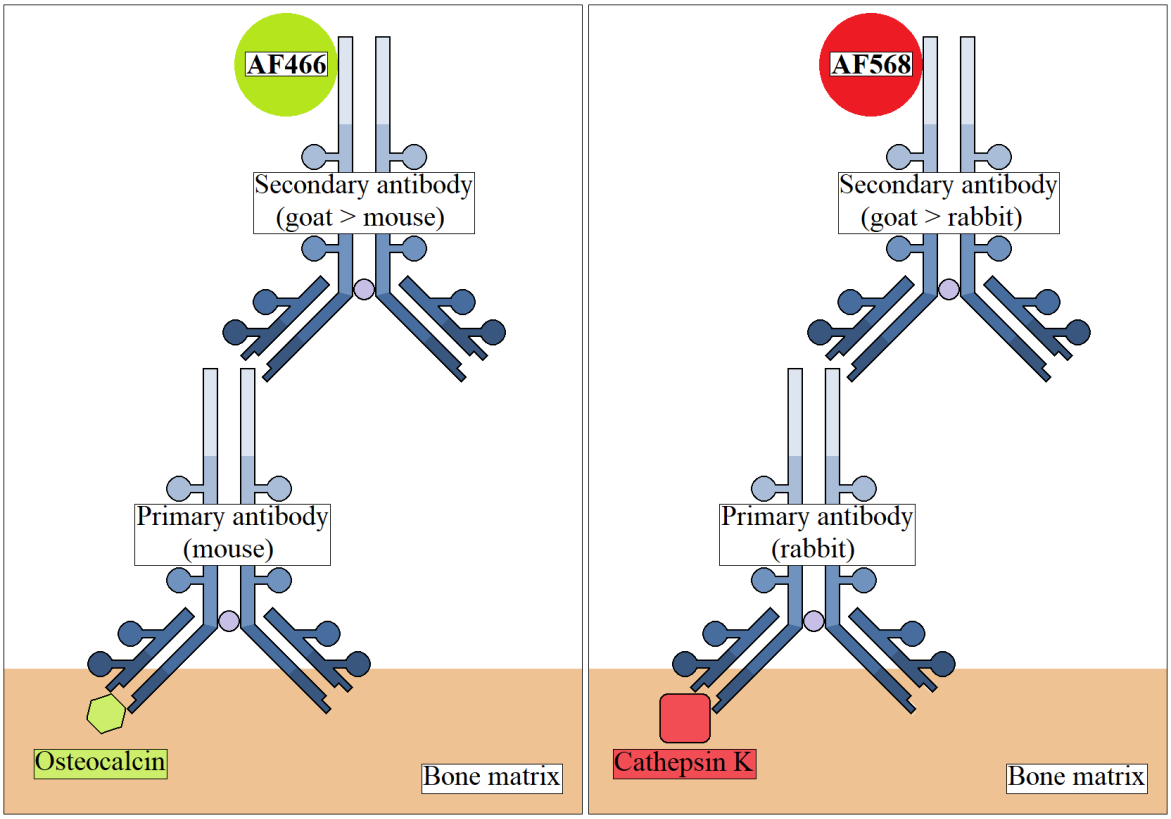

Fig. 24: **Binding cluster of primary and secondary antibodies in tissue.**
Left: antibodies binding to osteocalcin, right: antibodies binding to cathepsin K.

To remove the paraffin from the samples, slides were dewaxed in a solution of 250 ml Roti-Histol (Carl Roth GmbH + Co. KG, Karlsruhe, Germany) ‘for 10 minutes twice’, and subsequently within a ‘descending alcohol series’ starting at 100 % for two minutes twice, then in 95 % and 80 % each for two minutes twice, and finally in ‘distilled water’ again for two minutes twice. 200 µl of the blocking buffer were poured onto each sample slide. The slides were subsequently incubated ‘at 37 °C for 1 hour’. After pouring the primary antibody onto the slides, with a subsequent incubation for again one hour at 37 °C, slides were rinsed ‘in 1 x PBS for five minutes twice’. The same rinsing procedure was performed after the pouring of the secondary antibody and an incubation for 30 min at 37 °C. Finally, cover slips were mounted onto the sample front using ‘a mounting medium’ Fluoromount-G® (Fluoromount-G®, Southern Biotech Inc., Birmingham, Alabama, USA) (Becker et al. 2021).

2.3.2. Evaluation of the Immunofluorescence Samples

With a ‘fluorescence microscope (Operetta CLS™ high-content analysis system, PerkinElmer Inc., Waltham, Massachusetts, USA)’, single images of a magnification of 5x [Fig. 25, Fig. 26] and 40x were obtained (Becker et al. 2021). In addition to the three color channels (blue, green and red), single greyscale images for separate signals in the reflection of a wavelength of 488 nm (green, for osteocalcin), of 568 nm (red, for cathepsin K) and 358 nm (blue, for DAPI) were recorded.

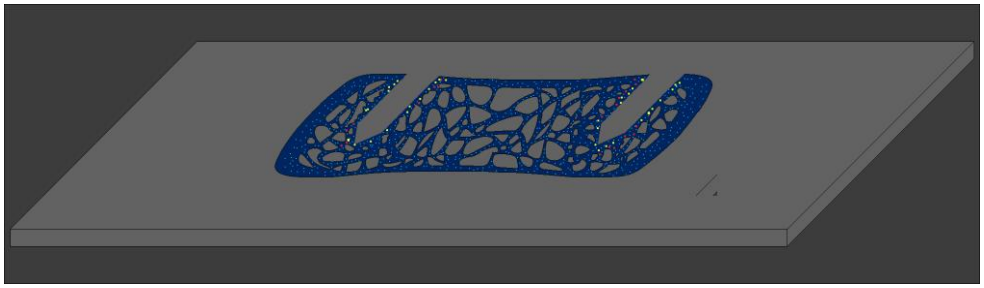

Fig. 25: **Immunofluorescent stained specimen on glass slide, scheme**

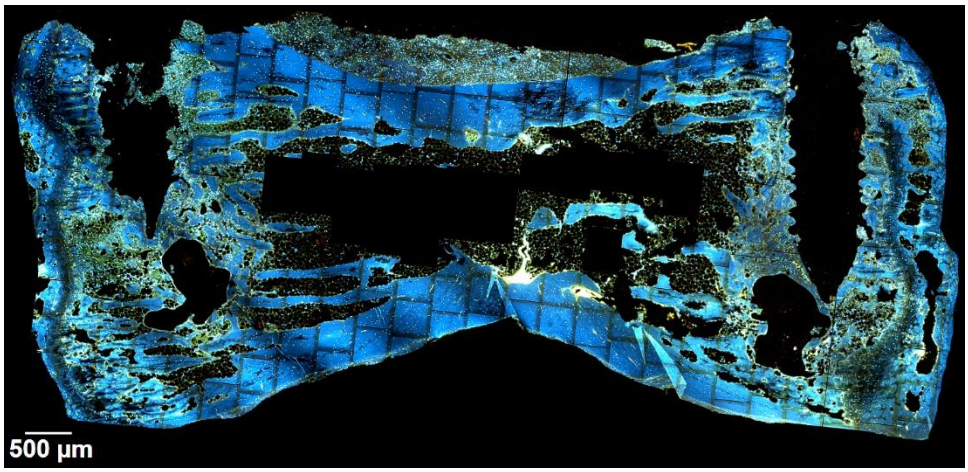

Fig. 26: **Analysis of immunofluorescence stained specimens, slide (magnification 5x)**

The greyscale images at a magnification of 40 were then stitched together to form a large new image using the plugin function of ‘Grid/Collection stitching’ in ‘ImageJ (FIJI distribution)’ (Preibisch et al. 2009) (Becker et al. 2021). This was done for each channel, so that three new greyscale images were generated. For each implant, a mask of 500 µm around the former implant position was generated using the FIJI tool ‘Make Band’. These ‘regions of interest (ROI)’ were subdivided into four single images according to the localization around the former implant position: ‘lateral top’, ‘lateral bottom’, ‘medial top’

and ‘medial bottom’. The areas ‘lateral top’ and ‘medial bottom’ were summarized to regions where mechanical tension was expected, while the compartments ‘medial top’ and ‘lateral bottom’ were grouped to regions that were supposedly exposed to mechanical pressure (Becker et al. 2021). In order to quantify the ‘number of nuclei’ and ‘the amount of osteocalcin and cathepsin K’ (Becker et al. 2021), each greyscale image was uploaded into a special ‘open-source’ (Becker et al. 2021) software, called CellProfiler (Carpenter et al. 2006), which is – depending on the resolution and on whether the immunofluorescence signal is large enough to be displayed in at least one pixel - capable of counting the total number and the area covered by each nucleus, osteocalcin, and cathepsin K. ‘For each signal, the quotient of the *occupied area per tissue area’* (OA/TA) was extracted (Becker et al. 2021).

2.4. Statistical Analysis

The ‘open-source software Program R’ (R Core Team, 2018) (Becker et al. 2021) was used for the statistical analysis. The mean value as well as the standard deviation, the median, the quartiles and minimum and maximum values were calculated for each variable and group. ‘The R package lme4 [Bates, Maechler, Bolker, & Walker, 2015, Becker et al. 2021] was used to perform a linear mixed effects analysis of the relationship between the outcome variable, applied force, and localization (‘tension’/’pressure’ zone)’ (Becker et al. 2021). As fixed effects, the applied force was entered (0 N, 0.5 N, 1.0 N, and 1.5 N) as well as the localization. As random effects, animals were considered (Becker et al. 2021).

3. Results

Visual inspection of the residual plots did not reveal any obvious deviations from homoscedasticity or normality. p-values were obtained by likelihood ratio tests of the full model with the effect in question against the model without the effect in question. The results were found significant at $p < 0.05$ (Becker et al. 2021).

3.1. Force-Tension-Diagrams

The force/ tension analyses performed for each NiTi-spring generated the following tension-force-diagrams, with the tension ε [mm] on the x-axis, the resulting force F [N] on the y-axis, and a pseudo-elastical interval between 1 – 2.5 mm [Fig. 27].

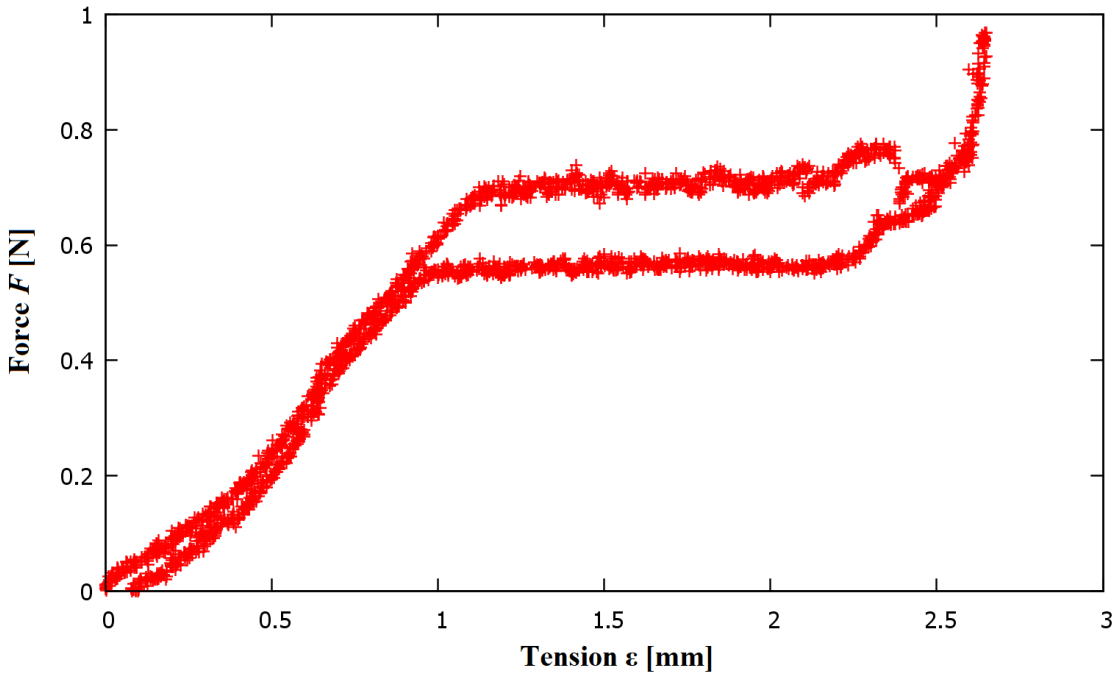

Fig. 27: **Force-tension-diagram of a NiTi-spring generated by a robotor (Stäubli RX 60) (modified after Becker et al. 2019)**

3.2. Gene expression analysis

Gene expression analysis focused on genes responsible for bone formation (Runx2 and SP7) and bone resorption (SOST and CTSK), at two and eight weeks after implant insertion and loading. Statistical analyses failed to reveal significant differences among the two groups (Becker et al. 2021). Nonetheless, genes were in general more expressed in the early healing phase.

3.2.1. Runx2

Although peri-implant stimulus (pressure or tension) and applied force did not have a significant impact on the expression of Runx2, neither after 2 nor after 8 weeks, a higher expression in regions of tension (lateral implant neck) was detected under the application of 1.5 N. The opposite finding was made for 0.5 N and 1.0 N, i.e. expression was more pronounced in the pressure zones [Fig. 28] (Becker et al. 2021).

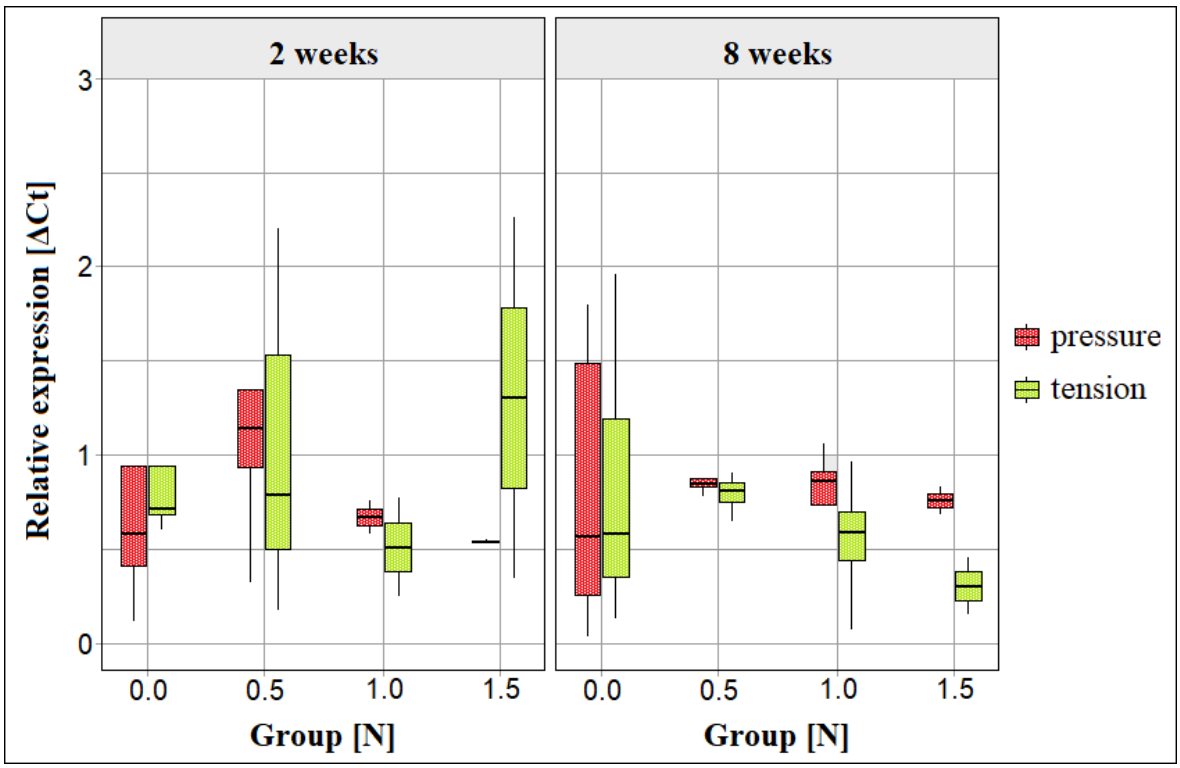

Fig. 28: **Peri-implant gene expression of Runx2 (modified after Becker et al. 2021)**

3.2.2. SP7/ Osterix

Like for Runx2, stimuli and force magnitude did not significantly influence gene expression of SP7 at week two and week eight. Generally, expression tended to be higher within regions exposed to tension ‘at 2 weeks’, whereas ‘at 8 weeks of loading, the opposite trend was observed’, as they were by trend higher in the pressure zones. A loading magnitude of 0.5 N led to ‘the highest’ gene expression observed at both time points [Fig. 29] (Becker et al. 2021).

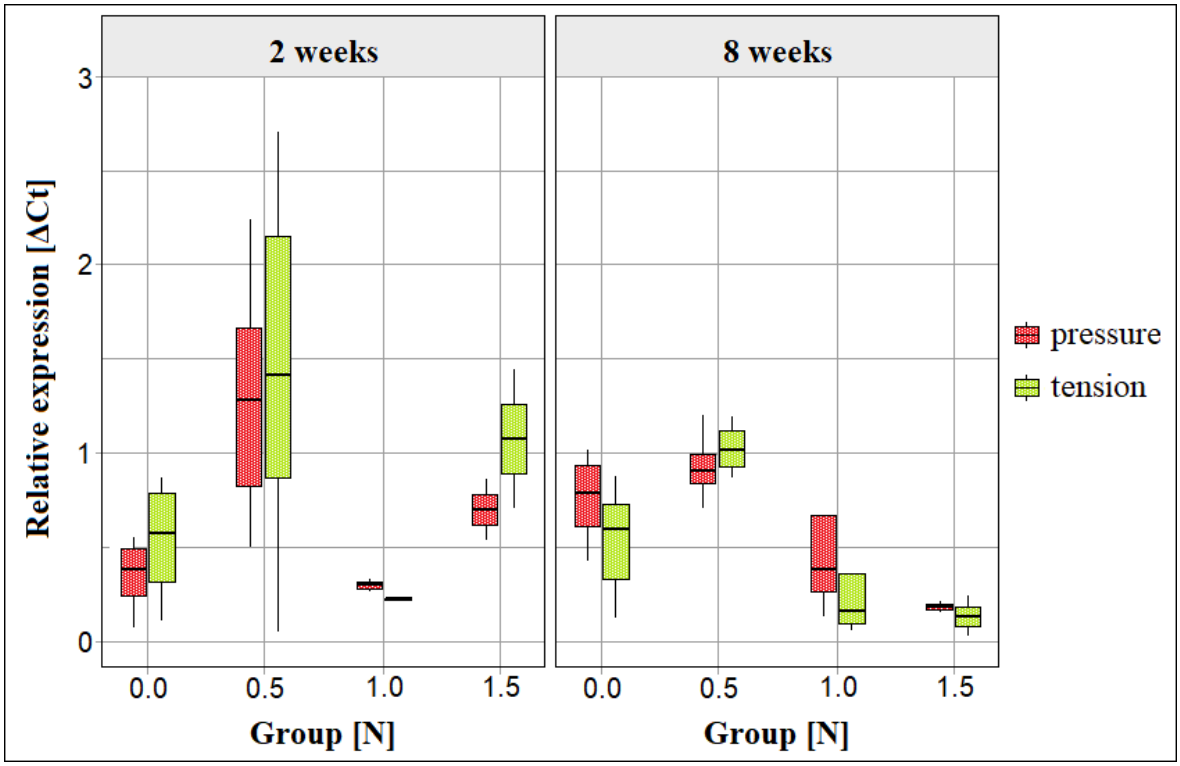

Fig. 29: **Peri-implant gene expression of SP7/ osterix (modified after Becker et al. 2021)**

3.2.3. SOST/ Sclerostin

According to the gene expression mentioned above, force and peri-implant localization did not have a significant impact on the expression. In opposite to Runx2 and SP7, SOST expression tended to be higher in regions of pressure in the test groups. The expression patterns were inverted under 0.5 N at 2 weeks and at 1.5 N at eight weeks, where expression was higher at tensions sites [Fig. 30] (Becker et al. 2021).

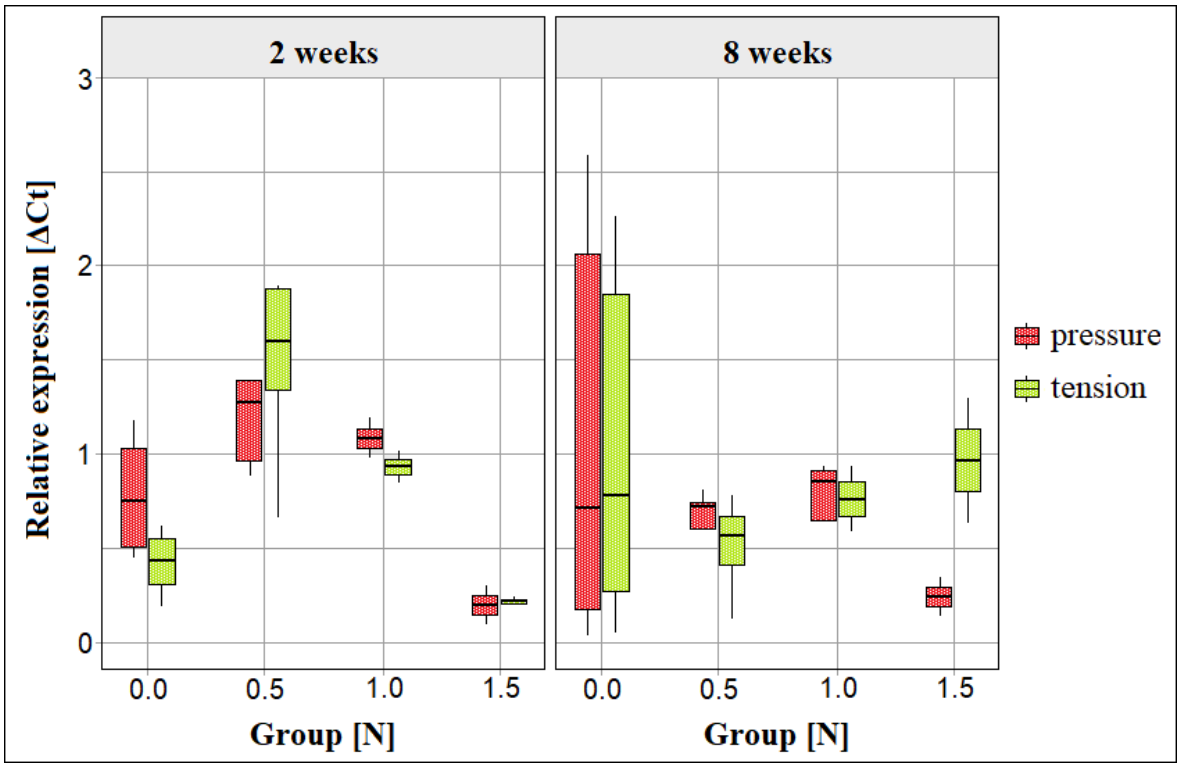

Fig. 30: **Peri-implant gene expression of SOST/ sclerostin (modified after Becker et al. 2021)**

3.2.4. CTSK

In accordance with the other genes, localization and force amplitude did not significantly affect the gene expression of CTSK. Its expression trended to be higher in regions of mechanical pressure, ‘except in the 1.5 N group at 2 weeks’ [Fig. 31] (Becker et al. 2021).

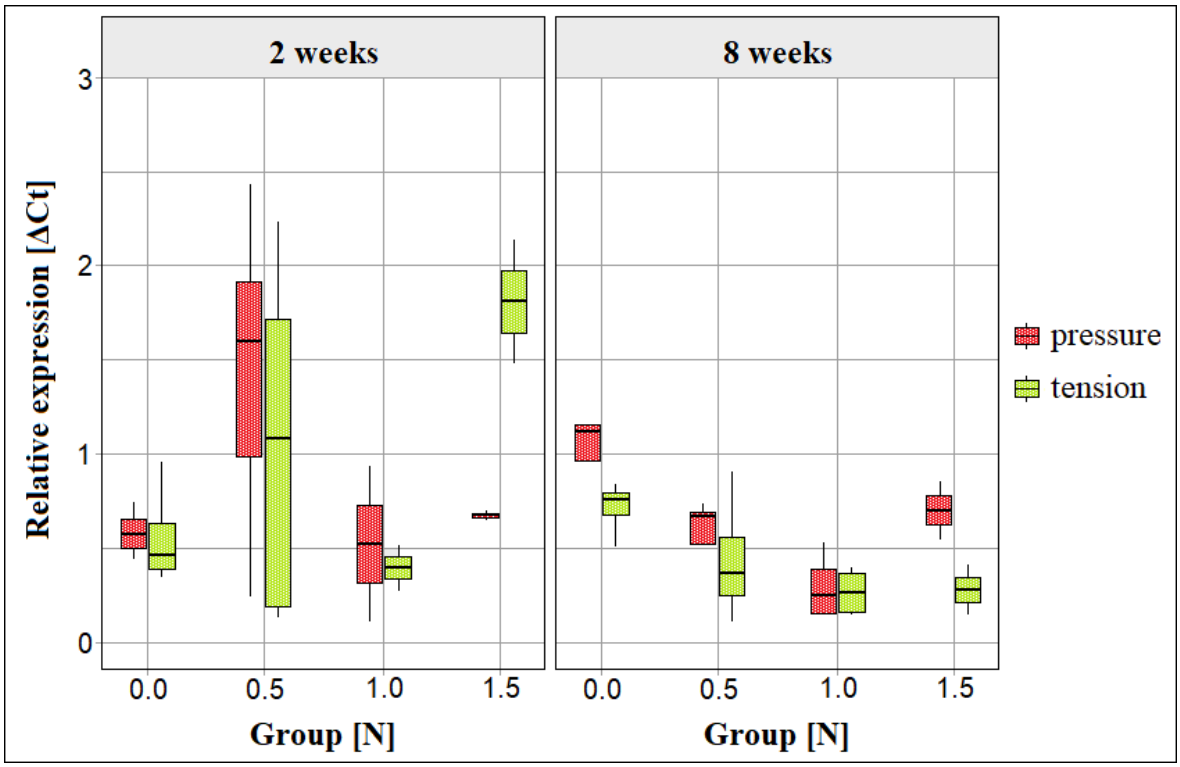

Fig. 31: **Peri-implant gene expression of CTSK (modified after Becker et al. 2021)**

3.3. Immunofluorescence analysis

Within the limits of the study, osteocalcin and cathepsin K 'were highly expressed in the early phase of healing, while their levels were dramatically reduced after 8 weeks', as they exhibited highest expressions under a force of 1.0 N after 2 weeks (as immunofluorescence samples applied to a force of 0.5 N were not evaluated owing to the very low sample size) (Becker et al. 2021). Osteocalcin has shown to be expressed 'to a higher extend in the 'tension'' than in pressure sites under 1.0 N, while cathepsin K was more expressed in regions of pressure under the same force magnitude (Becker et al. 2021). The immunofluorescence staining revealed that both osteocalcin and cathepsin K were more expressed after a healing period of two weeks compared to eight weeks (Becker et al. 2021). Cathepsin K expression was rarely seen after eight weeks, 'almost undetectable' (Becker et al. 2021). Like the gene expression, also protein expression seemed to have reached a steady state after eight weeks, as expression patterns of osteocalcin and cathepsin K decreased.

3.3.1. Osteocalcin

The peri-implant expression of osteocalcin decreased after a healing period of eight weeks in comparison to two weeks. At none of the two time points significant differences were found. Nonetheless, the expression trended to be higher in areas of mechanical tension. [Fig. 32] (Becker et al. 2021).

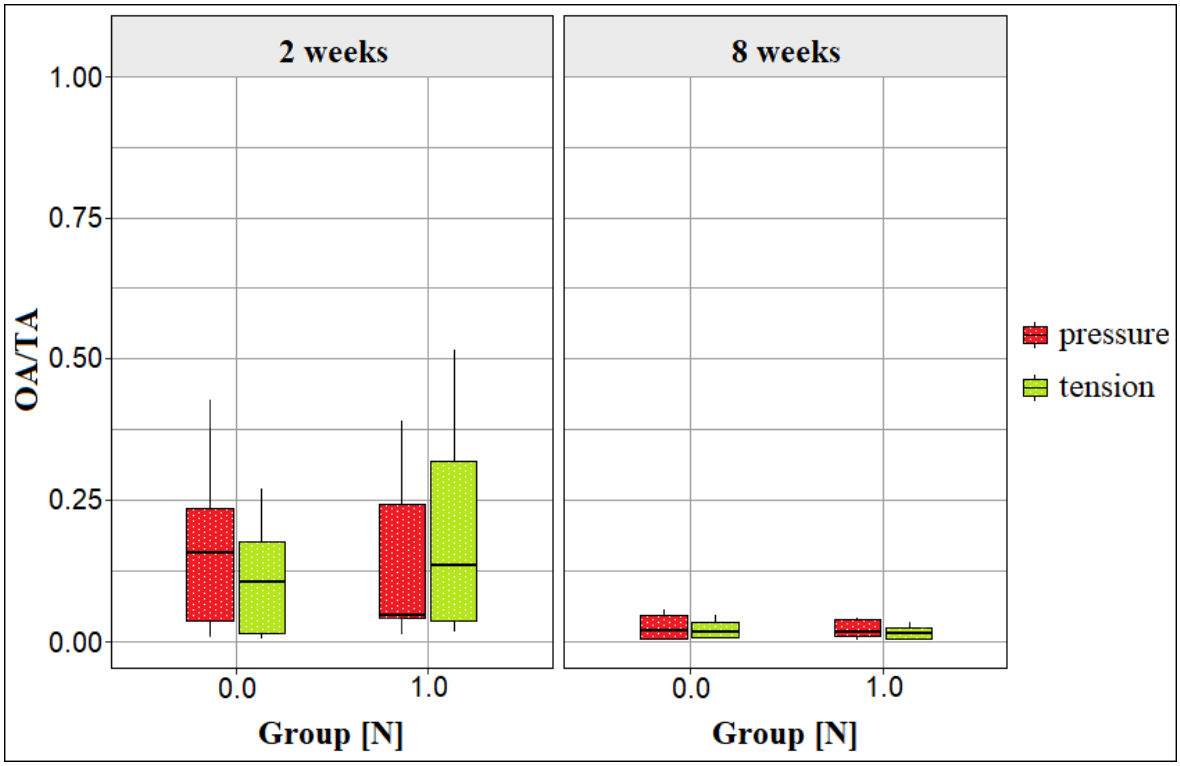

Fig. 32: **Peri-implant protein expression of osteocalcin (modified after Becker et al. 2021)**

3.3.2. Cathepsin K

Cathepsin K expression was slightly and by trend higher in regions of mechanical pressure, although no significant difference was detected at both time points. At 8 weeks, expression was clearly smaller compared to two weeks [Fig. 33] (Becker et al. 2021).

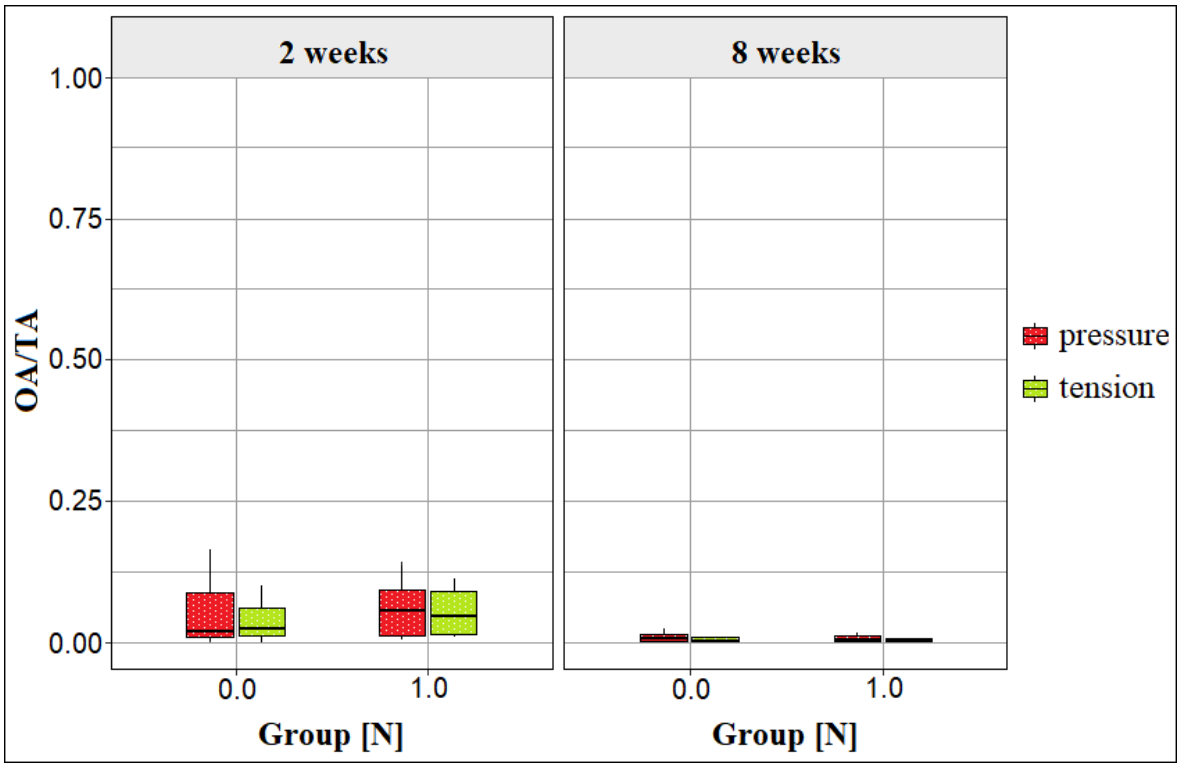

Fig. 33: **Peri-implant protein expression of cathepsin K (modified after Becker et al. 2021)**

4. Discussion

Implant migration has been supposed to be ‘facilitated’ (Becker et al. 2021) by bone resorption in the direction of implant movement and bone formation in the regions of the ‘former implant position’ (Becker et al. 2019). The present study aimed at investigating the biological backgrounds of this phenomenon in terms of gene and protein expression.

µCT-analyses performed in a prior study already confirmed a significant association between the amount of ongoing implant migration and the applied force. It has further shown that a decrease of implant migration velocity took place over time (Becker et al. 2019). The present thesis revealed that these findings go along with both a decreasing gene and protein expression after eight weeks of wound healing (Becker et al. 2021). Further investigations by our group confirmed that BIC-values ‘raised over time […] with increasing applied loads’ and were higher in the loading groups at the second time point, thus confirming that migrating implants did not lose their endosseous stability and that migration is ‘not a consequence of bone loss’, but remained in direct contact to their surrounding bone (Becker et al. 2021).

Mechanical force was shown to be a key stimulus for changes in bone structure through the process of bone remodeling (Kenkre/ Bassett 2018, Scheuren et al. 2020), especially in the peri-implant area (Stadelmann et al. 2013, Paul et al. 2018). It is driven by a cell response of osteocytes, osteoblasts and osteoclasts, depending on the force applied to the implant. Among other cells, the osteocytes ‘are recognized to be the principal sensory cells responding to mechanical stimuli’ (Becker et al. 2021), as they play a key role in maintaining bone homeostasis by orchestrating both the cells responsible for bone formation and those responsible for bone resorption: the cytokines they secrete in response to mechanical stress due to their mechanosensory capabilities have a reciprocal effect on osteoblasts and osteoclasts (Novack 2011, Goldring 2015). By determining the genetic differentiation of these effector cells (Scheuren et al. 2017), they are able to coordinate both bone formation and bone resorption. For this reason, gene expression analysis in this study was performed only with genes derived from osteocytes.

Within this study, Runx2, osterix and osteocalcin served as markers for bone formation, whereas sclerostin and cathepsin K were assumed to be responsible for bone resorption. While cathepsin K directly degrades the bone matrix by hydrolyzing collagen (Costa et al. 2011, Borel et al. 2012, Novinec/ Lenarčič 2013, Dai et al. 2020), sclerostin indirectly

inhibits bone formation by suppressing the Wnt-signaling pathway within osteocytes and therefore decreasing the expression of other cytokines such as Runx2 and SP7 (Robling et al. 2008, Lin et al. 2009, Tu et al. 2012, Spatz et al. 2015). Mechanical stimuli have shown to influence the peri-implant expression, as we have expected, bone resorption dominated in regions of mechanical pressure (Becker et al. 2021).

The Wnt-signaling, upon others activated by Runx2 (Komori 2020), and the NF-κB-signaling pathway both had influence on each other (Ma/ Hottiger 2016): the Wnt-signaling pathway may either activate or suppress the NF-κB-signaling pathway, dependent on the subsequent intracellular reactions of β-catenin (Ma/ Hottiger 2016). An analysis of the expression of genes that both activate and inhibit both signaling pathways might make an interpretation of their expression within the peri-implant area more challenging: Runx2, SP7, osteocalcin, SOST and cathepsin K all have an impact on the Wnt-signaling pathway, as Runx2 controls the expression of osterix via the Wnt-signaling pathway (Komori 2019, Komori 2020), and osterix itself is in charge of the expression of osteocalcin (Chen et al. 2019), which is a marker of bone formation (Brennan-Speranza/ Conigrave 2015). On the other hand, Runx2 can also both positively regulate the expression of osteocalcin (Komori 2019, Komori 2020) and SP7 (Komori 2018), but also the expression of SOST (Pérez-Campo et al. 2016).

As osterix is able to induce the expression of the bone resorption marker SOST (Yang et al. 2010), its role within the peri-implant process of bone remodeling is still controversial. On the other hand, sclerostin can inhibit the Wnt-signaling pathway (Lin et al. 2009, Tu et al. 2012). When bone is subjected to mechanical stimuli, the secretion of sclerostin decreases in favor for the Wnt-signaling pathway (Bellido 2014). It is not surprising that we could confirm a higher expression of osterix and osteocalcin in regions of tension, which control bone formation (Liu et al. 2020, Nakashima et la. 2002).

There is still a controversy regarding the findings of a higher expression of Runx2 in regions of pressure, as osterix is a downstream product of Runx2 (Komori 2006). A higher expression of Runx2 in regions of mechanical pressure might be explained by the fact that it induced the expression of another gene also being higher expressed in this region: SOST. Secondly, as mentioned above, SP7 is also a transcriptional factor in the expression of SOST (Sevetson et al. 2004, Yang et al. 2010, Pérez-Campo et al. 2016, Becker et al. 2021).

The dominance of CTSK in regions of pressure appears to be reasonable, as it controls the bone resorption processes (Dai et al 2020, Bonnet et al. 2017) that facilitate gaining space for the implant migration.

In return, osteocalcin plays a key role in increasing bone mineral density in terms of wound healing (Rodrigues et al. 2010, Berezovska et al. 2019): consequently, the initial hypothesis was supported by the finding of its expression to a larger extend within regions of tension, mostly after an observation period of two weeks. At this time point bone formation was most pronounced (Becker et al. 2021).

Although force did not have a significant impact, 0.5 N seemed to have a similar impact on gene expression of all the genes observed in this study, as their expression was highest under 0.5 N (Runx2, SP7, SOST and CTSK) (Becker et al. 2021).

1.5 N seems to be a critical limit for mechanical loading of the bone tissue, as an opposite gene expression of Runx2, SOST and CTSK with regard to the peri-implant area (tension vs. pressure) was found, predominantly expressed on the lateral implant site, in regions of tension (Becker et al. 2021). The inverted expression of SOST matches the findings of a downregulation in its expression under mechanical stimuli in other studies (Robling et al. 2008, Bullock et al. 2019, Lin et al. 2009, Spatz et al. 2015).

Microcracks within the surrounding bone tissue are suspected to occur during the mechanical loading. These cracks might affect the ‘canalicular network’ (Becker et al. 2021), which leads to an increase of osteocytic apoptosis (Bellido 2014). This apoptosis entails an increasing bone resorption in those regions (Jilka et al. 2013). The finding of an opposite expression might be explainable in reference to our previous µCT study, where the implants moved within the cortical bone only when forces were higher (Becker et al. 2019). Cortical bone is more difficult to be resorbed than trabecular bone, due to its smaller exposed surface, and has to bear larger forces than trabecular bone.

Only SP7, whose expression pattern differed from the other patterns anyway, showed an opposite distribution under a force of 1.0 N (Becker et al. 2021).

Unlike dental implants, mini-implants do not have a roughened, but a machined surface, which is why their anchorage in the bone is always lower than that of dental implants (Li et al. 2002). For this reason, their primary stability is also lower than their secondary stability during orthodontic loading (Vilani et al. 2015). Since primary stability was found to keep anchorage sufficient during orthodontic loading though, orthodontic forces can be applied

onto the mini-implants right after surgical placement without the need of a waiting period (Liou et al. 2004, Becker et al. 2018).

Over time, the 'velocity [of implant migration] within the bone' (Becker et al. 2021) in our prior study also showed a decrease (Becker et al. 2019). A decrease in the expression of both gene and protein expression from two weeks up to eight weeks leads to the assumption that the whole process of peri-implant bone remodeling reached a steady state within eight weeks. This means that after this wound healing period, bone formation already took place and adapted to the local stresses. As a result, the BIC has also shown to 'increase[d] with respect to the […] timing' and therefore be in trend higher after a period of eight weeks than it was two weeks after the implant insertion (Becker et al. 2021). Again, the BIC was shown to differ mostly in between week two and week eight under forces of both 0.5 N and 1.5 N. In this study, these two force levels also seemed to be responsible for both the highest gene expression in the genes analyzed (for 0.5 N), and secondly to lead to an opposite expression pattern according to the peri-implant localization (for 1.5 N) (Becker et al. 2021).

4.1. Discussion of the Method

In the end, issues in sample preparation for gene expression analysis and immunofluorescence are to be mentioned, as sample handling proved to be quite demanding. A low temperature storage for RNA downsampling - both during µCT scanning and sample preparation - was crucial to ensure osteocyte survival and to prevent mRNA degradation by *ribonucleases* (RNAses) at room temperature (Wan et al. 2010). The only way to keep osteocytes alive during scanning was to store them in a container with low thermal conductivity that was not radiopaque at the same time. A custom-made sample holder made of extruded polystyrene was able to meet these requirements due to its thermal insulating properties, as it prevented the sublimation of the dried ice during the scanning process (scan duration about one hour). In the design of the same, an optimum ratio had to be found between the inner volume for sample storage and a sufficient wall thickness to reduce evaporation.

Cryosectioning itself proved to be quite difficult as well, because, as mentioned earlier, samples were not meant to thaw at room temperature. Since decalcification was contraindicated because of the maintenance of the genetic material, the resulting rather solid bone tissue was hard to cut even with special blades mentioned above. Initial attempts in cryosectioning resulted in brittle bone fragments, whose former positions relative to the

implant surface could no longer be traced. In case a usable section was taken, the staining solutions washed away the bone fragments, which at this point were only fixed onto the slide by a thawing process. In addition, the sections gained without using a cryofilm were not in a plane, but protruded slightly from the slide surface. This led to the problem that the laser of the LCM microscope could not find a fixed focus for the cutting process and therefore osteocytes could hardly be extracted without damaging the surrounding tissue by thermal irritation.

It took several attempts (up to 6 months) and the help of the Kawamoto film to finally figure out a suitable method that 1) provided dimensionally stable sections 2) during the cutting and 3) the staining process while 4) preserving their genetic material at the same time. Using the Kawamoto film, I was finally able to bring one whole section into the slide level.

Furthermore, the problem of thawing samples could be circumvented by a process called thaw-mounting, a common method of usually mounting samples onto sample slides (Stumpf/ Roth 1966). In this process, the samples adhere onto the slide surface through the condensation of water within them (Cha et al. 2008, Le et al. 2018). As samples need to be refrozen again for further storage though, the forming of ice crystals within the sample might lead to cell destruction (Le et al. 2018). The use of the Kawamoto film allowed to adhere specimens to the slides without melting them - in a process known as freeze-drying (Kawamoto 2003).

Without the special temperature treatments, samples would have been unusable for further treatment with respect to handling nucleic acids. Finally, a promising method was found to preserve the three-dimensional information (at a histological level) and simultaneously use it for local gene expression analyses.

Another time-consuming issue was to obtain suitable immunofluorescence scans, as for our questioning, we were dependent on images containing one whole implant and its surrounding bone tissue at a 40x magnification. The microscope we initially used could only provide images at 40x magnification that contained small sections of the peri-implant bone tissue, but not an entire implant. Although it was possible to obtain images at 40x magnification with this microscope, these images could not be merged into a new whole image at the same magnification without artifacts. As a result, the peri-implant tissue could not be subdivided into the regions of interest (tension and pressure).

The use of immunofluorescence instead of immunohistochemistry in this study was advantageous, because it allowed the staining of one and the same specimen section with different antibodies in search for more than one antigen of interest.

Using an advanced immunofluorescence microscope (Operetta, see above), single images at a magnification of 40, scanned one after another with a small offset, could be obtained and then stitched together to a whole new image as they were adjacent to each other. However, these images were so large (up to 500 TB) that an enormous amount of storage space was required. The resulting need to transfer data from one storage medium to another further slowed down the evaluation process. Common immunofluorescence microscopes are usually not designed for such a sample size (additionally at this magnification). Currently, systems are being sought that allow 1) a faster scanning process as well as 2) a reduction in storage space while 3) still providing image information regarding the regions of interest. These three aspects should be considered in future studies regarding immunofluorescence analyses.

4.2. Limitations of the Study

For the present study, only osteocytic gene expression was analyzed. Although osteocytes have a similar gene expression as osteoblasts, proteins like the BAp and collagen type I are lower in osteocytes, while osteocalcin and sclerostin are even higher (Bellido 2014). Additionally, not much is known about the 'scarce' (Becker et al. 2021) force induced gene expression of Runx2 and SP7 in osteocytes, whereas more studies on the expression in osteoblasts can be found (Hojo/ Ohba 2020, Komori 2020). Consideration should be given to including the gene expression in 'additional types of cells' (Becker et al. 2021), such as osteoblasts and osteoclasts, in a future study as well, as many of them have shown to appear in a closer proximity to the implant surface. Furthermore, a greater distance than 100 µm to the former implant position should be taken into consideration, as the impact of cytokines involved in bone remodeling might exceed regions beyond 100 µm (Becker et al. 2021).

Overall, gene expression was only analyzed within 'the cortical compartment proximity to the implant surface' (Becker et al. 2021), but not the implant tip. This was due to the consideration that the remaining peri-implant bone areas should still be kept for future analysis of further genes, which are also related to bone remodeling (i.e. RANKL, OPG, ALP). Further analyses according to the gene expression in regions around the implant tip might therefore highlight the understanding of implant migration to a greater extend.

The genes analyzed in this study represent only a few genes that take part in the complex process of bone remodeling. Their expression patterns might only give a small clue about how bone formation and resorption are balanced in regions close to a mini-implant. Analyses in protein expression were restricted to specimens that had been subjected to a force of 0 N and 1.0 N.

The reason why the statistics of this study have only been descriptive is up to the fact that there was a 'limited number of animals available' (Becker et al. 2021) for each question (gene or protein expression) observed. This was due to the fact that as many different questions as possible were of interest, which should be answered with as few available animals as possible due to the 3Rs requirement (Russell/ Burch 1960). Thanks to our previous study, that was performed to investigate X-ray based morphological changes in the peri-implant bone structure by performing µCT analysis (Becker et al. 2019), peri-implant bone remodeling could already be assessed in a total of n = 61 animals, but only radiologically. These results were supposed to be corroborated in follow-up studies against the background of different biological questions, each of which can be divided into 1) gene and protein expression (in this study) 2) 'angiogenesis' (Hüfner et al. 2022) and 3) histological questionings such as 'BIC' (Becker et al. 2021), peri-implant cell number and distribution, and *bone volume fraction* (BV/ TV) (Becker et al. 2021). The handling of the tissue samples (decalcification/ non-decalcification; hard tissue histology; storage and handling of samples at room temperature or at - 80°C) for these different questions have already been reported above. This also required a different embedding of the same depending on the research question, which is why the samples intended for the analysis of gene expression had to be stored in a freeze-embedding medium, those for the study of protein expression embedded within in paraffin due to staining with antibodies, and samples for the study of BIC within in PMMA due to hard tissue histology.

Furthermore, the implant surface has to be considered as an important factor for processes in bone remodeling and resulting implant stability. Due to the mini-implants' surfaces, we can distinguish machined from rough surfaces. Regarding the latter, there is only one manufacturer who offers mini-implants with a *sandblasted, large-grit, acid-etched* (SLA) surface under the name C-Implants (Chung et al. 2005). Those with a machined surface were the ones used within this study. Implants with a roughened surface need a shoter time period for reaching their stability in terms of wound healing and show a greater osseointegration

than smooth surfaces do (Nasatzky et al. 1993, Shalabi et al. 2006). Mini-implants with a machined surface show a smaller secondary stability than those with rough surfaces (Nienkemper et al. 2014). The impact of the implants' 'surface roughness' (Becker et al. 2019) as well as 'different loading time points' (Becker et al. 2021), like differences between an 'immediate' and a 'delayed loading' (Becker et al. 2019) (Freire et al. 2007, Garg/ Gupta 2015, Serra et al. 2010) might therefore be another interesting aspect to be investigated in future studies.

5. Conclusions

Within the limits of the study, implant migration has been shown to be accompanied by peri-implant force and time dependent bone remodeling, which is documented by local changes in gene and protein expression in the peri-implant area. Over time (two to eight weeks from implant loading), bone adapted to local stresses and therefore limited implant migration.

SOST and CTSK controlling bone resorption were most pronounced in regions subjected to mechanical pressure, whereas bone formation controlled by SP7 and Runx2 dominated in regions subjected to mechanical tension in the early healing phase. In line with the decrease of implant migration velocity over time, associated gene and protein expression also decreased at eight weeks when compared to the findings at two weeks of loading.

Future analyses on the impact of the implant surface microstructure and loading time may be needed to further elucidate the phenomenon of implant migration. In addition, further genes and proteins may be explored in future investigations.

6. References

Alves, A., Cacho, A., San Roman, F., Gerós, H., Afonso, A.: Mini implants osseointegration, molar intrusion and root resorption in Sinclair minipigs. International Orthodontics. 2019;17(4):733-43.

Anderson, D.M., Maraskovsky, E., Billingsley, W.L., Dougall, W.C., Tometsko, M.E., Roux, E.R., Teepe, M.C., DuBose, R.F., Cosman, D., Galibert, L.: A homologue of the TNF receptor and its ligand enhance T-cell growth and dendritic-cell function. Nature. 1997;390:175–179.

Angle, E.H.: Treatment of Malocclusion of the Teeth and Fractures of the Maxillae: Angle's System. Philadelphia: White Dental Manufacturing Co. 1900;6:81-150.

Animal Protection Act 24.07.1972, Section 5, § 7a (1) b)

Animal Protection Act 24.07.1972, Section 5, § 7a (2)

Arthur, G.: Albert Coons: harnessing the power of the antibody. The Lancet Respiratory Medicine. 2016;4(3):181-2.

Asok, N., Chandra, P., Singh, K., Tandon, R.: Mandibular molar intrusion with mini-implants and the multiloop edgewise archwire technique. American Journal of Orthodontics and Dentofacial Orthopedics. 2019;155(2):157.

Auricchio, F., Taylor, R.L.: Shape-Memory Alloys: Modeling and Numerical Simulations of the Finite-Strain Superelastic Behavior. Computer Methods in Applied Mechanics and Engineering. 1996;143:175–194.

Auricchio, F., Lubliner, J.: Shape-Memory Alloys: Macromodelling and Numerical Simulations of the Superelastic Behavior. Computer Methods in Applied Mechanics and Engineering, 1997;146:281–312.

Badea, C.T., Drangova, M., Holdsworth, D.W., Johnson, G.A.: In vivo small-animal imaging using micro-CT and digital subtraction angiography. Physics in Medicine and Biology. 2008;53(19):R319-50.

Bailey, S., Karsenty, G., Gundberg, C., Vashishth, D.: Osteocalcin and osteopontin influence bone morphology and mechanical properties. Annals of the New York Academy of Sciences. 2017;1409(1):79-84

Bates, D., Maechler, M., Bolker, B., Walker, S.: Fitting Linear Mixed-Effects Models Using lme4. Journal of Statistical Software. 2015; 67(1):1-48.

Becker, K., Drescher, D., Hönscheid, R., Golubovic, V., Mihatovic, I., Schwarz, F.: Biomechanical, micro-computed tomographic and immunohistochemical analysis of early osseous integration at titanium implants placed following lateral ridge augmentation using extracted tooth roots. Clinical Oral Implants Research. 2017;28(3):334-40.

Becker, K., Klitzsch, I., Stauber, M., Schwarz, F.: Three-dimensional assessment of crestal bone levels at titanium implants with different abutment microstructures and insertion depths using micro-computed tomography. Clinical Oral Implants Research. 2017;28(6):671-676.

Becker, K., Pliska, A., Busch, C., Wilmes, B., Wolf, M., Drescher, D.: Efficacy of orthodontic mini implants for en masse retraction in the maxilla: a systematic review and meta-analysis. International Journal of Implant Dentistry. 2018;4(1):35.

Becker, K., Wilmes, B., Grandjean, C., Vasudavan ,S., Drescher, D.: Skeletally anchored mesialization of molars using digitized casts and two surface-matching approaches : Analysis of treatment effects. Journal of Orofacial Orthopedics. 2018;79(1):11-18.

Becker, K., Schwarz, F., Rauch, N.J., Khalaph, S., Mihatovic, I., Drescher, D.: Can implants move in bone? A longitudinal in vivo micro-CT analysis of implants under constant forces in rat vertebrae. Clinical Oral Implants Research. 2019;30(12):1179-1189.

Becker, K., Rauch, N., Brunello, G., Azimi, S., Beller, M., Hüfner, M., Nienkemper, M., Schwarz-Herzke, B., Drescher, D.: Bone remodelling patterns around orthodontic mini-implants migrating in bone: an experimental study in rat vertebrae. European Journal of Orthodontics. 2021; 1;43(6):708-717.

Bellido, T.: Osteocyte-driven bone remodeling. Calcified Tissue International. 2014;94(1):25-34.

Berezovska, O., Yildirim, G., Budell, W.C., Yagerman, S., Pidhaynyy, B., Bastien, C., van der Meulen, M.C.H., Dowd, T.L..: Osteocalcin affects bone mineral and mechanical properties in female mice. Bone. 2019; 128:115031.

Blazsek, I., Goldschmidt, E., Machover, D., Misset, J.L., Benavides, M., Comisso, M., Ceresi, E., Canon, C., Labat, M.L., Mathe, G.: Excess of lympho-reticular cell complexes in the bone marrow linked to t cell mediated dysmyelopoiesis. Biomedicine & Pharmacotherapy.1986; 40(1):28-32.

Block, M.S., Hoffman, D.R.: A new device for absolute anchorage for orthodontics. American Journal of Orthodontics and Dentofacial Orthopedics. 1995;107(3):251-8.

Boerckel, J.D., Mason, D.E., McDermott, A.M., Alsberg, E.: Microcomputed tomography: approaches and applications in bioengineering. Stem Cell Research & Therapy. 2014;5(6):144.

Bonnet, N., Brun, J., Rousseau, J.C., Duong, L.T., Ferrari, S.L.: Cathepsin K Controls Cortical Bone Formation by Degrading Periostin. Journal of Bone and Mineral Research. 2017;32(7):1432-1441.

Borel, O., Gineyts, E., Bertholon, C., Garnero, P.: Cathepsin K preferentially solubilizes matured bone matrix. Calcified Tissue International. 2012;91(1):32-9.

Brånemark, P.I.: Osseointegration and its experimental background. The Journal of Prosthetic Dentistry. 1983;50(3):399-410.

Brennan-Speranza, T.C., Conigrave, A.D.: Osteocalcin: an osteoblast-derived polypeptide hormone that modulates whole body energy metabolism. Calcified Tissue International. 2015;96(1):1-10.

Bresler, S.C., Bavarian, R., Granter, S.R., Woo, S.B.: Direct immunofluorescence is of limited utility in patients with low clinical suspicion for an oral autoimmune bullous disorder. Oral Diseases. 2020;26(1):81-8.

Brown, R.N., Sexton, B.E., Gabriel Chu, T.M., Katona, T.R., Stewart, K.T., Kyung, H.M.: Comparison of stainless steel and titanium alloy orthodontic miniscrew implants: a mechanical and

histologic analysis. American Journal of Orthodontics and Dentofacial Orthopedics. 2014;145(4):496-504.

Bollero, P., Di Fazio, V., Pavoni, C., Cordaro, M., Cozza, P., Lione, R.: Titanium alloy vs. stainless steel miniscrews: an in vivo split-mouth study. European Review for Medical and Pharmacological Sciences. 2018;22(8):2191-2198.

Bonucci, E., Ascenzi, A., Vittur, F., Pugliarello, M.C., De Bernard, B.: Density of osteoid tissue and osteones at different degree of calcification. Calcified Tissue Research. 1970;5(2):100-7.

Bullock, W.A., Pavalko, F.M., Robling, A.G.: Osteocytes and mechanical loading: The Wnt connection. Orthodontics & Craniofacial Research. 2019;22 Suppl 1:175-179.

Bushinsky, D.A., Frick, K.K.: The effects of acid on bone. Current Opinion in Nephrology and Hypertension. 2000;9(4):369-79.

Calvo-Guirado, J.L., Pérez-Albacete, C., Aguilar-Salvatierra, A., de Val Maté-Sánchez, J.E., Delgado-Ruiz, R.A., Abboud, M.: Narrow- versus mini-implants at crestal and subcrestal bone levels. Experimental study in beagle dogs at three months. Clinical Oral Investigations. 2015;19(6):1363-9.

Cano-Sánchez, J., Campo-Trapero, J., Gonzalo-Lafuente, J.C., Moreno-López, L.A., Bascones-Martínez, A.: Undecalcified bone samples: a description of the technique and its utility based on the literature. Medicina Oral, Patologia Oral y Cirugia Bucal. 2005;10 Suppl 1:E74-87.

Carlson, C., Sung, J., McComb, R.W., Machado, A.W., Moon, W.: Microimplant-assisted rapid palatal expansion appliance to orthopedically correct transverse maxillary deficiency in an adult. American Journal of Orthodontics and Dentofacial Orthopedics. 2016;149(5):716-28.

Cha, S., Zhang, H., Ilarslan, H.I., Wurtele, E.S., Brachova, L., Nikolau, B.J., Yeung, E.S.: Direct profiling and imaging of plant metabolites in intact tissues by using colloidal graphite-assisted laser desorption ionization mass spectrometry. The Plant Journal. 2008;55(2):348-60.

Chang, C.H., Lin, J.S., Roberts, W.E.: Failure rates for stainless steel versus titanium alloy infrazygomatic crest bone screws: A single-center, randomized double-blind clinical trial. The Angle Orthodontist. 2019;89(1):40-46.

Cao, X., Chen, D.: The BMP signaling and in vivo bone formation. Gene. 2005;357(1):1-8.

Carpenter, A.E., Jones, T.R., Lamprecht, M.R., Clarke, C., Kang, I.H., Friman, O.: CellProfiler: image analysis software for identifying and quantifying cell phenotypes. Genome Biology. 2006;7(10):R100.

Chambers, T.J.: Osteoblasts release osteoclasts from calcitonin-induced quiescence. Journal of Cell Science. 1982;57:247-60.

Chen, Z., Song, Z., Yang, J., Huang, J., Jiang, H.: Sp7/osterix positively regulates dlx2b and bglap to affect tooth development and bone mineralization in zebrafish larvae. Journal of Biosciences. 2019;44(6):127.

Chen, K., Jiao, Y., Liu, L., Huang, M., He, C., He, W., Hou, J., Yang, M., Luo, X., Li, C.: Communications Between Bone Marrow Macrophages and Bone Cells in Bone Remodeling. Frontiers in Cell and Developmental Biology. 2020;22;8:598263.

Chhabra, S., Minz, R.W., Saikia, B.: Immunofluorescence in dermatology. Indian Journal of Dermatology, Venereology and Leprology. 2012;78(6):677-91.

Chiquet, M., Renedo, A.S., Huber, F., Flück, M.: How do fibroblasts translate mechanical signals into changes in extracellular matrix production? Matrix Biology. 2003;22(1):73-80.

Chiquet, M., Gelman, L., Lutz, R., Maier, S.: From mechanotransduction to extracellular matrix gene expression in fibroblasts. Biochimica et Biophysica Acta. 2009;1793(5):911-20.

Cho, S.W., Soki, F.N., Koh, A.J., Eber, M.R., Entezami, P., Park, S.I., van Rooijen, N., McCauley, L.K.: Osteal macrophages support physiologic skeletal remodeling and anabolic actions of parathyroid hormone in bone. Proceedings of the National Academy of Sciences of the United States of America (PNAS). 2014;28;111(4):1545-50.

Chung, K., Kim. S.H., Kook, Y.: C-orthodontic microimplant for distalization of mandibular dentition in Class III correction. The Angle Orthodontist. 2005;75(1):119-28.

Coons, A.H., Creech, H.J., Jones, R.N.: Immunological Properties of an Antibody Containing a Fluorescent Group. Proceedings of the Society for Experimental Biology and Medicine. 1941;47(2):200-202.

Costa, A., Raffainl, M., Melsen, B.: Miniscrews as orthodontic anchorage: a preliminary report. The International Journal of Adult Orthodontics & Orthognathic Surgery. 1998;13(3):201-9.

Costa, A.G., Cusano, N.E., Silva, B.C., Cremers, S., Bilezikian, J.P.: Cathepsin K: its skeletal actions and role as a therapeutic target in osteoporosis. Nature Reviews Rheumatology. 2011;7(8):447-56.

Cotrim-Ferreira, F.A., Quaglio, C.L., Peralta, R.P., Carvalho, P.E., Siqueira, D.F.: Metallographic analysis of the internal microstructure of orthodontic mini-implants. Brazilian Oral Research. 2010;24(4):438-42.

Creekmore, T.D., Eklund, M.K.: The possibility of skeletal anchorage. Journal of Clinical Orthodontics: JCO. 1983;17(4):266-9.

Curran, S., McKay, J.A., McLeod, H.L., Murray, G.I.: Laser capture microscopy. Molecular Pathology: MP. 2000;53(2):64-8.

Dai, R., Wu, Z., Chu, H.Y., Lu, J., Lyu, A., Liu, J.: Cathepsin K: The Action in and Beyond Bone. Frontiers in Cell and Developmental Biology. 2020;8:433

Dallas, S.L., Prideaux, M., Bonewald, L.F.: The osteocyte: an endocrine cell ... and more. Endocrine Reviews. 2013;34(5):658-90.

Davidovitch, Z.: Tooth movement. Critical Reviews in Oral Biology & Medicine. 1991;2(4):411-50.

Deguchi, T., Takano-Yamamoto, T., Kanomi, R., Hartsfield, J.K. Jr., Roberts, W.E., Garetto. L.P.: The use of small titanium screws for orthodontic anchorage. Journal of Dental Research. 2003;82(5):377-81.

de Morais, L.S., Serra, G.G., Albuquerque Palermo, E.F., Andrade, L.R., Müller, C.A., Meyers, M.A., Elias, C.N.: Systemic levels of metallic ions released from orthodontic mini-implants. American Journal of Orthodontics and Dentofacial Orthopedics. 2009;135(4):522-9.

Dhaliwal, J.S., Albuquerque, R.F. Jr., Murshed, M., Feine, J.S.: Osseointegration of standard and mini dental implants: a histomorphometric comparison. International Journal of Implant Dentistry. 2017;3(1):15.

Diercks, G.F., Pas, H.H., Jonkman, M.F.: Immunofluorescence of Autoimmune Bullous Diseases. Surgical Pathology Clinics. 2017;10(2):505-12.

Donaldson, J.G.: Immunofluorescence staining. Current Protocols in Cell Biology. 2015;69:4.3.1-4.3.7.

Donath, K., Breuner, G.: A method for the study of undecalcified bones and teeth with attached soft tissues. The Säge-Schliff (sawing and grinding) technique. Journal of Oral Pathology. 1982;11(4):318-26.

Dyment, M.L., Synge, J.L.: Elasticity of periodontal membrane. Oral Health. 1935;25:105

El-Beialy, A.R., Abou-El-Ezz, A.M., Attia, K.H., El-Bialy, A.M., Mostafa, Y.A.: Loss of anchorage of miniscrews: a 3-dimensional assessment. American Journal of Orthodontics and Dentofacial Orthopedics. 2009;136(5):700-7.

Emmert-Buck, M.R., Bonner, R.F., Smith, P.D., Chuaqui, R.F., Zhuang, Z., Goldstein, S.R.: Laser capture microdissection. Science. 1996;274(5289):998-1001.

Enlow, D.H., Moyers, R.E., Hunter, W.S., McNamara, J.A. Jr.: A procedure for the analysis of intrinsic facial form and growth. An equivalent-balance concept. American Journal of Orthododontics. 1969;56(1):6-23.

Everts, V., Delaissé, J.M., Korper, W., Jansen, D.C., Tigchelaar-Gutter, W., Saftig, P.: The bone lining cell: its role in cleaning Howship's lacunae and initiating bone formation. Journal of Bone and Mineral Research. 2002;17(1):77-90.

Fanghänel, J., Proff, P., Dietze, S., Bayerlein, T., Mack, F., Gedrange, T.: The morphological and clinical relevance of mandibular and maxillary bone structures for implantation. Folia Morphologica (Warsz). 2006;65(1):49-53.

Farkasdi, S., Pammer, D., Rácz, R., Hriczó-Koperdák, G., Szabó, B.T., Dobó-Nagy, C.: Development of a quantitative preclinical screening model for implant osseointegration in rat tail vertebra. Clinical Oral Investigations. 2019;23(7):2959-73.

Farrar, J. N.: Treatise on Irregularities of the Teeth and Their Correction. DeVinne Press. 1888;2:758.

Felsenthal, N., Zelzer, E.: Immunofluorescent Staining of Adult Murine Paraffin-Embedded Skeletal Tissue. Methods in Molecular Biology. 2021;2230:337-44.

Franceschi, R.T., Xiao, G., Jiang, D., Gopalakrishnan, R., Yang, S., Reith, E.: Multiple signaling pathways converge on the Cbfa1/Runx2 transcription factor to regulate osteoblast differentiation. Connective Tissue Research. 2003;44 Suppl 1(Suppl 1):109-16.

Franz-Odendaal, T.A., Hall, B.K., Witten, P.E.: Buried alive: how osteoblasts become osteocytes. Developmental Dynamics. 2006;235(1):176-90.

Freire, J.N., Silva, N.R., Gil, J.N., Magini, R.S., Coelho, P.G.: Histomorphologic and histomophometric evaluation of immediately and early loaded mini-implants for orthodontic anchorage. American Journal of Orthodontics and Dentofacial Orthopedics. 2007;131(6):704.e1-9.

Freitas, G.P., Lopes, H.B., Martins-Neto, E.C., de Oliveira, P.T., Beloti, M.M., Rosa, A.L.: Effect of Surface Nanotopography on Bone Response to Titanium Implant. Journal of Oral Implantology. 2016;42(3):240-7.

Frost, H.M.: Skeletal structural adaptations to mechanical usage (SATMU): 2. Redefining Wolff's law: the remodeling problem. The Anatomical Record. 1990;226(4):414-22.

Gainsforth, B.L., Higley, L.B.: A study of orthodontic anchorage possibilities in basal bone. American Journal of Orthodontics and Oral Surgery. 1945;31:406-417.

Gao, Y., Jheon, A., Nourkeyhani, H., Kobayashi, H., Ganss, B.: Molecular cloning, structure, expression, and chromosomal localization of the human Osterix (SP7) gene. Gene. 2004;341:101-10.

Garg, K.K., Gupta, M.: Assessment of stability of orthodontic mini-implants under orthodontic loading: A computed tomography study. Indian Journal of Dental Research. 2015;26(3):237-43.

Geoghegan, I.P., Hoey, D.A., McNamara, L.M.: Integrins in Osteocyte Biology and Mechanotransduction. Current Osteoporosis Reports. 2019;17(4):195-206.

Glass, D.A. 2nd, Bialek, P., Ahn, J.D., Starbuck, M., Patel, M.S., Clevers, H.: Canonical Wnt signaling in differentiated osteoblasts controls osteoclast differentiation. Developmental Cell. 2005;8(5):751-64.

Going, J.J., Lamb, R.F.: Practical histological microdissection for PCR analysis. The Journal of Pathology. 1996;179(1):121-4.

Goldring, S.R.: The osteocyte: key player in regulating bone turnover. RMD open. 2015;1(Suppl 1):e000049

Goldsworthy, S.M., Stockton, P.S., Trempus, C.S., Foley, J.F., Maronpot, R.R.: Effects of fixation on RNA extraction and amplification from laser capture microdissected tissue. Molecular Carcinogenesis. 1999;25(2):86-91.

Gotfredsen, K., Budtz-Jörgensen, E., Jensen, L.N.: A method for preparing and staining histological sections containing titanium implants for light microscopy. Stain Technology. 1989;64(3):121-7.

Graham, R.C. Jr., Karnovsky, M.J.: The early stages of absorption of injected horseradish peroxidase in the proximal tubules of mouse kidney: ultrastructural cytochemistry by a new technique. Journal of Histochemistry & Cytochemistry. 1966;14(4):291-302.

Granke, M., Gourrier, A., Rupin, F., Raum, K., Peyrin, F., Burghammer, M.: Microfibril orientation dominates the microelastic properties of human bone tissue at the lamellar length scale. PLOS ONE. 2013;8(3):e58043.

Granke, M., Does, M.D., Nyman, J.S.: The Role of Water Compartments in the Material Properties of Cortical Bone. Calcified Tissue International. 2015;97(3):292-307.

Greco, T.L., Takada, S., Newhouse, M.M., McMahon, J.A., McMahon, A.P., Camper, S.A.: Analysis of the vestigial tail mutation demonstrates that Wnt-3a gene dosage regulates mouse axial development. Genes & Development. 1996;10(3):313-24.

Greco, M., Derton, N.: Orthodontic extrusion for a preprosthetic approach: a bracketless mini-implant-based mechanics. Orthodontics : the art and practice of dentofacial enhancement. 2012;13(1):210-5.

Gurgel, J.d.A., Pinzan-Vercelino, C.R., Bramante, F.S., Rivera, A.P.: Distalization of maxillary molars using a lever arm and mini-implant. Orthodontics : the art and practice of dentofacial enhancement. 2013;14(1):e140-9.

Haagerup, A., Hertz, J.M., Christensen, M.F., Binderup, H., Kruse, T.A.: Cathepsin K gene mutations and 1q21 haplotypes in at patients with pycnodysostosis in an outbred population. European Journal of Human Genetics : EJHG. 2000;8(6):431-6.

Hamrick, M.W.: A role for myokines in muscle-bone interactions. Exercise and Sport Sciences Reviews. 2011;39(1):43-7.

Harada, N., Watanabe, Y., Sato, K., Abe, S., Yamanaka, K., Sakai, Y., Kaneko, T., Matsushita, T.: Bone regeneration in a massive rat femur defect through endochondral ossification achieved with chondrogenically differentiated MSCs in a degradable scaffold. Biomaterials. 2014;35(27):7800-10.

Hart, T.R., Cousley, R.R., Fishman, L.S., Tallents, R.H.: Dentoskeletal changes following mini-implant molar intrusion in anterior open bite patients. The Angle Orthodontist. 2015;85(6):941-8.

Hojo, H., Ohba, S.: Gene regulatory landscape in osteoblast differentiation. Bone. 2020;137:115458.

Hounsfield, G.N.: Computerized transverse axial scanning (tomography). 1. Description of system. The British Journal of Radiology. 1973;46(552):1016-22.

Hourfar, J., Kanavakis, G., Goellner, P., Ludwig, B.: Fully customized placement of orthodontic miniplates: a novel clinical technique. Head & Face Medicine. 2014;3;10:14.

Hsu, S.M., Raine, L., Fanger, H.: A comparative study of the peroxidase-antiperoxidase method and an avidin-biotin complex method for studying polypeptide hormones with radioimmunoassay antibodies. American Journal of Clinical Pathology. 1981;75(5):734-8.

Hsu, S.M., Raine, L., Fanger, H.: The use of antiavidin antibody and avidin-biotin-peroxidase complex in immunoperoxidase technics. American Journal of Clinical Pathology. 1981;75(6):816-21.

Hsu, S.M., Raine, L., Fanger, H.: Use of avidin-biotin-peroxidase complex (ABC) in immunoperoxidase techniques: a comparison between ABC and unlabeled antibody (PAP) procedures. Journal of Histochemistry & Cytochemistry. 1981;29(4):577-80.

Huang, X., Ackland, G.J., Rabe, K.M.: Crystal structures and shape-memory behaviour of NiTi. Nature Materials. 2003;2(5):307-11.

Hüfner, M., Rauch, N., Schwarz-Herzke, B., Knorr, I.J., Sager, M., Drescher, D., Becker, K.: Micro-angiogenic patterns around orthodontic implants migrating in bone: A micro-CT study in the rat tail model. Journal of Clinical Periodontology. 2022;49(2):188-197.

Idleburg, C., Lorenz, M.R., DeLassus, E.N., Scheller, E.L., Veis, D.J.: Immunostaining of Skeletal Tissues. Methods in Molecular Biology. 2021;2221:261-73.

Im, K., Mareninov, S., Diaz, M.F.P., Yong, W.H.: An Introduction to Performing Immunofluorescence Staining. Methods in Molecular Biology. 2019;1897:299-311.

Iwayama, T., Okadam, T., Ueda, T., Tomita, K., Matsumoto, S., Takedachi, M.: Osteoblastic lysosome plays a central role in mineralization. Science Advances. 2019;5(7):eaax0672.

Jain, R.K., Kumar, S.P., Manjula, W.S.: Comparison of intrusion effects on maxillary incisors among mini implant anchorage, j-hook headgear and utility arch. Journal of Clinical and Diagnostic Research : JCDR. 2014;8(7):Zc21-4.

Jain, S., Basavaraj, V.: Direct Immunofluorescence Studies in Lichen Planus. Turkish Journal of Pathology. 2019;35(3):193-7.

Jansen, I.D., Vermeer, J.A., Bloemen, V., Stap, J., Everts, V.: Osteoclast fusion and fission. Calcified Tissue International. 2012;90(6):515-22.

Jilka, R.L., Noble, B., Weinstein, R.S.: Osteocyte apoptosis. Bone. 2013;54(2):264-71.

Kampschulte, M., Langheinirch, A.C., Sender, J., Litzlbauer, H.D., Althöhn, U., Schwab, J.D.: Nano-Computed Tomography: Technique and Applications. RöFo : Fortschritte auf dem Gebiete der Röntgenstrahlen und der Nuklearmedizin. 2016;188(2):146-54.

Kanomi, R.: Mini-implant for orthodontic anchorage. Journal of Clinical Orthodontics: JCO. 1997;31(11):763-7.

Kawamoto, T.: Use of a new adhesive film for the preparation of multi-purpose fresh-frozen sections from hard tissues, whole-animals, insects and plants. Archives of Histology and Cytology. 2003;66(2):123-43.

Kawamoto, T., Kawamoto, K.: Preparation of thin frozen sections from nonfixed and undecalcified hard tissues using Kawamot's film method (2012). Methods in Molecular Biology. 2014;1130:149-64.

Kaur, S., Raggatt, L.J., Batoon, L., Hume, D.A., Levesque, J.P., Pettit, A.R.: Role of bone marrow macrophages in controlling homeostasis and repair in bone and bone marrow niches. Seminars in Cell and Developmental Biology. 2017;61:12-21.

Kennedy, O.D., Herman, B.C., Laudier, D.M., Majeska, R.J., Sun, H.B., Schaffler, M.B.: Activation of resorption in fatigue-loaded bone involves both apoptosis and active pro-osteoclastogenic signaling by distinct osteocyte populations. Bone. 2012;50(5):1115-22.

Kennedy, O.D., Laudier, D.M., Majeska, R.J., Sun, H.B., Schaffler, M.B.: Osteocyte apoptosis is required for production of osteoclastogenic signals following bone fatigue in vivo. Bone. 2014;64:132-7.

Komori, T.: Regulation of osteoblast differentiation by transcription factors. Journal of Cellular Biochemistry. 2006;99(5):1233-9.

Komori, T.: Regulation of osteoblast differentiation by Runx2. Advances in Experimental Medicine and Biology. 2010;658:43-9.

Komori, T.: Runx2, an inducer of osteoblast and chondrocyte differentiation. Histochemistry and Cell Biology. 2018;149(4):313-23.

Komori, T.: Regulation of Proliferation, Differentiation and Functions of Osteoblasts by Runx2. International Journal of Molecular Sciences. 2019;20(7):1694.

Komori, T.: Molecular Mechanism of Runx2-Dependent Bone Development. Molecules and Cells. 2020;43(2):168-175.

Kovács, B., Vajda, E,. Nagy, E.E.: Regulatory Effects and Interactions of the Wnt and OPG-RANKL-RANK Signaling at the Bone-Cartilage Interface in Osteoarthritis. International Journal of Molecular Sciences. 2019;20(18):4653.

Kenkre, J.S., Bassett, J.: The bone remodelling cycle. Annals of Clinical Biochemistry. 2018;55(3):308-27.

Feldkamp, L.A., Davis, L.Ca, Kress, J.W.: Practical cone-beam algorithm, Journal of the Optical Society of America, A 1, 1984;612-619

Kuphasuk, C., Oshida, Y., Andres, C.J., Hovijitra, S.T., Barco, M.T., Brown, D.T.: Electrochemical corrosion of titanium and titanium-based alloys. Journal of Prosthetic Dentistry. 2001;85(2):195-202.

Lacey, D.L., Timms, E., Tan, H.L., Kelley, M.J., Dunstan, C.R., Burgess, T., Elliott, R., Colombero, A,. Elliott, G., Scully, S.: Osteoprotegerin ligand is a cytokine that regulates osteoclast differentiation and activation. Cell. 1998;93:165–176.

Lambert, L.J., Challa, A.K., Niu, A., Zhou, L., Tucholski, J., Johnson, M.S.: Increased trabecular bone and improved biomechanics in an osteocalcin-null rat model created by CRISPR/Cas9 technology. Disease Models & Mechanisms. 2016;9(10):1169-79.

Lawrie, L.C., Curran, S.: Laser capture microdissection and colorectal cancer proteomics. Methods in Molecular Biology. 2005;293:245-53.

Le, M.U.T., Son. J.G., Shon, H.K., Park, J.H., Lee, S.B., Lee, T.G.: Comparison between thaw-mounting and use of conductive tape for sample preparation in ToF-SIMS imaging of lipids in Drosophila microRNA-14 model. Biointerphases. 2018;13(3):03B414.

Lee, C.W., Ren, Y.J., Marella, M., Wang, M., Hartke, J., Couto, S.S.: Multiplex immunofluorescence staining and image analysis assay for diffuse large B cell lymphoma. Journal of Immunological Methods. 2020;478:112714.

Li, D., Ferguson, S.J., Beutler, T., Cochran, D.L., Sittig, C., Hirt, H.P., Buser, D.: Biomechanical comparison of the sandblasted and acid-etched and the machined and acid-etched titanium surface for dental implants. Journal of Biomedical Materials Research. 2002;60(2):325-32.

Li, X., Zhang, Y., Kang, H., Liu, W., Liu, P., Zhang, J.: Sclerostin binds to LRP5/6 and antagonizes canonical Wnt signaling. Journal of Biological Chemistry. 2005;280(20):19883-7.

Lin, C., Jiang, X., Dai, Z., Guo, X., Wenig, T., Wang, .J.: Sclerostin mediates bone response to mechanical unloading through antagonizing Wnt/beta-catenin signaling. Journal of Bone and Mineral Research. 2009;24(10):1651-61.

Liou, E.J., Pai, B.C., Lin, J.C.: Do miniscrews remain stationary under orthodontic forces? American Journal of Orthodontics and Dentofacial Orthopedics. 2004;126(1):42-7.

Liu, Q., Li, M., Wang, S., Xiao, Z., Xiong, Y., Wang, G.: Recent Advances of Osterix Transcription Factor in Osteoblast Differentiation and Bone Formation. Frontiers in Cell and Developmental Biology. 2020;8:601224.

Lombardo, L., Albertini, P., Cervinara, F., Brucculeri, L., Siciliani, G.: Early class III treatment with hybrid rapid palatal expander combined with facemask. International Orthodontics. 2020;18(3):624-635.

Lyu, C.X., Yang, L., Chen, L.L., Yu, F.Y., Lu, H.P.: [Advance and review: miniscrew-assisted rapid palatal expansion]. Zhonghua Kou Qiang Yi Xue Za Zhi = Chinese Journal of Stomatology. 2019;54(11):778-782. Chinese. doi: 10.3760/cma.j.issn.1002-0098.2019.11.011. PMID: 31683387.

Ma, B., Hottiger, M.O.: Crosstalk between Wnt/β-Catenin and NF-κB Signaling Pathway during Inflammation. Frontiers in Immunology. 2016;7:378.

Mahamid, J., Sharir, A., Addadi, L., Weiner, S.: Amorphous calcium phosphate is a major component of the forming fin bones of zebrafish: Indications for an amorphous precursor phase. Proceedings of the National Academy of Sciences of the United States of America. 2008;105(35):12748-53.

Maliszewska-Olejniczak, K., Dróżdż, A., Waluś, M., Dorosz, M., Gryziński, M.A.: Immunofluorescence Imaging of DNA Damage and Repair Foci in Human Colon Cancer Cells. Journal of Visualized Experiments : JoVE. 2020(160).

Marek, A., Schüler, C., Satué, M., Haigl, B., Erben, R.G.: A Laser Capture Microdissection Protocol That Yields High Quality RNA from Fresh-frozen Mouse Bones. Journal of Visualized Experiments : JoVE. 2019(151).

Martin, T.J., Ng, K.W.: Mechanisms by which cells of the osteoblast lineage control osteoclast formation and activity. Journal of Cellular Biochemistry. 1994;56(3):357-66.

Matos, L.L., Trufelli, D.C., de Matos, M.G., da Silva Pinhal, M.A.: Immunohistochemistry as an important tool in biomarkers detection and clinical practice. Biomarker Insights. 2010;5:9-20.

Mavrogenis, A.F., Dimitriou, R., Parvizi, J., Babis, G.C.: Biology of implant osseointegration. Journal of Musculoskeletal & Neuronal Interactions. 2009;9(2):61-71.

McNamara, L.M., Majeska, R.J., Weinbaum, S., Friedrich, V., Schaffler, M.B.: Attachment of osteocyte cell processes to the bone matrix. Anatomical Record (Hoboken). 2009;292(3):355-63.

McNerny, E.M., Gong, B., Morris, M.D., Kohn, D.H.: Bone fracture toughness and strength correlate with collagen cross-link maturity in a dose-controlled lathyrism mouse model. Journal of Bone and Mineral Research. 2015;30(3):455-64.

Mecenas, P., Espinosa, D.G., Cardoso, P.C., Normando, D.: Stainless steel or titanium mini-implants? The Angle Orthodontist. 2020;90(4):587-97.

Melsen, B.: Mini-implants: Where are we? Journal of Clinical Orthodontics: JCO. 2005;39(9):539-47.

Meyns, J., Brasil, D.M., Mazzi-Chaves, J.F., Politis, C., Jacobs, R.: The clinical outcome of skeletal anchorage in interceptive treatment (in growing patients) for class III malocclusion. International journal of oral and maxillofacial surgery. 2018;47(8):1003-10.

Miller, S.C., Bowman, B.M.: Rapid inactivation and apoptosis of osteoclasts in the maternal skeleton during the bone remodeling reversal at the end of lactation. The Anatomical Record (Hoboken). 2007;290(1):65-73.

Miyamoto, T.: Regulators of osteoclast differentiation and cell-cell fusion. The Keio Journal of Medicine. 2011;60(4):101-5.

Moorer, M.C., Riddle, R.C.: Regulation of Osteoblast Metabolism by Wnt Signaling. Endocrinology and Metabolism (Seoul). 2018;33(3):318-30.

Moriishi, T., Ozasa, R., Ishimoto, T., Nakano, T., Hasegawa, T., Miyazaki, T.: Osteocalcin is necessary for the alignment of apatite crystallites, but not glucose metabolism, testosterone synthesis, or muscle mass. PLOS Genetics. 2020;16(5):e1008586

Müller, R.: Hierarchical microimaging of bone structure and function. Nature Reviews Rheumatology. 2009;5(7):373-81.

Mundlos, S.: Cleidocranial dysplasia: clinical and molecular genetics. Journal of Medical Genetics. 1999;36(3):177-82.

Muruganandhan, J., Sujatha, G., Patil, S., Raj, A.T.: Laser Capture Microdissection in Oral Cancer. The Journal of Contemporary Dental Practice. 2018;19(5):475-6.

Nagasaka, H., Sugawara, J., Kawamura, H., Nanda, R.: "Surgery first" skeletal Class III correction using the Skeletal Anchorage System. Journal of Clinical Orthodontics. 2009;43(2):97-105.

Nahm, K.Y., Heo, J.S., Lee, J.H., Lee, D.Y., Chung, K.R., Ahn, H.W.: Gene profiling of bone around orthodontic mini-implants by RNA-sequencing analysis. BioMed Research International. 2015;2015:538080

Nakane, P.K., Pierce, G.B. Jr.: Enzyme-labeled antibodies: preparation and application for the localization of antigens. Journal of Histochemistry & Cytochemistry. 1966;14(12):929-31.

Nakashima, K., Zhou, X., Kunkel, G., Zhang, Z., Deng, J.M., Behringer, R.R., de Crombrugghe, B.: The novel zinc finger-containing transcription factor osterix is required for osteoblast differentiation and bone formation. Cell. 2002;108(1):17-29.

Nasatzky, E., Gultchin J., Schwartz, Z.: [The role of surface roughness in promoting osteointegration]. Refuat Hapeh Vehashinayim (1993). 2003;20(3):8-19, 98.

Nefussi, J.R., Sautier, J.M., Nicolas, V., Forest, N.: How osteoblasts become osteocytes: a decreasing matrix forming process. Journal de Biologie Buccale. 1991;19(1):75-82.

Nelson, C.A., Warren, J.T., Wang, M.W., Teitelbaum, S.L., Fremont, D.H.: RANKL employs distinct binding modes to engage RANK and the osteoprotegerin decoy receptor. Structure. 2012;20(11):1971-82.

Nienkemper, M., Wilmes, B., Lübberink, G., Ludwig, B., Drescher D.: Extrusion of impacted teeth using mini-implant mechanics. Journal of Clinical Orthodontics. 2012;46(3):150-5.

Nienkemper, M., Wilmes, B., Pauls, A., Drescher, D.: Impact of mini-implant length on stability at the initial healing period: a controlled clinical study. Head & Face Medicine. 2013;9:30.

Nienkemper, M., Handschel, J., Drescher, D.: Systematic review of mini-implant displacement under orthodontic loading. International Journal of Oral Science. 2014;6(1):1-6.

Nienkemper, M., Wilmes, B., Pauls, A., Drescher, D.: Mini-implant stability at the initial healing period: a clinical pilot study. The Angle Orthodontist. 2014;84(1):127-33.

Ning, X., Bao, H., Liu, X., Fu, H., Wang, W., Huang, J.: Long-term in vivo CT tracking of mesenchymal stem cells labeled with Au@BSA@PLL nanotracers. Nanoscale. 2019;11(43):20932-41.

Nojima, L.I., Nojima, M.D.C.G., Cunha, A.C.D., Guss, N.O., Sant'Anna, E.F.: Mini-implant selection protocol applied to MARPE. Dental Press Journal of Orthodontics. 2018;23(5):93-101.

Nomura, S., Takano-Yamamoto, T.: Molecular events caused by mechanical stress in bone. Matrix Biology. 2000;19(2):91-6.

Nosouhian, S., Rismanchian, M., Sabzian, R., Shadmehr, E., Badrian, H., Davoudi, A.: A Mini-review on the Effect of Mini-implants on Contemporary Orthodontic Science. Journal of International Oral Health : JIOH. 2015;7(Suppl 1):83-7.

Novack, D.V.: Role of NF-κB in the skeleton. Cell Research. 2011;21(1):169-82

Novinec, M., Lenarčič, B.: Cathepsin K: a unique collagenolytic cysteine peptidase. Biological Chemistry. 2013;394(9):1163-79.

Ortín, J., Delaey, L.: Hysteresis in shape-memory alloys. International Journal of Non-Linear Mechanics, 2002;37:1275-1281

Otsuka, K., Wayman, C.M.: Shape memory materials. Cambridge University Press. 1999;58-66.

Pacheco, E., Hu, R., Taylor, S.: Laser Capture Microdissection and Transcriptional Analysis of Sub-Populations of the Osteoblast Lineage from Undecalcified Bone. Methods in Molecular Biology. 2018;1723:191-202.

Papadopoulos, M.A., Papageorgiou, S.N., Zogakis, I.P.: Clinical effectiveness of orthodontic miniscrew implants: a meta-analysis. Journal of Dental Research. 2011;90(8):969-76.

Papageorgiou, S.N., Zogakis, I.P., Papadopoulos, M.A.: Failure rates and associated risk factors of orthodontic miniscrew implants: a meta-analysis. American Journal of Orthodontics and Dentofacial Orthopedics. 2012;142(5):577-95.e7.

Paul, G.R., Malhotra, A., Müller, R.: Mechanical Stimuli in the Local In Vivo Environment in Bone: Computational Approaches Linking Organ-Scale Loads to Cellular Signals. Current Osteoporosis Reports. 2018;16(4):395-403.

Pauls, A., Nienkemper, M., Drescher, D.: Accuracy of torque-limiting devices used for mini-implant placement--an in vitro study. Journal of Orofacial Orthopedics. 2013;74(2):124-36.

Pérez-Campo, F.M., Santurtún, A., García-Ibarbia, C., Pascual, M.A., Valero, C., Garcés, C., Sañudo, C., Zarrabeitia, M.T., Riancho, J.A.: Osterix and RUNX2 are Transcriptional Regulators of Sclerostin in Human Bone. Calcified Tissue International. 2016;99(3):302-9.

Peterlik, H., Roschger, P., Klaushofer, K., Fratzl, P:. From brittle to ductile fracture of bone. Nature Materials. 2006;5(1):52-5.

Pinzan-Vercelino, C.R.M., Bramante, F.S., de Araújo Gurgel, J., Vergani, E., de Souza Gregório, R.: Intrusion of maxillary molar using mini-implants: A clinical report and follow-up at 5 years. The Journal of Prosthetic Dentistry. 2017;118(1):1-4.

Pittman, J.W., Navalgund, A., Byun, S.H., Huang, H., Kim, A.H., Kim, D.G.: Primary migration of a mini-implant under a functional orthodontic loading. Clinical Oral Investigations. 2014;18(3):721-8.

Preibisch, S., Saalfeld, S., Tomancak, P.: Globally optimal stitching of tiled 3D microscopic image acquisitions. Bioinformatics (Oxford, England). 2009;25(11):1463-5.

Pugliarello, M.C., Vittur, F., De Bernard, B., Bonucci, E., Ascenzi, A.: Chemical modifications in osteones during calcification. Calcified Tissue Research. 1970;5(2):108-14.

Qin, L., Liu, W., Cao, H., Xiao, G.: Molecular mechanosensors in osteocytes. Bone Research. 2020;8:23.

R Core Team (2018) R: A Language and Environment for Statistical Computing. R Foundation for Statistical Computing, Vienna.

Renaud, M., Farkasdi, S., Pons, C., Panayotov, I., Collart-Dutilleul, P.Y., Taillades, H.: A New Rat Model for Translational Research in Bone Regeneration. Tissue Engineering Part C Methods. 2016;22(2):125-31.

Rey, C., Miquel, J.L., Facchini, L., Legrand, A.P., Glimcher, M.J.: Hydroxyl groups in bone mineral. Bone. 1995;16(5):583-6.

Rey, C., Combes, C., Drouet, C., Glimcher, M.J.: Bone mineral: update on chemical composition and structure. Osteoporosis International. 2009;20(6):1013-21.

Reznikov, N., Chase, H., Brumfeld, V., Shahar, R., Weiner, S.: The 3D structure of the collagen fibril network in human trabecular bone: relation to trabecular organization. Bone. 2015;71:189-95.

Riquelme, M.A., Cardenas, E.R., Xu, H., Jiang, J.X.: The Role of Connexin Channels in the Response of Mechanical Loading and Unloading of Bone. International Journal of Molecular Sciences. 2020;21(3):1146.

Roberts, W.E., Marshall, K.J., Mozsary, P.G.: Rigid endosseous implant utilized as anchorage to protract molars and close an atrophic extraction site. The Angle Orthodontist. 1990;60(2):135-52.

Robinson, R.A.: Bone tissue: composition and function. The Johns Hopkins Medical Journal. 1979;145(1):10-24.

Robling, A.G., Niziolek, P.J., Baldridge, L.A.: Mechanical stimulation of bone in vivo reduces osteocyte expression of Sost/sclerostin. Journal of Biological Chemistry. 2008;283(9):5866-75.

Rodrigues, L.E., Mônica, D.S., Chiantelli, C.C., Alves, M.L., Rangel, G.I., Okamoto, T., Okamoto, R.: Temporal localization of osteocalcin protein during healing of tooth extraction sockets in rats. Minerva Stomatologica. 2010;59(6):355-61.

Rodríguez de Guzmán-Barrera, J., Sáez Martínez, C., Boronat-Catalá, M., Montiel-Company, J.M., Paredes-Gallardo, V., Gandía-Franco, J.L.: Effectiveness of interceptive treatment of class III malocclusions with skeletal anchorage: A systematic review and meta-analysis. PLOS ONE. 2017;12(3):e0173875.

Romaniuk, A., Lyndina, Y., Sikora, V., Lyndin, M., Karpenko, L., Gladchenko, O., Masalitin, I.: Structural features of bone marrow. Interventional Medicine and Applied Science. 2016;8(3):121-126.

Russell, W.M.S., Burch, R.L.: The principles of humane experimental technique. Medical Journal of Australia. 1960;1: 500-500.

Sandstedt, C.: Einige Beiträge zur Theorie der Zahnregulierung, Nordisk Tandläkare Tidskrift. 1904;5:236–256.

Saulacic, N., Bosshardt, D.D., Bornstein, M.M., Berner, S., Buser, D.: Bone apposition to a titanium-zirconium alloy implant, as compared to two other titanium-containing implants. European Cells & Materials. 2012;23:273-86.

Schaller, S., Henriksen, K., Sørensen, M.G., Karsdal, M.A.: The role of chloride channels in osteoclasts: ClC-7 as a target for osteoporosis treatment. Drug News & Perspectives. 2005;18(8):489-95.

Scheele, W.: The Collected Papers of Carl Wilhelm Scheele. Nature.1931;128, 1023–1024. https://doi.org/10.1038/1281023a0

Scheuren, A., Wehrle, E., Flohr, F., Müller, R.: Bone mechanobiology in mice: toward single-cell in vivo mechanomics. Biomechanics and Modeling in Mechanobiology. 2017;16(6):2017-2034.

Scheuren, A.C., Kuhn, G.A., Müller, R.: Effects of long-term in vivo micro-CT imaging on hallmarks of osteopenia and frailty in aging mice. PLOS ONE. 2020;15(9):e0239534.

Scheuren, A.C., Vallaster, P., Kuhn, G.A., Paul, G.R., Malhotra, A., Kameo, Y., Müller, R.: Mechano-Regulation of Trabecular Bone Adaptation Is Controlled by the Local in vivo Environment and Logarithmically Dependent on Loading Frequency. Frontiers in Bioengineering and Biotechnology. 2020;8:566346.

Schlesinger, P.H., Mattsson, J.P., Blair, H.C.: Osteoclastic acid transport: mechanism and implications for physiological and pharmacological regulation. Mineral and Electrolyte Metabolism. 1994;20(1-2):31-9.

Schlesinger, P.H., Blair, H.C., Teitelbaum, S.L., Edwards, J.C.: Characterization of the osteoclast ruffled border chloride channel and its role in bone resorption. The Journal of Biological Chemistry. 1997;272(30):18636-43.

Schrof, S., Varga, P., Hesse, B., Schöne, M., Schütz, R., Masic, A.: Multimodal correlative investigation of the interplaying micro-architecture, chemical composition and mechanical properties of human cortical bone tissue reveals predominant role of fibrillar organization in determining microelastic tissue properties. Acta Biomaterialia. 2016;44:51-64.

Seidal, T., Balaton, A.J., Battifora, H.: Interpretation and quantification of immunostains. The American Journal of Surgical Pathology. 2001;25(9):1204-7.

Semënov, M., Tamai, K., He, X.: SOST is a ligand for LRP5/LRP6 and a Wnt signaling inhibitor. The Journal of Biological Chemistry. 2005;280(29):26770-5.

Serra, G., Morais, L.S., Elias, C.N., Meyers, M.A., Andrade, L., Müller, C.A., Müller, M.: Sequential bone healing of immediately loaded mini-implants: histomorphometric and fluorescence analysis. American Journal of Orthodontics and Dentofacial Orthopedics. 2010;137(1):80-90.

Sevetson, B., Taylor, S., Pan, Y.: Cbfa1/RUNX2 directs specific expression of the sclerosteosis gene (SOST). The Journal of Biological Chemistry. 2004;279(14):13849-58.

Shalabi, M.M., Gortemaker, A., Van't Hof, M.A., Jansen, J.A., Creugers, N.H.: Implant surface roughness and bone healing: a systematic review. Journal of Dental Research. 2006;85(6):496-500.

Shapiro, P.A., Kokich, V.G.: Uses of implants in orthodontics. Dental Clinics of North America. 1988 Jul;32(3):539-50.

Sheldon, H., Robinson, R.A.: Electron microscope studies of crystal-collagen relationships in bone. IV. The occurrence of crystals within collagen fibrils. The Journal of Biophysical and Biochemical Cytology. 1957;3(6):1011-6.

Shibata, D., Hawes, D., Li, Z.H., Hernandez, A.M., Spruck, C.H., Nichols, P.W.: Specific genetic analysis of microscopic tissue after selective ultraviolet radiation fractionation and the polymerase chain reaction. The American Journal of Pathology. 1992;141(3):539-43.

Shoulders, M.D., Raines, R.T.: Collagen structure and stability. Annual Review of Biochemistry. 2009;78:929-58.

Siebenlist, U., Franzoso, G., Brown, K.: Structure, regulation and function of NF-kappa B. Annual Review of Cell and Developmental Biology. 1994;10:405-55.

Silasi, D.A., Alvero, A.B., Mor, J., Chen, R., Fu, H.H., Montagna, M.K.: Detection of cancer-related proteins in fresh-frozen ovarian cancer samples using laser capture microdissection. Methods in Molecular Biology. 2008;414:35-45.

Simonet, W.S., Lacey, D.L., Dunstan, C.R., Kelley, M., Chang, M.S., Lüthy, R., Nguyen, H.Q., Wooden, S., Bennett, L., Boone, T.: Osteoprotegerin: a novel secreted protein involved in the regulation of bone density. Cell. 1997;89:309–319.

Singh, V.M., Salunga, R.C., Huang, V.J., Tran, Y., Erlander, M., Plumlee, P.: Analysis of the effect of various decalcification agents on the quantity and quality of nucleic acid (DNA and RNA) recovered from bone biopsies. Annals of Diagnostic Pathology. 2013;17(4):322-6.

Smith, R.J., Burstone, C,J.: Mechanics of tooth movement. American Journal of Orthodontics. 1984;85(4):294-307.

Sosly, R., Mohammed, H., Rizk, M.Z., Jamous, E., Qaisi, A.G., Bearn, D.R.: Effectiveness of miniscrew-supported maxillary incisor intrusion in deep-bite correction: A systematic review and meta-analysis. The Angle Orthodontist. 2020;90(2):291-304.

Soysa, N.S., Alles, N.: Positive and negative regulators of osteoclast apoptosis. Bone reports. 2019;11:100225.

Spatz, J.M., Wein, M.N., Gooi, J.H., Qu, Y., Garr, J.L., Liu, S.: The Wnt Inhibitor Sclerostin Is Up-regulated by Mechanical Unloading in Osteocytes in Vitro. The Journal of Biological Chemistry. 2015;290(27):16744-58.

Stadelmann: VA, Conway, C.M., Boyd, S.K.: In vivo monitoring of bone-implant bond strength by microCT and finite element modelling. Computer Methods in Biomechanics and Biomedical Engineering. 2013;16(9):993-1001.

Stumpf, W.E., Roth, L.J.: High resolution autoradiography with dry mounted, freeze-dried frozen sections. Comparative study of six methods using two diffusible compounds 3H-estradiol and 3H-mesobilirubinogen. Journal of Histochemistry & Cytochemistry. 1966;14(3):274-87.

Supanchart, C., Kornak, U.: Ion channels and transporters in osteoclasts. Archives of Biochemistry and Biophysics. 2008;473(2):161-5.

Surace, M., DaCosta, K., Huntley, A., Zhao, W., Bagnall, C., Brown, C.: Automated Multiplex Immunofluorescence Panel for Immuno-oncology Studies on Formalin-fixed Carcinoma Tissue Specimens. Journal of Visualized Experiments : JoVE. 2019(143).

Tanne, K., Sakuda, M., Burstone, C.J.: Three-dimensional finite element analysis for stress in the periodontal tissue by orthodontic forces. American Journal of Orthodontics and Dentofacial Orthopedics. 1987;92(6):499-505.

Takada, S., Stark, K.L., Shea, M.J., Vassileva, G., McMahon, J.A., McMahon, A.P.: Wnt-3a regulates somite and tailbud formation in the mouse embryo. Genes & Development. 1994;8(2):174-89.

Tertuliano, O.A., Greer, J.R.: The nanocomposite nature of bone drives its strength and damage resistance. Nature materials. 2016;15(11):1195-202.

Tozlu, M., Nalbantgil, D., Ozdemir, F.: Effects of a newly designed apparatus on orthodontic skeletal anchorage. European Journal of Dentistry. 2013;7(Suppl 1):S083-s8.

Trelenberg-Stoll, V., Drescher, D., Wolf, M., Becker, K.: Automated tooth segmentation as an innovative tool to assess 3D-tooth movement and root resorption in rodents. Head & Face Medicine. 2021;17(1):3.

Triaca, A., Antonini, M., Wintermantel, E.: Ein neues Titan-Flachschrauben-Implantat zur orthodontischen Verankerung am anterioren Gaumen. Inf. Orthodont. Kieferorthop. 24.1992:251–257.

Tsuda, E., Goto, M., Mochizuki, S., Yano, K., Kobayashi, F., Morinaga, T., Higashio, K.: Isolation of a novel cytokine from human fibroblasts that specifically inhibits osteoclastogenesis. Biochemical and Biophysical Research Communications. 1997;234:137–142.

Tu, X., Rhee, Y., Condon, K.W., Bivi, N., Allen, M.R., Dwyer, D.: Sost downregulation and local Wnt signaling are required for the osteogenic response to mechanical loading. Bone. 2012;50(1):209-17.

Umemori, M., Sugawara, J., Mitani, H., Nagasaka, H., Kawamura, H.: Skeletal anchorage system for open-bite correction. American Journal of Orthodontics and Dentofacial Orthopedics. 1999;115:166-74

Upadhyay, M., Yadav, S., Patil, S.: Mini-implant anchorage for en-masse retraction of maxillary anterior teeth: a clinical cephalometric study. American Journal of Orthodontics and Dentofacial Orthopedics. 2008;134(6):803-10.

Upadhyay, M., Yadav, S., Nagaraj, K., Nanda, R.: Dentoskeletal and soft tissue effects of mini-implants in Class II division 1 patients. The Angle Orthodontist. 2009;79(2):240-7.

Upadhyay, M., Yadav, S., Nagaraj, K., Uribe, F., Nanda, R.: Mini-implants vs fixed functional appliances for treatment of young adult Class II female patients: a prospective clinical trial. The Angle Orthodontist. 2012;82(2):294-303.

Upendran, A., Gupta, N., Salisbury, H.G.: Dental Mini-Implants. StatPearls [Internet]. Treasure Island (FL): StatPearls Publishing. 2021.

Van Hul, W., Balemans, W., Van Hul, E., Dikkers, F.G., Obee, H., Stokroos, R.J.: Van Buchem disease (hyperostosis corticalis generalisata) maps to chromosome 17q12-q21. American Journal of Human Genetics. 1998;62(2):391-9.

Vande Vannet, B., Sabzevar, M.M., Wehrbein, H., Asscherickx, K.: Osseointegration of miniscrews: a histomorphometric evaluation. European Journal of Orthodontics. 2007;29(5):437-42.

Vandesompele, J., De Preter, K., Pattyn, F., Poppe, B., Van Roy, N., De Paepe, A., Speleman, F.: Accurate normalization of real-time quantitative RT-PCR data by geometric averaging of multiple internal control genes. Genome Biology. 2002;3(7):RESEARCH0034.

Vilani, G.N., Ruellas, A.C., Elias, C.N., Mattos, C.T.: Stability of smooth and rough mini-implants: clinical and biomechanical evaluation - an in vivostudy. Dental Press Journal of Orthodontics. 2015;20(5):35-42.

Wan, E., Akana, M., Pons, J., Chen, J., Musone, S., Kwok, P.Y.: Green technologies for room temperature nucleic acid storage. Current Issues in Molecular Biology. 2010;12(3):135-42.

Wang, M.L., Massie, J., Perry, A., Garfin, S.R., Kim, C.W.: A rat osteoporotic spine model for the evaluation of bioresorbable bone cements. The Spine Journal. 2007;7(4):466-74.

Wang, Y., McNamara, L.M., Schaffler, M.B., Weinbaum, S.: A model for the role of integrins in flow induced mechanotransduction in osteocytes. Proceedings of the National Academy of Sciences of the United States of America. 2007;104(40):15941-6.

Wang, L., Liu, S., Zhao, Y., Liu, D., Liu, Y., Chen, C.: Osteoblast-induced osteoclast apoptosis by fas ligand/FAS pathway is required for maintenance of bone mass. Cell Death & Differentiation. 2015;22(10):1654-64.

Wassermann, F., Yaeger, J.A.: Fine structure of the osteocyte capsule and of the wall of the lacunae in bone. Zeitschrift für Zellforschung 67, 1965:636–652

Webster, D., Schulte, F.A., Lambers, F.M., Kuhn, G., Müller, R.: Strain energy density gradients in bone marrow predict osteoblast and osteoclast activity: a finite element study. Journal of Biomechanics. 2015;48(5):866-74.

Wehrbein, H., Glatzmaier, J., Mundwiller, U., Diedrich, P.: The Orthosystem--a new implant system for orthodontic anchorage in the palate. Journal of Orofacial Orthopedics = Fortschritte der Kieferorthopadie. 1996;57(3):142-53.

Wehrbein, H., Merz, B.R., Diedrich, P., Glatzmaier, J.: The use of palatal implants for orthodontic anchorage. Design and clinical application of the orthosystem. Clinical Oral Implants Research. 1996;7(4):410-6.

Wehrle, E., Tourolle Né Betts, D.C., Kuhn, G.A., Scheuren, A.C., Hofmann, S., Müller, R.: Evaluation of longitudinal time-lapsed in vivo micro-CT for monitoring fracture healing in mouse femur defect models. Scientific Reports. 2019;9(1):17445.

Wei, J., Karsenty, G.: An overview of the metabolic functions of osteocalcin. Current Osteoporosis Reports. 2015;13(3):180-5.

Wijenayaka, A.R., Kogawa, M., Lim, H.P., Bonewald, L.F., Findlay, D.M., Atkins, G.J.: Sclerostin stimulates osteocyte support of osteoclast activity by a RANKL-dependent pathway. PLOS ONE. 2011;6(10):e25900.

Wilmes, B., Drescher, D., Nienkemper, M.: A miniplate system for improved stability of skeletal anchorage. Journal of Clinical Orthodontics: JCO. 2009;43(8):494-501.

Wilmes, B., Nienkemper, M., Ludwig, B., Kau, C.H., Drescher, D.: Early Class III treatment with a hybrid hyrax-mentoplate combination. Journal of Clinical Orthodontics. 2011 Jan;45(1):15-21.

Wilmes, B., Katyal, V., Drescher, D.: Mini-implant-borne Pendulum B appliance for maxillary molar distalisation: design and clinical procedure. Australian Orthodontic Journal. 2014;30(2):230-9.

Wilmes, B., Vasudavan, S., Drescher, D.: Maxillary molar mesialization with the use of palatal mini-implants for direct anchorage in an adolescent patient. American Journal of Orthodontics and Dentofacial Orthopedics. 2019;155(5):725-32.

Woittiez, R.D., Baan, G.C., Huijing, P.A., Rozendal, R.H.: Functional characteristics of the calf muscles of the rat. Journal of Morphology. 1985;184(3):375-87.

Wolff, J.D.: Das Gesetz der Transformation der Knochen, Hirschwald Verlag, Berlin, 1982:40-92.

Wong, B.R., Josien, R., Lee, S.Y., Sauter, B., Li, H.L., Steinman, R.M., Choi, Y.: TRANCE (tumor necrosis factor [TNF]-related activation-induced cytokine), a new TNF family member predominantly expressed in T cells, is a dendritic cell-specific survival factor. Journal of Experimental Medicine. 1997;186:2075–2080.

Wróbel, E., Witkowska-Zimny, M., Przybylski, J.: Biological mechanisms of implant osseointegration. Ortopedia, Traumatologia, Rehabilitacja. 2010;12(5):401-9.

Wu, M., Kriti, D., van Bakel, H., Jabs, E.W., Holmes, G.: Laser Capture Microdissection of Mouse Embryonic Cartilage and Bone for Gene Expression Analysis. Journal of visualized experiments : JoVE. 2019(154).

Xin, X., Jiang, X., Lichtler, A., Kronenberg, M., Rowe, D., Pachter, J.S.: Laser-Capture Microdissection and RNA Extraction from Perfusion-Fixed Cartilage and Bone Tissue from Mice Implanted with Human iPSC-Derived MSCs in a Calvarial Defect Model. Methods in Molecular Biology. 2018;1723:385-96.

Xing, L., Boyce, B.F.: Regulation of apoptosis in osteoclasts and osteoblastic cells. Biochemical and Biophysical Research Communications. 2005;328(3):709-20.

Xing, L., Xiu, Y., Boyce, B.F.: Osteoclast fusion and regulation by RANKL-dependent and independent factors. World Journal of Orthopedics. 2012;3(12):212-22.

Yang, F., Tang, W., So, S., de Crombrugghe, B., Zhang, C.: Sclerostin is a direct target of osteoblast-specific transcription factor osterix. Biochemical and Biophysical Research Communications. 2010. 400:684–688

Yang, J., Pham, S.M., Crabbe, D.L.: High-resolution Micro-CT evaluation of mid- to long-term effects of estrogen deficiency on rat trabecular bone. Academic Radiology. 2003;10(10):1153-8.

Yang, N., Liu, Y.: The Role of the Immune Microenvironment in Bone Regeneration. International Journal of Medical Sciences. 2021;18(16):3697-3707.

Yang, X.S., Sun, S., Wu, X.L.: Dissecting the Mechanism of Martensitic Transformation via Atomic-Scale Observations. Scientific Reports. 4, 2014:6141

Yasuda, H., Shima, N., Nakagawa, N., Yamaguchi, K., Kinosaki, M., Mochizuki, S., Tomoyasu, A., Yano, K., Goto, M., Murakami, A.: Osteoclast differentiation factor is a ligand for osteoprotegerin/osteoclastogenesis-inhibitory factor and is identical to TRANCE/RANKL. Proceedings of the National Academy of Sciences of the United States of America. 1998;95:3597–3602.

Yoshikawa, D.K.: Biomechanical principles of tooth movement. Dental clinics of North America. 1981;25(1):19-26.

Zhang, C., Cho, K., Huang, Y., Lyons, J.P., Zhou, X., Sinha, K.: Inhibition of Wnt signaling by the osteoblast-specific transcription factor Osterix. Proceedings of the National Academy of Sciences of the United States of America. 2008;105(19):6936-41.

Zhu, J., Zeng, Q., Fu, T.: An updated review on TiNi alloy for biomedical applications. Corrosion Reviews. 2019;37:539-552.

Zhuang, Z., Bertheau, P., Emmert-Buck, M.R., Liotta, L.A., Gnarra, J., Linehan, W.M.: A microdissection technique for archival DNA analysis of specific cell populations in lesions < 1 mm in size. The American Journal of Pathology. 1995;146(3):620-5.

7. Acknowledgments

My sincere thanks go to Prof. Dr. Dieter Drescher, for both providing the present topic and supervising this dissertation.

I would also like to sincerely thank PD Dr. Kathrin Becker, not only for the conception of the present topic and her continuous supervision, but also for her scientific and emotional support, both during the experimental part and the writing process itself.

Many thanks go to Prof. Dr. Ralph Müller, head of the Institute of Biomechanics at the ETH Zurich, as well as Dr. Gisela Kuhn and Ph.D. Ariane Scheuren, for making it possible to hospitate in their institute and learn about their exciting suggestions in the technical handling of bone samples for gene expression analysis.

To Dr. Beryl Schwarz-Herzke I would like to express my sincere thanks, for her support in both performing the gene expression analysis and preparing the immunofluorescence stains, but also for her scientific suggestions apart from this work.

I would also like to thank Jun.-Prof. Mathias Beller for his help in the challenging generation of the immunofluorescence scans, as well as his subsequent training in handling the software CellProfiler.

Furthermore, PD Dr. Alberto Pérez Bouza and Simone Enders from the Institute for Pathology and Cytology in Troisdorf deserve a huge thank for their instructions in the persisting preparation of the paraffin sections.

Apart from the scientific inputs to this work, I would like to thank all the ones who have supported me emotionally - perhaps unknowingly - during the preparation of this work.

In this regard, grateful thanks go to Prof. Dr. Jürgen Becker, also for enabling my specialist education in the field of oral surgery.

Sincere thanks also go to Dr. Gordon John and Dr. Andreas Künzel, Caro, Annemarie, Florian, Alex, Giulia, Mira and Viktoria for their open ears - during, but also after work. You have not insignificantly advanced the progress of this work.

Additionally, I would like to thank Sebastian, firstly for his continued support in providing the LCM microscope, but moreover for exciting tales from another world.

In the end, infinite thanks go to my parents, who have always been supportive in times of discouragement - things that cannot be put into words appropriate enough.

Last but not least, *my greatest thanks* go to my grandpa though, to whom this work is dedicated with love.